Efficient Algorithms for Image Denoising using Wavelets

A thesis

submitted in the fulfillment of the

requirement for the award of the degree of

Doctor of Philosophy

Submitted by:

Ram Paul

Registration no. 950911008

School of Mathematics

Thapar Institute of Engineering and Technology

Patiala, Punjab, INDIA-147004

June, 2019

Certificate

I hereby certify that the work which is being presented in this thesis entitled "Efficient Algorithms for Image Denoising using Wavelets", in partial fulfillment of the requirements for the award of degree of **DOCTOR OF PHILOSOPHY** submitted in School of Mathematics, Thapar Institute of Engineering and Technology, Patiala, is an authentic record of my own work carried out under the supervision of Dr. Rajesh Kumar Gupta, Associate Professor, Department of Mathematics, Central University of Haryana, Mahendergarh and Dr. Singara Singh Kasana, Associate Professor, Computer Science and Engineering Department, TIET and refers duly listed other researcher works in the reference section. All the presented matter in this thesis has not been proposed or submitted for the award of any other research or degree of this or any other University.

Paul

(Ram Paul)

Registration Number: 950911008

This is to certify that the above stated matter by the candidate is correct and true to the best of my knowledge and belief.

(Dr. Rajesh Kumar Gupta)
Associate Professor
Department of Mathematics
Central University of Haryana
Mahendergarh-123029, Haryana, India
Supervisor

(Dr. Singara Singh Kasana)
Associate Professor
Computer Science and Engineering Department
Thapar Institute of Engineering and Technology
Patiala-147004, Punjab, India
Supervisor

Acknowledgments

I have an obligation to pay the grace of almighty, whose divine light provided me more in the form of the perseverance, inspiration, faith, guidance enormous patience, and great strength to carry out this research work.

I would like to express my earnest gratitude to my supervisors, **Dr. Rajesh Kumar Gupta**, Associate Professor, Department of Mathematics, Central University of Haryana, Mahendergarh and **Dr. Singara Singh Kasana**, Associate Professor, Computer Science and Engineering Department, Thapar Institute of Engineering and Technology, Patiala for their learn able guidance and simulation throughout this work of research, providing me constructive comments and learning support. I am extremely indebted to them for providing time to listen and give their valuable suggestions.

I express my sincere thanks to **Dr. Satish Kumar Sharma**, Head, School of Mathematics, Thapar Institute of Engineering and Technology, Patiala for his support and suggestions.

I am grateful to the Doctoral committee comprising **Dr. Satwinder Singh Bhatia**, Professor, School of Mathematics, **Dr. Rajendra Kumar Sharma**, Professor, Computer Science and Engineering Department and **Dr. Ajay Kumar**, Associate Professor, Computer Science and Engineering Department for monitoring the progress and providing valuable suggestions for the improvement of this work. I thank all the staff members of Computer Science and Engineering Department and School of Mathematics, Thapar Institute of Engineering and Technology for their support and cooperation.

I am highly thankful to **Dr. Rekha Aggarwal**, Professor and Director, Amity School of Engineering and Technology, Amity University, Noida, for her moral support, cheering concern and optimistic attitude for doing things. My special thanks go to **Dr. Pinki Nayak**, Head CSE deptt., ASET, for her great help and assistance in all regards, from technical to personal problems.

Words are inadequate in paying regards to my father late **Sh. Raghuvir Singh**, mother **Smt. Parkashi Devi** and my in laws for their blessings, continuous encouragement and patience. I express deep gratitude to my brother **Ramesh Kumar** whose love, care and support have been an invaluable source of encouragement to me.

It is not possible for me to quantify and express in words the constant help and great moral support of my dear wife **Ms. Sulakshna Rana**. Her support and divine advice have always strengthen me not only in this research work but at every stage of my life. I acknowledge support from my loving daughters **Mitali Singh**, **Anvika Singh** and **Ashita Singh** during this doctoral research.

I would like to express thanks to all who made their contribution directly or indirectly during this journey of research work to make my Ph. D., a successful event.

(Ram Paul)

Abstract

The fundamental ideas of this thesis are based on the observation that there are high scopes of enhancing the efficiency in Image Denoising Algorithms (IDAs). Noises in the digital images are induced during their acquisition and transmission due to the imperfect nature of digital instruments. For instance, Additive White Gaussian Noise (AWGN) is cased by poor quality image acquisition equipment and also inherited in communication channels. Various IDAs have been proposed to reduce the noise from images in spatial as well as transform domains. The IDAs in spatial domain can be further subdivided according to linear and non-linear approach. The transform domain IDAs are based on the choice of basis functions.

After reviewing standard IDAs in spatial and transform domain, this thesis embarks on the endeavor of developing and experimenting new IDAs in wavelet domain that perform not only noise reduction but also preservation of image fine details and color components. Wavelet transform achieved more popularity in transform domain due to sparsity and multiresolution property. Discrete Wavelet Transform (DWT) of a noisy image can generate very sparse wavelet coefficients. Wavelet coefficient thresholding is achieved by calculating the threshold value adaptively. This can avoid the over-smoothening of noisy images and their fine details especially edges. DWT, Undecimated DWT (UDWT) and Dual-Tree Complex Wavelet Transform (DT-CWT) are the efficient wavelet transform functions for IDAs and used in this work.

It is necessary to reduce the noises for further image processing while preserving the edges present in the image. An edge preserving adaptive algorithm for gray and color image denoising is proposed. The noisy images are decomposed using DWT to obtain their coefficients. The edges of an image are detected using the Canny edge detector in all the details subbands. Then two thresholds are

calculated by using the Bayesian estimator. The adaptive standard threshold is used for flatten region and its updated version is used for edge region as the noise has low visual perception on the edges. These threshold values are applied through soft thresholding to the wavelet coefficients. The results of this proposed adaptive algorithm are compared by Peak Signal-to-Noise Ratio (PSNR) and visual perception of denoisied images with existing adaptive IDAs.

An efficient and adaptive IDA to preserve the edges in wavelet domain is proposed. A noisy image is decomposed into subbands by using DWT. An optimal threshold value is calculated from the wavelet coefficients of diagonal details subband of first decomposition level using the Bayesian estimator. Then wavelet coefficients hard thresholding is achieved by the application of selected threshold value to all the details subbands. After that morphological operations are performed with the thresholded wavelet coefficient of the test image to preserve the edges from any degradation by hard thresholding. A denoised image is reconstructed from these modified and enhanced wavelet coefficients by using the inverse DWT (IDWT). The experimental results show the effectiveness and efficiency of proposed IDA. Also, the results of the proposed algorithm are compared with state-of-art existing IDAs using PSNR and visual perception.

Three color components namely hue (the dominant wavelength), saturation (purity o color) and luminance (the intensity of light) are not preserved during traditional IDAs. It is very important to preserve the edges and these color information of a color image. The standard DWTs propose a facility of implementing a multi-scale analysis, but shift-invariance and directional selectivity are not supported by them which are necessary for color image processing. This is due to the decimation used in traditional DWT and can be covered by UDWT. An adaptive color IDA using spatial correlation in UDWT is proposed that preserves the color image features more efficiently. The noisy color image is decomposed into four subbands using the UDWT. Then the spatial correlation of wavelet coefficients in a noisy color image is achieved by the coefficient multiplication of adjacent decomposition levels. The threshold value is calculated by computing the noise standard deviation from the correlated diagonal subband of first and second decomposition levels. The soft thresholding is applied here to denoise all the correlated coefficients for each details correlated subbands. The experimental results confirm that this proposed algorithm preserves image edges and color components very well while

reducing noise. The efficiency and performance of existing state-of-the-art and proposed IDAs are compared by using PSNR values and visual perception.

Further, the traditional DWT has the drawbacks of being shift-invariant, directional selectivity and lacking the capacity to process phase information of edges in images. The traditional DWT based IDAs leave lots of residual noise in the denoised images. An adaptive IDA using pre-filtering in the Double-density Dual-Tree Complex Wavelet Transform (DDT-CWT) is proposed which preserves the image features like edges more efficiently. Firstly, the noisy image is pre-filtered using standard Wiener filtering. Secondly, this pre-filtered output image is decomposed into different subbands using the DDT-CWT. Then a threshold value is calculated by computing the noise standard deviation from the diagonal subband of first decomposition level of the real part of DDT-CWT coefficients. The soft thresholding is applied after finalizing the threshold value. The improved experimental results are compared with Wiener filtering in wavelet domain, DT-CWT based IDA.

Abbreviations

ANFIS	Adaptive Neuro-Fuzzy Inference System
AWGN	Additive White Gaussian Noise
BM3D	Block Matching and 3-D
CBIR	Content based Image Retrieval
CWM	Central Weighted Median
CWT	Complex Wavelet Transform
DCT	Discrete Cosine Transform
DDT-CWT	Double-density Dual Tree CWT
DFT	Discrete Fourier Transform
DT-CWT	Dual Tree - CWT
DWT	Discrete Wavelet Transform
EPAT	Edge Preserving Adaptive Thresholding
EQ	Estimation-Quantization
FFT	Fast Fourier Transform
FMRF	Finite Markov Random Fields
GGD	Generalized Gaussian Distribution
GGM	Generalized Gaussian Mixture
GMM	Gaussian Mixture Model
HH	High-High pass subband
HL	High-Low pass subband
ICA	Independent Component Analysis

IDAs	Image Denoising Algorithms
IDWT	Inverse Discrete Wavelet Transform
i.i.d.	independent identically distributed
IQI	Image Quality Index
LET	Linear Expansion of Thresholds
LH	Low-High Pass Subband
LL	Low-Low Pass Subband
LMMSE	Linear Minimum Mean Square Error
LS-SVM	Least Square - Support Vector Machine
LPG	Local Pixel Grouping
MAP	Maximum-a-Posteriori
MDL	Minimum Description Length
MF	Mapping Function
ML	Maximum Likelihood
MM	Mathematical Morphology
MMSE	Minimum Mean Square Error
MRF	Markov Random Field
MSE	Mean Square Error
MTF	Modulation Transfer Function
NLM	Non-Local Mean
pdf	probability density function
PCA	Principal Component Analysis
PSF	Points Spreading Function
PSNR	Peak Signal to Noise Ratio
RGB	Red, Green and Blue
SAR	Synthetic Aperture Radar
SE	Structuring Element
SIWPD	Sift Invariant Wavelet Packet Decomposition

SNR	Signal-to-Noise Ratio
SSIM	Structural Similarity Index Measure
SURE	Steins Unbiased Risk Estimate
SVM	Support Vector Machine
TI	Translation-Invariant
TV	Total Variation
TLS	Total Least Square
UDWT	Undecimated Wavelet Transform
WP	Wavelet Packet

Notations and Symbols

I	Original image
$\tilde{I}$	Noisy image
μ_I	Mean of original image
$\mu_{\tilde{I}}$	Mean of noisy image
$\eta(i,j)$	Noise intensity at (*i, j*) coordinates
H	Low-pass filters
G	High-pass filters
m	Image mean
(M,N)	Size of the image
σ_n	Noise standard deviation
σ_n^2	Noise variance
b	Bit depth of the image
μ_I	Mean luminance of the free images
$\mu_{\tilde{I}}$	Mean luminance of the noisy image
σ_I	Standard deviation of original image
$\sigma_{\tilde{I}}$	Standard deviation of noisy image
σ_I^2	Noise variance of the original images
$\sigma_{\tilde{I}}^2$	Noise variance of the noisy image
$\sigma_{I\tilde{I}}$	Local measures of noise-free and noisy images correlation
z	Gray level of image

Contents

List of Figures

List of Tables

List of Publications

1. **Ram Paul**, Rajesh Kumar Gupta and Singara Singh Kasana, "Performance Analysis of Impulse Denoising Techniques in Magnetic Resonance Imaging", *International Journal of Computer Applications*, vol. 136, no. 12, pp. 17-22, 2016.

2. **Ram Paul**, Singara Singh Kasana and Rajesh Kumar Gupta, "An Edge-preserving Adaptive Image Denoising using Discrete Wavelet Transform", *International Journal of Imaging and Robotics*, vol. 18, no. 4, pp. 155-164, 2018, *SCOPUS* Indexed.

3. **Ram Paul**, Singara Singh Kasana and Rajesh Kumar Gupta, "Performance Analysis of Adaptive Image Denoising Techniques for Different Levels of Wavelet Decomposition using Orthogonal and Compactly Supported Wavelet Families", *International Journal of Engineering and Applied Sciences*, vol. 5, no. 7, pp. 51-58, 2018.

4. **Ram Paul**, Singara Singh Kasana and Rajesh Kumar Gupta, "Efficient Edge-preserving Adaptive Image Denoising using Morphological Operations in Wavelet Domain", *International Journal of Applied Engineering Research*, vol.13, no. 16, pp. 12941-12949, 2018, *SCOPUS* Indexed.

5. **Ram Paul**, Singara Singh Kasana and Rajesh Kumar Gupta, "Improved Color Image Denoising using Spatially Adaptive Statistical Dependency in Undecimated Wavelet Transform Coefficients", *Ain Shams Engineering Journal*, (Communicated) ***SCI* Indexed.**

6. **Ram Paul**, Singara Singh Kasana and Rajesh Kumar Gupta, "An Adaptive Image Denoising using Pre-filtering in Double-density Dual Tree Complex wavelet Transform", *International Journal of Signal and Imaging Systems Engineering*, (Communicated) *SCOPUS* Indexed.

Chapter 1

Introduction

Digital images is generally encoded as a matrix of gray level or color values. These have a key role in the area of visual information sharing applications like multimedia computing, biometrics, pattern recognition, image data communication, texture understanding, remote sensing, Content Based Image Retrieval (CBIR) and so on. In these fields of image processing, images do not exist without noise. Noise is induced in the images during their acquisition and transmission (Donoho and Johnstone 1994). The major factors which induce the noise in the images during their acquisition are the light levels and temperature of the sensors used in the camera. If dust particles are present on the scanner screen, they can also introduce noise in the image. A digital image may be corrupted mainly due to the interferences in channel used for its transmission. Following types of noise are induced in the images:

(i) **Additive Noise**: It is the error induced in the original intensity values of the image in additive manner. Model o this noise follows Gaussian distribution *i.e.* the noise is equally spread over the entire image. Examples are AWGN and salt-and-pepper noise.

(ii) **Multiplicative Noise**: It is the error induced in the original image intensity values in multiple manner. It uses the multiplication operation pointwise in image intensity. Two type of multiplicative noises are speckle and brown noise.

These categories are further divided into sub-categories and are explained further in next section.

These noises in imaging pose great problems for visual quality and automated analysis operations. Noise must be removed in the pre-processing step for further information utilization of images. The severe effects in visual perception promote to study the noise types and its models in-depth.

The process of noise reduction from the noisy image while retaining its important features like textures, corners and edges is called image denoising. The main objective of an IDA is to preserve the original image features, color components and other fine details (Donoho 1995). An efficient IDA is a great challenge to the researchers due to the different complexities of the images and densities of noises. The denoising of an image has been one of the most important field in the area of image processing. It is an important and mandatory pre-processing in wide range of image processing applications. Examples are natural image analysis, medical images, radio astronomy *etc.* (Coifman and Donoho 1995). Each application may be based on its own particular requirements. In other words, noise reduction in natural images must be handled with specific care, since denoising may cause the loss of image fine details like edges, textures *etc* due to their same high frequency spectrum as per induced noise.

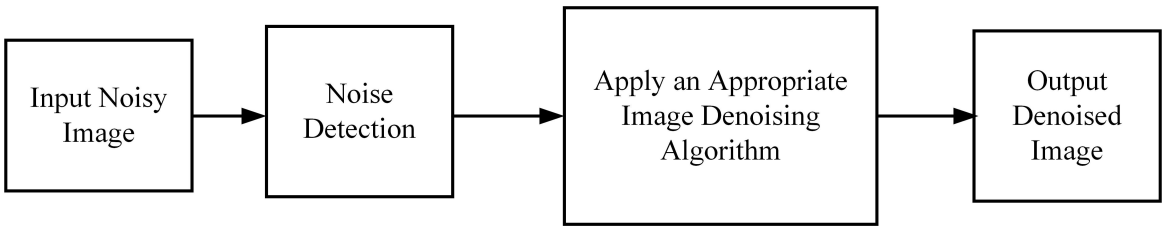

Figure 1.1: Basic Image Denoising System

The basic image denoising system is given in Figure 1.1 with all the required steps. In its first step, a noisy image with required noise standard deviation is made from the original image and intensity of noise as well as its type is detected next so that an appropriate IDA is applied. Third step can finalized the applicable IDA to reduce the noise with preserving the fine details and color components of the image. After that an output denoised image is reconstructed which is similar to original image.

During the image denoising, the main aim is to suppress the noise without paying any attention in preserving the fine details and color components of the image. So in traditional IDAs, the edges may be disturbed due to their over-smoothening (Chen and Lien 2008). The edges of a natural image have a major role in visual perception of the images. So there is a great need to preserve the edges during

image denoising (Chen and Lien 2008, Faghih and Smith 2002, Jain and Tyagi 2015). The edges have a major role in sharpness of an image. So image denoising with edge preserving continues to attract researcher's attention from other disciplines like image compression, pattern recognition, computer graphics and multimedia, computer vision and psychology (Hassan and Saparon 2011, Islam et al. 2017).

It is not practically possible to completely remove the noise from an image but a researcher can work towards the better reduction of noise from the noisy image (Abramovich and Benjamini 1996). A huge literature of IDAs have been proposed by researchers based on different mathematical tools like probability and statistics, partial differential equations, spatial-domain filtering and transform-domain filtering. Wiener filtering, Block Matching and 3-D (BM3D) filtering, bilateral filtering and many more have achieved better objective and subjective performance. It is important and necessary that the IDAs have no bluffing, distortion effect and induced no artifacts to the denoised images. All the important image features must be preserved so that a realness of image can be recovered completely.

All the noises produce undesirable effects such as artifacts, false edges, corners, unseen geometric elements, blurred objects and disturbs background of the image. Most of the existing IDAs also consider noise as high frequency contents which confuse the edges as a noise components and get smoothen them during the process of image denoising. The solution of all these problems may be achieved through the analysis of noise models. The majority of existing IDAs are specifically applicable for the reduction of AWGN and salt-and-pepper noise in images (Hammond and Simoncelli 2006, Lin and Lingfu 2009). So far, various IDAs have been proposed to deal with noise reduction, which can be categorized into two main groups: image denoising in the spatial domain *i.e.* time or space domain and image denoising in the transform domain *i.e.* Fourier or wavelet transform. These IDAs may be based on linear or non-linear approach. Linear IDAs are not so effective for noisy images since the spectrum of fine details of images are similar to the spectrum of noise (Brox et al. 2008). Non-linear IDAs based on sparsity *i.e.* the main energy of an image can be represented by a few wavelet coefficients within the transform domain while the noise energy is spread among all the wavelet coefficients (Cho et al. 2009, Azzalini et al. 2005).

Selecting an appropriate algorithm plays a major role in image denoising depending on induced noise model in the image. For example, an IDA for natural images may not be well suitable for denoising the medical images with different type of noises. To analyze and quantify the performance of the various IDAs, a set of high quality gray and color images are taken in this work and additive noise of different intensities are added to it. The corrupted images are used as an input to the IDAs, which produce the denoised images close to the original images.

1.1 Mathematical Noise Models in an Image

To go into depth of image denoising, it is mandatory to know mathematically model of noise present in the digital images very clear. Theoretically, a noise is an intensity error acting on each pixel location separately and characterized by random variables (Beghdadi and Khellaf 1997). Induced noise in an image can be modeled by using histogram or statistical measurement using probability density function (pdf) or Points Spreading Function (PSF) and Modulation Transfer Function (MTF). The quantitative analysis of noise models are essential to reduce these undesirable effects for further processing of information or image (Hamza and Krim 2001). They are categorized into two broad categories: additive and multiplicative noises as shown in Figure 1.2. Different type of noises under these two categories are also well organized in this Figure. Their theoretical details with mathematical representations are given in coming subsections.

1.1.1 Additive Noise Model

The simplest noise model is an additive noise model in which the some intensity of noise gets embedded to the original image pixel evenly to produce a corrupted noisy image (Danielyan and Foi 2009). It can be mathematically represented by the equation (1.1) with realization of independent identical distribution (*i.i.d.*) random variable:

$$\tilde{I}(x,y) = I(x,y) + \eta(x,y) \tag{1.1}$$

where $\tilde{I}(x,y)$ represents a noisy image, $I(x,y)$ is an original image and $\eta(x,y)$ is an induced

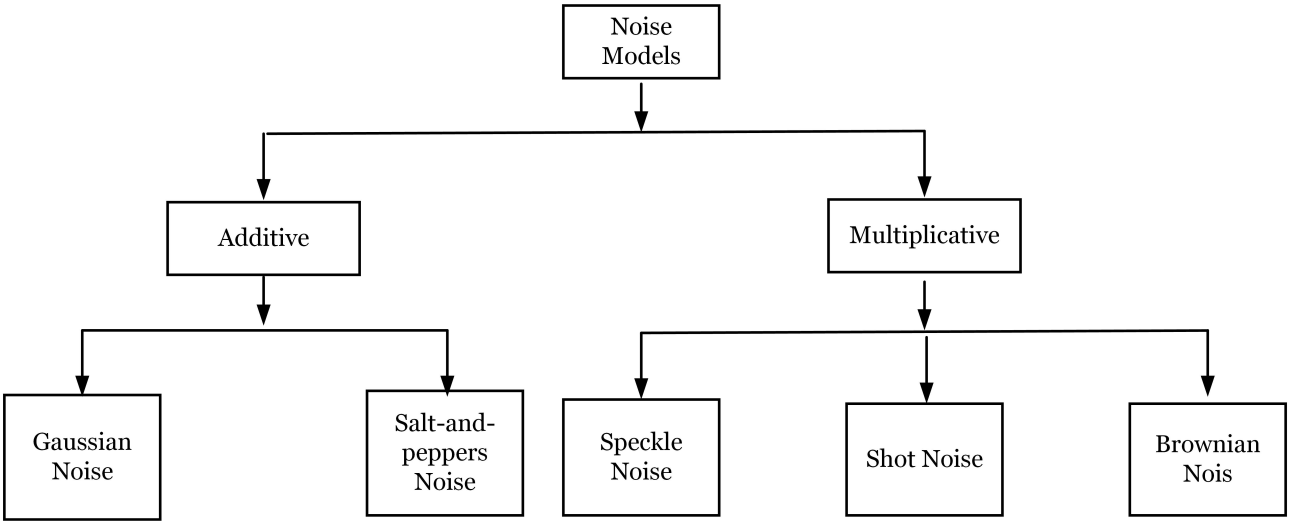

Figure 1.2: Noise Models in Digital Images

noise. Mainly two type of noises follow this noise model: Gaussian noise and salt-and-pepper noise.

1.1.1.1 Gaussian Noise

In Gaussian noise, the induced noise is evenly distributed over the entire image *i.e.* it follows a random Gaussian distribution in which each noisy image pixel value is the sum of original pixel value and noise pixel value (Rank and Unbehauen 1992). This noise model has a *pdf* of the normal distribution of gray values in an image (Hammond and Simoncelli 2006, Moulin and Liu 1999). A Gaussian noise mathematical model represents the more accurate approximation of noises in the images. The main sources of additive noises are the electronic noise in amplifiers or detectors. AWGN is the special case of additive noise (Selesnick 2008).

Mathematically, it is represented by:

$$p(z) = \frac{1}{\sqrt{2\pi\sigma^2}} e^{\frac{-(z-m)^2}{2\sigma^2}} \tag{1.2}$$

where z represents a gray level, m is mean of the image, and σ is the noise standard deviation.

This type of additive noise follows a Generalized Gaussian Distribution (GGD) (Beghdadi and Khellaf 1997). This noise model is represented by bell shaped curve due to the equal randomness of the normalized Gaussian pattern, as shown in Figure 1.3.

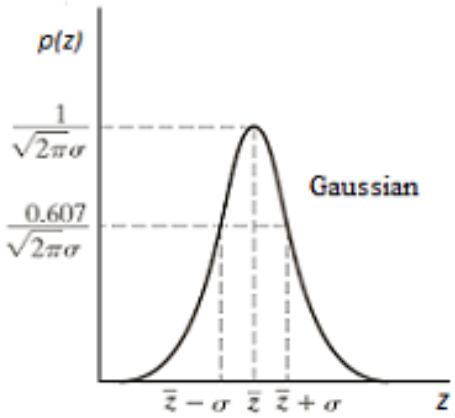

Figure 1.3: Gaussian Noise Distribution

1.1.1.2 Salt-and-Pepper Noise

It is also called impulse noise, shot noise or spike noise and has only two possible values, $I(x, y)$ of original true image and $\eta(x, y)$ of noise value with the probability of salt or pepper is usually less than 0.1. A corrupted pixels in the noisy images are set alternatively to a maximum value as a *salt* or to a minimum value as a *pepper* while non-affected pixels remain unchanged (Chen and Lien 2008). The main sources of salt-and-pepper noise are faulty memory locations, malfunctioning pixel elements in the camera sensors, or there can be the process timing errors during digitization.

Mathematically it is given by

$$p(z) = \begin{cases} P_a & ; \quad \text{for} z = a \\ P_b & ; \quad \text{for} z = b \\ 0 & ; \quad \text{o}therwise \end{cases} \tag{1.3}$$

If either P_a=0 or P_b=0 =¿ unipolar impulse noise, If either P_a= P_b=0 =¿ bipolar impulse noise or salt-and-pepper noise. Normally, a=0 (black) and b=0 (white)

The pepper noise is represented by 0 and salt noise is 255 for an 8-bit gray image representation and is given in Figure 1.4.

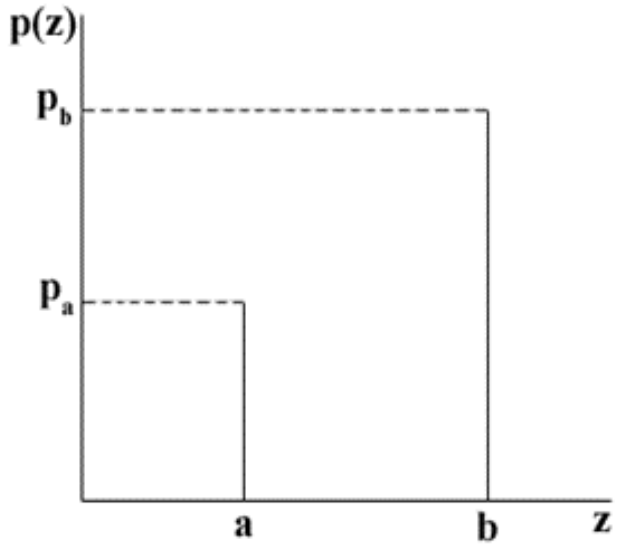

Figure 1.4: Salt-and-pepper Noise Distribution

1.1.2 Multiplicative Noise Model

In this noise model, pixel value of noisy image is the product of noise pixel value and original image pixel value (Hawwar and Reza 2002). The multiplicative noise model is represented mathematically as:

$$\hat{I}(i,j) = I(i,j) \times \eta(i,j) \tag{1.4}$$

where $\hat{I}(i,j)$ represents a noisy image, $I(i,j)$ is a true image and $\eta(i,j)$ is induced noise. Basically, two types of noises follow the multiplicative noise model in the digital images and are discussed in the coming sub-sections.

1.1.2.1 Speckle Noise

Speckle noise has the characteristic of multiplicative noise model. The main sources of speckle noise are some special imaging systems like laser imaging and Synthetic Aperture Radar (SAR). The speckles are developed by these sources of noise by random interference in the images.

Mathematically, it is given by

$$P(z) = \frac{g^{\alpha-1}}{(\alpha-1)!a^{\alpha}} e^{\frac{-z}{a}} \tag{1.5}$$

where a^{α} is noise variance and z represents the gray level.

This multiplicative noise follows a gamma distribution as shown in Figure 1.5:

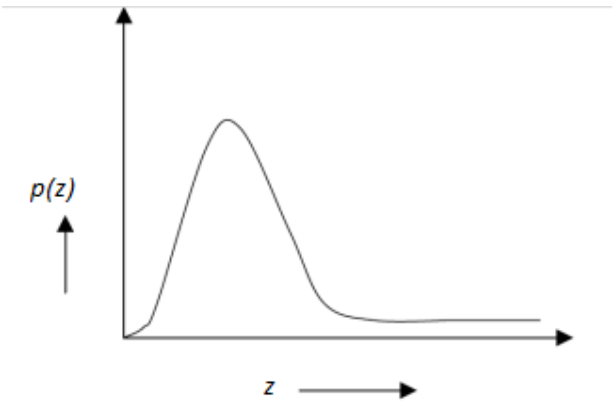

Figure 1.5: Gamma Noise Distribution

1.1.2.2 Brownian Noise

Colored noise has many names such as Brownian noise or pink noise or flicker noise or 1/f noise. Brownian noise follows non-stationary stochastic process with normal distribution. Brownian noise is a particular case of $1/f$ noise and also called as fractal noise. The power spectral density of Brownian noise is proportional to the square of frequency and obtained by integrating white noise in the images. The mathematical model for this noise is given by two equations: a zero mean Gaussian process (B_H):

$$B_H(0) = 0 \tag{1.6}$$

and an expected value of fractional Brownian motion:

$$B|B_H(t) - B_H(t-\delta)|^2 = \sigma^2 |\delta|^{2H} \tag{1.7}$$

where σ^2 is noise variance.

1.2 Image Denoising Quality Parameters

The image denoising quality is evaluated for comparing the various IDAs subjectively and objectively. In this section, different image quality parameters are discussed with their importance and applications. The quality of a denoised image may be evaluated objectively by numeric results and/or subjectively by visual perception. The main approach in objective evaluation is PSNR and used in this work due to its accuracy and efficiency in image denoising. Some others are the Image Quality Index (IQI) and Structural Similarity Index Measure (SSIM). In the subjective approach, the denoised image is compared with original image by human visual perception analysis.

1.2.1 Objective Quality Evaluation

The objective image quality evaluation is a measure mathematically used to quantify the similarities and distinguishes between the denoised image $\tilde{I}$ and the original true image I. Mostly used metrics to quantify the image quality evaluation are Mean Square Error (MSE) and PSNR.

$$MSE = \frac{1}{M \times N} \sum_{x=1}^{M} \sum_{y=1}^{N} [I(x,y) - \tilde{I}(x,y)]^2 \tag{1.8}$$

where $I(x,y)$ represents an original image, $\tilde{I}(x,y)$ is denoised image and $M \times N$ is image size.

MSE is often normalized by the square of the maximum value of the image intensity. It is mathematically represented in a logarithmic scale. Statistically, the Signal-to-Noise Ratio (SNR) is a measure of the standard deviations of an image against the standard deviations of noise in the image (Blu and Luisier 2007). Therefore, larger the SNR, better the noisy image recovered.

$$SNR = 10 \log_{10} \left[\frac{\sum_{x=1,}^{M} \sum_{y=1}^{N} I^2(x,y)}{MSE} \right] \tag{1.9}$$

where $I(x,y)$ represents a original image, $M \times N$ represents image size and MSE is given in equation (1.8).

PSNR is given as a ratio among maximum possible image intensity power and the noise power of corrupted image that degrade the fidelity of image representation. Mathematically PSNR is given as:

$$PSNR = 10 \log_{10} \left[\frac{(2^b - 1)^2}{MSE} \right] \tag{1.10}$$

where b is the bit depth of the image.

SSIM approach of image quality assessment is also popular and new measures of image quality that better correlate with human visual perception (Ghouti and Bouridane 2005). The similarity between the original and denoised images are measured by SSIM based on visible structures in the images (Rehman and Wang 2011). SSIM index is calculated on various windows of sample images. The measure between original image $I(x, y)$ and denoised image $\tilde{I}(x, y)$ of common image size $M \times N$ is given as:

$$SSIM[I(x, y), \tilde{I}(x, y)] = l[I(x, y), \tilde{I}(x, y)] \times c[I(x, y), \tilde{I}(x, y)] \times s[I(x, y), \tilde{I}(x, y)] \tag{1.11}$$

where

$$l(I, \tilde{I}) = \frac{2\mu_I \mu_{\tilde{I}} + C_1}{\mu_I^2 + \mu_{\tilde{I}}^2 + C_1} \tag{1.12}$$

$$c(I, \tilde{I}) = \frac{2\sigma_I \sigma_{\tilde{I}} + C_2}{\sigma_I^2 + \sigma_{\tilde{I}}^2 + C_2} \tag{1.13}$$

$$s(I, \tilde{I}) = \frac{\sigma_{I\tilde{I}} + C_3}{\sigma_I \sigma_{\tilde{I}} + C_3} \tag{1.14}$$

SSIM between original image $I(x, y)$ and denoised image $\tilde{I}(x, y)$ considers three similarities as described ahead:

- The first term $l(I, \tilde{I})$ given in the equation (1.12) is the luminance similarity comparison function which measures the mean luminance of the noisy image $\mu_{\tilde{I}}$ and original images μ_I;
- The second term $c(I, \tilde{I})$ explained in the equation (1.13) is the contrast similarity comparison function and it evaluates a noise standard deviation of the noisy image $\sigma_{\tilde{I}}$ and standard deviation of original image σ_I as well as the noise variance of the noisy image $\sigma_{\tilde{I}}^2$ and variance of the original image σ_I^2;

- The third term $s(I, \tilde{I})$ presented in the equation (1.14) is the structure similarity comparison function which evaluates the standard deviations of the noisy image and original images, as well as their correlated local measures $\sigma_{I\tilde{I}}$.

1.2.2 Subjective Quality Evaluation

Subjective analysis is the pictorial representation of the noise standard deviations, noisy image and denoised image. When the original image is not available, it is not practically feasible to get an objective measure of the similarity. But there are many reference-free algorithms to provide the subjective quality:

Human visual perception: It is a better way to evaluate the image denoising quality by human judgment. A subjectivity gets decreased as the number of human subjects increase (Bolster et al. 2003). The human attention is towards the artifacts visibility and edges sharpness for subjective evaluation.

Subjective Quality Attributes:

1. Color of an image can be represented by using hue and saturation, except lightness.
2. Lightness of an image can range from *light* to *dark* and is used to separate it from color.
3. Contrast can be represented by the global and local differences in lightness and chromaticity within the image.
4. Sharpness of an image describes the clarity of fine details and definition of edges.
5. Artifacts can degrade the quality of an image if they are detectable.

1.3 Image Denoising Algorithms

In this section, all the major categories of IDAs have been discussed. Most of the existing IDAs equally consider noise and image edges as high frequency contents and smooth the edges during

image denoising process. All the existing IDAs are grouped in two broad categories: spatial domain denoising and transform domain denoising. The spatial domain denoising algorithms can be further subdivided in linear and non-linear IDAs. The images are not so effectively denoised by linear IDAs due to their wide-band spectrum similarity. Non-linear IDAs can overcomes this drawback of linear approaches.

The induced noise in an image is of additive nature during the image acquisitions and transmissions process. The actual degradation of the noisy image is vary depending on the type of noise induced in the image. An IDA must be chosen as per the percentage of image quality degradation as well as noise type. The traditional algorithms of noise reduction include Non-Local Mean (NLM) filter, Total Variation (TV) method and non-linear shrinkage models in different version of wavelet transforms. DWT, UDWT and DT-CWT are the efficient transforms for IDAs in the image processing literature (Buades et al. 2005b).

Independent Component Analysis (ICA) is an important and is popular in IDAs based on data-adaptive transform. It is used for Gaussian and non-Gaussian noise distribution. It has a major drawback of computational cost as compared to wavelet based algorithms because a sliding window and required sample of noise free data is used. In most of situations, the noise free training data for an image is not available easily.

1.3.1 Image Denoising in Spatial Domain

In all the spatial domain IDAs, individual pixels of a noisy image have been operated directly. The main assumption in the real world is that a digital image has many uniform intensity regions and that mostly insignificant variations of intensity changes in these regions are due to the noise induced (Buades et al. 2005a). The local variance is important and estimated by window masks of size $m \times m$ pixels of the image. It is important to finalize the option of window size from which a local variance is estimated. It should at least 5×5 for better noise estimation but to ensure local image stationarity, it must also be small enough. The weighted average of values of a central point pixel and the neighborhood pixels of an image is achieved by all these algorithms for the purpose of image denoising (Eng and Ma 2001).

A variety of spatial filters that attempt to suppress noise without corrupting the significant features of the image have been developed over the years. Spatial domain filters are of two types: linear spatial filters and non-linear spatial filters. The linear filtering algorithms require the information about the noise and the original image frequency spectrum. Main examples of this type filters are mean filter and Wiener filter. The non-linear filtering algorithms reduce the noise without explicitly identifying the noise spectrum and the original image signal. Non-linear filters are widely used for additive noise reduction and edge detection. Basic examples are different type of median filter and bilateral filter.

1.3.1.1 Linear Image Denoising in Spatial Domain

A filtering method is linear when the output is a weighted sum of the input pixels. Most of the classical linear IDAs are based on the assumption that image processing applications in which both edge enhancement and noise reduction are mutually considered. A mean filter is a common class of spatial averaging filters of all equal weights (Thaipanich et al. 2010).

Another spatially-based image denoising filter more adaptive than the mean filter is Lee filter. Lee filter is a local statistics filter that employs local masks whose coefficients are functions of the local image and noise characteristics. Lee filter is expected to perform little or no smoothing near edges or high contrast texture regions and extra smoothing in the regions of the image.

Wiener filtering in spatial domain always gives optimal experimental results when the corruption of image is modeled as a Gaussian random process and the criteria of accuracy is the minimum MSE (Ozkan et al. 1992). Wiener filtering in spatial domain based on minimum MSE (MMSE) gives the much visually displeasing denoised images than the input original noisy images. It successfully reduces the MSE for low noise densities well.

One of the limitations of conventional linear filtering algorithms for image denoising is that they are based on the consideration that the image signal is stationary and formed through a linear process. They blur the sharp edges, disturb lines and fine details of an image (Yoo and Ahn 2014). The main drawback of the Wiener filter is that it considers the original image and noise as a globally stationary components that remain relatively constant throughout the image.

1.3.1.2 Non-linear Image Denoising in Spatial Domain

A filtering method is non-linear when the output is not a weighted sum of the input pixels. All the non-linear filtering algorithms modify the each pixel value in a noisy image based on the returned value of a non-linear function. Non-linear spatial filters reduce the additive noise to a desired extent but at the cost of image blurring due to which the edges are not preserved in denoised image (Beghdadi and Khellaf 1997). In last two decade, a broad class of non-linear median type filtering algorithms has been developed to overcome the weaknesses of linear filters. Examples are weighted median, relaxed median filter *etc*.

A bilateral filtering is a non-linear image denoising filter with edge preserving. A weighted combination of the central pixel with relative location and the neighborhood pixels is achieved in the bilateral filtering. A pixel value may change dynamically until a convergence criterion is met in this filter.

1.3.2 Image Denoising in Transform Domain

Spatial domain IDAs reduce the noise to a reasonable extent but tend to blur sharp edges, destroy lines and other fine details of images. Transform domain algorithms overcome these problems due to their convolution property where the convolutions are transformed into multiplication of the spectrum. An image transform is a mathematical tool and may be used to apply to the image for its conversion from one domain to other domain.

Consider this equation to understand the image transformation:

$$G(x, y) = T\{I(x, y)\} \tag{1.15}$$

where, $I(x, y)$ is input image for transformation, $G(x, y)$ is output image after transformation, and T is the transformation function for image decomposition.

1.3.2.1 Image Denoising in Frequency Spatial Domain

Frequency domain IDAs are another way of approaching image restoration and image enhancement. It overcomes the main difficulties associated with the spatial domain image filtering algorithms. Their computational complexity involved in performing the convolution well with solving the deconvolution problem. As the noises occupy a higher region of frequency spectrum, then a low-pass filtering is preferred for image denoising in frequency domain. Fourier convolution property can overcome these problems using frequency domain algorithms where convolution is transformed into multiplication of the spectra (Oktem and Ponomarenko 2007). A frequency-based denoising algorithm often adopt some form of low-pass filtering to suppress most of the high frequency components since most of the energy of a typical image is concentrated in the low frequency range and the energy of noise is often spread across all frequency components (white noise). These IDAs are mainly under two groups: Discrete Fourier transform (DFT) based IDAs and Discrete Cosine Transform (DCT) based IDAs.

DFT based Algorithms: DFT has a major role in most of the image processing operations. Fast Fourier Transform (FFT) speeds up DFT of $O(N^2)$ operations by computing it using $O(Nlog_2N)$ operations. Image denoising may be achieved in the transform domain by first computing DFT or FFT to achieve its transform domain values for modifications and then applying an inverse transform to get the recovered image.

DCT based Algorithms: produces a finite sequence of cosine functions sum oscillating at different frequencies (Foi et al. 2007). DCTs are mainly used in different image processing operations like lossy compression and image denoising where small number of high-frequency elements can be rejected. The use of cosine function in place of sine functions is necessary for image compression and denoising, since it described that a small amount of cosine functions are required to approximate a typical noisy image, whereas the cosines represent a particular choice of boundary conditions for differential equations.

However, this approach is generally not effective because it involves suppressing two distinct types of high frequency components that are randomly mixed within the noisy images. On the one hand, visible edges, which are the significant features of an image from a human viewing perspective, are represented by desirable high-frequency components in the power spectrum of an image.

On the other hand, noise is also modeled as high frequency data, representing the undesirable high frequency component that one seeks to eliminate or suppress. Thus, it becomes difficult to suppress the noise without also causing some degree of degradation of the significant features of the image. Consequently, most of the generic frequency-based IDAs often result in over-smoothened denoised images where the edges and other high-frequency fine details of the noisy image have been blurred.

1.3.2.2 Image Denoising in Wavelet Domain

The computation of frequency domain IDAs is slow and the results are not good in preserving the edges of an image. This section discusses the fundamental basics of wavelet and its features. It is an oscillatory form of time-limited vanishing wave. A wavelet is a mathematical tool with different vanishing moments used in digital image processing operations. Its principles are similar to those of Fourier analysis. Many researchers have started image compression and image denoising using wavelets.

The different version of wavelet families can be linked to several works in this research area, starting by Haar in 1909 with the first wavelet. Grossmann and Morlet (Grossmann et al. 1989) have proposed the formulations of continuous wavelet transform. The orthogonal wavelets with compact support is given by Ingrid Daubechies and Stéphane Mallat who proposed an implementation algorithm for the filter-bank of DWT.

The image structural information are finalized by using the mother wavelet with different scales and translations. It is allowed to change the size of window freely in the particularity of wavelet analysis *i.e.* to make it suitable analysis function for the required resolution. All the sudden changes for high resolution in time-frequency domain analysis are captured by using a the mother wavelet special version in high resolution in time-frequency domain analysis (Bacchelli and Papi 2004).

From last two decades, image processing operations using applied mathematical tools have been developed by researchers. DWT poses a powerful wavelet based tool for the multi-scale representation and analysis of images (Donoho et al. 1996). These mathematical tools are the advance generation of the traditional Fourier transform techniques as they localize the image information in time-frequency plane (Lin and Lingfu 2009). DWT has the ability of trading the resolution from one type to an-

other, which makes them especially suitable for the image denoising and compression (Hosseini et al. 2016). When orthogonal wavelets are used with periodic boundary conditions, the orthogonality of DWT leads to ensure that AWGN is transformed into equally distributed (white) noise in wavelet coefficients.

The IDAs in time-frequency domain is sub-divided as per the choice of basis functions. These basis functions may be a data adaptive and non-adaptive used in time-frequency domain filtering.

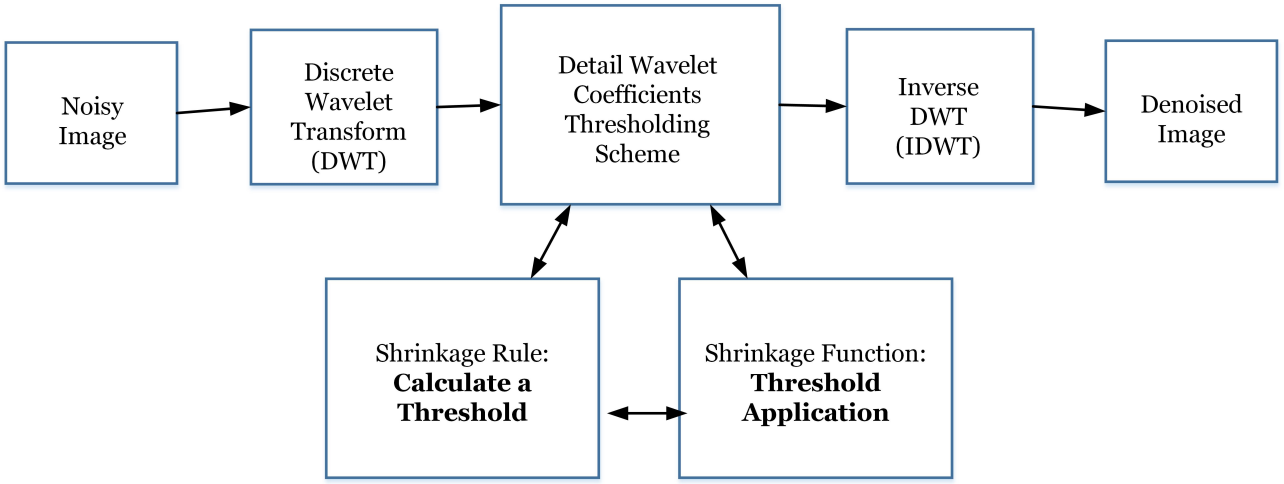

Figure 1.6: Image Denoising using Wavelets

The localization property of wavelets in space and scale makes them suitable for spatial adaptive methodology (Nandal and Kumar 2018). Wavelet-based IDAs as shown in Figure 1.6 are the popular state-of-the-art in image denoising methodologies, both in forms of performance and computational efficiency. A simple IDA based on DWT is achieved as shown in Figure 1.6 and details description is given ahead.

- **DWT of Noisy Image:** These two things are finalized before proceeding DWT of noisy image:

  i) Choice of a wavelet function (*e.g.* Daubechies, coiflets *etc.*) and

  ii) Number of levels for the wavelet decomposition.

The *mother* wavelet should be selected carefully to better approximate and capture the transient changes of the noisy image. The mother wavelet selection choice can be based on eyeball inspection of the structural details of an image, or it can be finalized based on correlation between the image

of interest and required output image. The selection of mother wavelet may be based on the spatial correlation of the image information (Krishnamoorthi 2007). DWT is a highly successful technique of image decomposition, as it separates image and AWGN in the wavelet domain effectively (Hedaoo and Godbole 2011). Their special features make them to be more suitable in visual information processing. It is an important feature that makes the separation of image from noise in wavelet domain.

The wavelet function may not necessarily be best adapted to an underlying image complexity. When an image includes more complex structures with fine details, it becomes necessary to adaptively select an appropriate best basis which provides the best image estimate upon thresholding the noisy coefficients (Thakur 2013). The efficiency of a wavelet basis to handle the complex structures of an image is according to its symmetry and regularity properties. These properties are well fulfilled by orthogonal and compactly supported wavelets like Daubechies, Symlets and Coiflets families. A search of best basis in the wavelet families are analyzed (Weyrich and Warhola 1998).

The localization property of wavelets in space and scale makes them suitable for adaptive approaches (Abramovich and Benjamini 1996, Banham and Katsaggelos 1996). DWT decomposes the noisy images into four sub-images of different spatial domain and independent frequency domain. DWT separates image signal and noise signal in the wavelet domain effectively using the sparsity property. DWT maps AWGN of the image into the white noise in the transform domain (Abramovich and Benjamini 1996, Dengwen and Wengang 2008). Before computation of DWT of the noisy image, one must finalize the type of selected wavelet and level of decomposition. There is no universal wavelet basis which suites all types of the image complex structures (Hassan and Saparon 2011).

DWT is achieved by selecting a wavelet type with suitable vanishing moments using different decomposition levels. The maximum decomposition levels to apply DWT depend on how many pixels contain in a given image (Radi et al. 2011). Generally, the denoised image from the lower noise density have higher SNR than that of the higher noise density. So more DWT decomposition levels are needed for reducing the most of noise in a high density noisy image (Luo 2006). After that only the severe noise exist in the wavelet coefficients.

IDAs using DWT can be subdivided into four categories: linear IDAs, non-linear IDAs, non-

orthogonal IDAs and wavelet coefficient model based IDAs. Linear IDA like Wiener filtering in wavelet domain performs better for low noise densities but not at higher. The non-linear wavelet coefficients thresholding is mostly used in wavelet based IDAs. The statistical modeling of wavelet coefficients is also used to achieve the better results with preserving the fine details of an image. The non-orthogonal wavelet transform overcome the pitfalls of orthogonal wavelet based IDAs (Khmag et al. 2015). They support the shift-invariant, directional selectivity and phases of edges **additional features** which are more necessary for high structural and color images. These features provide better subjective and objective results for color image denoising with color components preserving well.

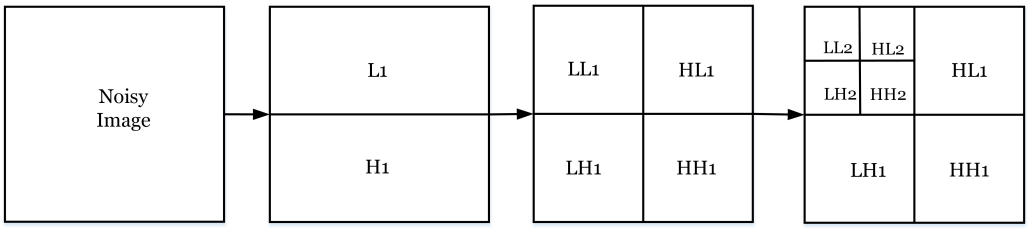

Figure 1.7: Two Levels of Wavelet Decomposition

The wavelet decomposition of a noisy image is achieved as follows: To apply wavelet decomposition of the input noisy image into four different subbands shown in Figure 1.8 with downsampling. If LL_j subband is used as an initial input, then LL_{j+1}, HL_{j+1}, LH_{j+1} and HH_{j+1}, $j = 1, 2, ..., J$, where j-th is the current decomposition level and J represents the largest decomposition level (Chaux et al. 2007). These subbands identify all constructive information of the noisy image. The approximation subband LL_{j+1} is achieved by low-pass filtering along the x and y axes. The HL_{j+1}, LH_{j+1} and HH_{j+1} subbands describe the horizontal, vertical and diagonal details of the image respectively. A significant amount of noise is contained by the highest subband HH_1 of first decomposition level. The LL_{j+1} subband can be repetitively decomposed to get the HL_{j+2}, LH_{j+2} and HH_{j+2} subbands (Hussain et al. 2015).

When using DWT, the translations of an image lead to different wavelet coefficients with downsampling. This problem can be overcome by providing a facility for more complete characteristic representation of an image with shift-invariant transformations such as the UDWT (Lang et al. 1996). Further enhancements can be achieved with spatially adaptive thresholding schemes which consolidate inter-scale and intra-scale dependencies. A proposal idea is concentrated to work out a new

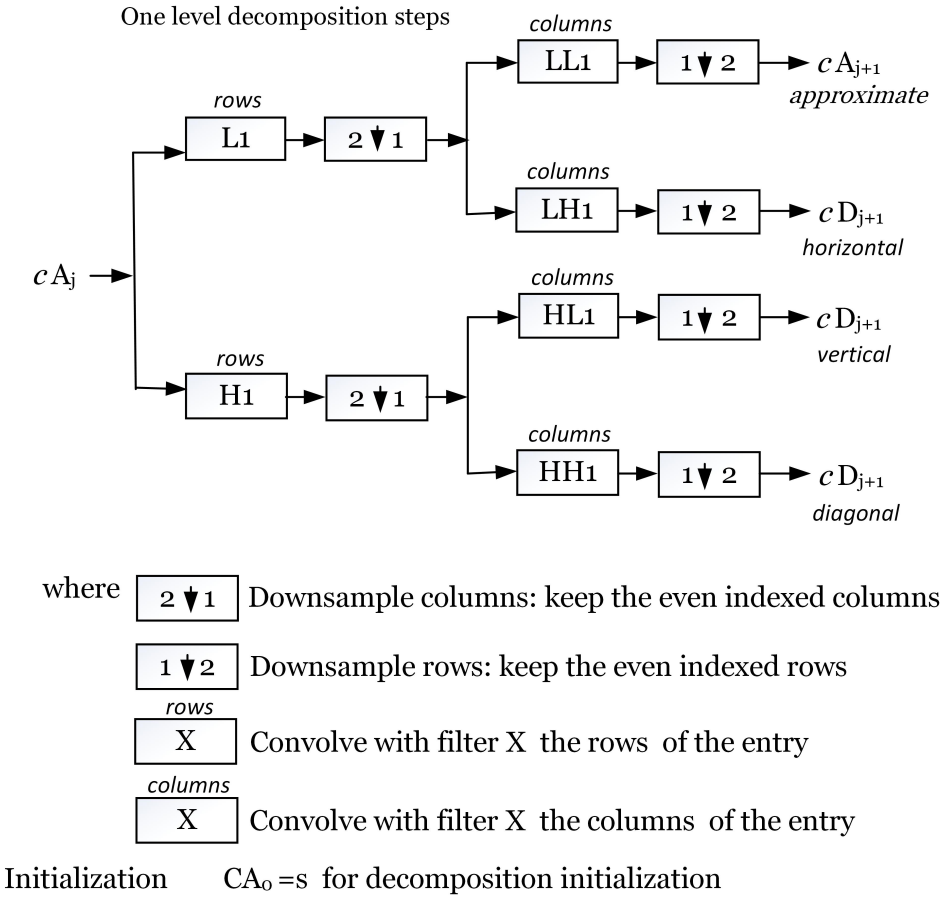

Figure 1.8: One level 2D DWT Wavelet Decomposition

IDA using UDWT coefficients thresholding based on the Bayesian estimator. The important property of UDWT is that it doesn't support decimation of the noisy images. It is not a limitation of today's scenario to require the larger storage space and more computations as needed by UDWT. This kind of redundant, translation-invariant transform is especially useful for denoising, which is one of the most important wavelet applications.

- **DWT Coefficients Thresholding:** After wavelet decomposition is performed on the noisy image, it is needed to do wavelet coefficients thresholding. Non-linear thresholding of forward transformed wavelet coefficients has two parameters and is achieved as:

  i) Shrinkage Rule: Estimation of a threshold value.

  ii) Shrinkage Function: Application of the threshold value to the details coefficients by hard or soft thresholding.

The shrinkage rule is how to calculate the threshold value, and shrinkage function is how to apply the calculated threshold value to the noisy DWT coefficients. Researchers published different thresholding schemes for the threshold estimation and its application to the decomposed wavelet coefficients.

Threshold Selection: The threshold value selection is called shrinkage rule. The selection of a suitable threshold value is the challenging issue of a wavelet-based image denoising methodologies (Banham and Katsaggelos 1996). The noisy coefficients are retained by selecting small threshold value and the fine details of images are smoothened by large threshold. The threshold value may be adaptive and non-adaptive approach across the wavelet scales and locations. The non-adaptive approach reveals a universal threshold initiated by Donoho and Johnstone (Donoho and Johnstone 1995) and an adaptive approach can give a level or subband adaptive threshold. This threshold value is estimated by using the noise standard deviation computed from the first diagonal subband as it has maximum noise density.

The single threshold for all the wavelet coefficients is called universal threshold given by Donoho and Johnstone. This threshold estimation criterion is known as VisuShrink (Donoho and Johnstone 1995). The same threshold value is used for all decomposition levels. The universal threshold is not

capable to differentiate the smooth (flat) and non-smooth (feature-based) region of the image and is applicable only when noise level is low.

An adaptive thresholding is also used by fixing the optimum thresholding value depending on the decomposition level. The wavelet coefficients spatial configuration can effectively classified the noise and image fine details under the high noise circumstance (Hawwar and Reza 2002, Pizurica 2002). The threshold value must be estimated adaptively based on scale and space of wavelet coefficients to preserve the important features of the image like edges. An adaptive threshold is computed by fixing the optimum noise standard deviation depending on the decomposition level and subbands. This threshold estimation scheme is called Bayesian estimator (Vidakovic 1998, Ho and Hwang 2013).

A popular and effective noise level was estimated by Donoho and Johnstone. This is calculated using median absolute deviation based on the details coefficients first decomposition level. Most of DWT based image denoising is achieved by choosing the optimal threshold value using a hybrid of any two threshold selection schemes like universal threshold and the Stein's Unbiased Risk Estimator (SURE) threshold and it gives better results than a single threshold like VISUShrink (Blu and Luisier 2007). VISUShrink is non-adaptive and depends on the noise densities and image local information (Donoho and Johnstone 1994). BayesShrink mainly minimizes Bayesian risk estimator function by considering generalized Gaussian prior and thus provides a data adaptive threshold. BayesShrink technique exceeds SUREShrink in most of the cases for different noise densities.

The selection of a suitable threshold value is a critical issue of a wavelet-based IDAs. The neighboring wavelet coefficients spatial configuration can provide better noise-image classifications under the high noise densities Bolster et al. (2003). The threshold value must be estimated adaptively based on scale and space of wavelet coefficients which is different for different region of image. The limit is selected such that satisfactory noise reduction with image features preserving is achieved. An orthogonal wavelet transform is applied to the noisy image with AWGN and the transformed image preserves the Gaussian nature of the noise.

An estimation of noise standard deviations using the median absolute value of high amplitudes wavelet coefficients. The optimal threshold value is calculated from the diagonal subband (HH_1) of first decomposition level and is applied for all desired levels (Cho et al. 2009). The noise standard

deviation is calculated by

$$\hat{\sigma}_n = \frac{median(|HH_1|)}{0.6745}. \tag{1.16}$$

where $\hat{\sigma}_n$ is the estimated noise standard deviation. The scale factor in denominator is according to the distribution of $|HH_1|$, and is equal to 0.6745 for a Gaussian distributed data (Donoho 1995).

This noise standard deviation is the basis for each type of threshold calculation. Universal or global threshold is also the optimal threshold value and minimizes the cost function of the differences (Donoho and Johnstone 1994) which is given by:

$$\delta_u = \hat{\sigma}_n \sqrt{2logM} \tag{1.17}$$

An adaptive threshold value may be calculated by using the local information of an image. There are many approaches for threshold selection under the adaptive or spatially adaptive criteria.

Threshold Application: The threshold application is called shrinkage function. In DWT domain, the AWGN is uniformly spread throughout the coefficients, while most of the image information are concentrated in few significant coefficients (Bolster et al. 2003). Therefore, one straightforward way of distinguishing information from noise in the wavelet domain is to threshold the wavelet coefficients. The application of threshold to the wavelet transformed coefficients is known as thresholding (Abramovich and Benjamini 1996, Azzalini et al. 2005). Two types of thresholding scheme used in literature are: *hard* thresholding and, soft thresholding.

The hard thresholding is a scheme used to keep or kill the coefficients. It removes the small wavelet coefficients while others are left untouched and is described mathematically in equation (1.18). In this way some artifacts in the images are generated due to the unsuccessful attempts of reducing large noise coefficients. The hard thresholding demerits are overcome/removed by soft thresholding. In this type of thresholding scheme, the wavelet coefficients smaller than the threshold value are removed while larger coefficients are shrunk by the actual value of the threshold itself. This type of thresholding follows the keep or shrink rule which is explained mathematically in equation (1.19).

$$T_{hard}(w) = \begin{cases} w & \text{if } |w| > T \\ 0 & \text{otherwise} \end{cases} \tag{1.18}$$

$$T_{soft}(w) = \begin{cases} sign(w)(w-t) & \text{if } |w| > T \\ 0 & \text{otherwise} \end{cases} \tag{1.19}$$

As the soft thresholding scheme is continuous so it provides better smoother results as compared to the hard thresholding scheme and also more visually pleasant denoised images. Hard thresholding preserves the edge better in comparison with the soft thresholding scheme but with artifacts. In most of the situations, it might be good to apply the soft thresholding to few decomposition level details, and the hard thresholding to the rest. The application of hard thresholding over-smoothen the images at discontinuity, due to which artifacts are reconstructed in denoised images.

Inverse DWT of Thresholded Coefficients: Denoised images are achieved by using IDWT of the modified (thresholded) wavelet coefficients. After trimming down the small wavelet coefficients, *i.e.* after removing the noisy wavelet coefficients from all the details subband coefficients, image reconstruction is performed using the same wavelet function type and version as used at the time of decomposition of the image. The image reconstruction is an exact reverse process of wavelet decomposition (Malfait and Roose 1997) by finding IDWT of thresholded wavelet coefficients. The additive low pass and high pass synthesis filters are used to sample the approximation and details coefficients through the same number of decomposition levels as used in DWT.

The *à-trous* algorithm and Beylkin's algorithm are used to compute UDWT of a noisy image (Bhonsle and Dewangan 2012). These two algorithms proceed in different ways for the noisy image decomposition. The UDWT reconstruction of approximation coefficients and details coefficients from the thresholded wavelet coefficients of the noisy image is achieved in the same way as traditional DWT (Wang et al. 2010). In this way, up-sampling is discarded as in the traditional DWT but are instead retained with a redundancy.

The DT-CWT generates a set of real and imaginary parts of complex wavelet coefficients by us-

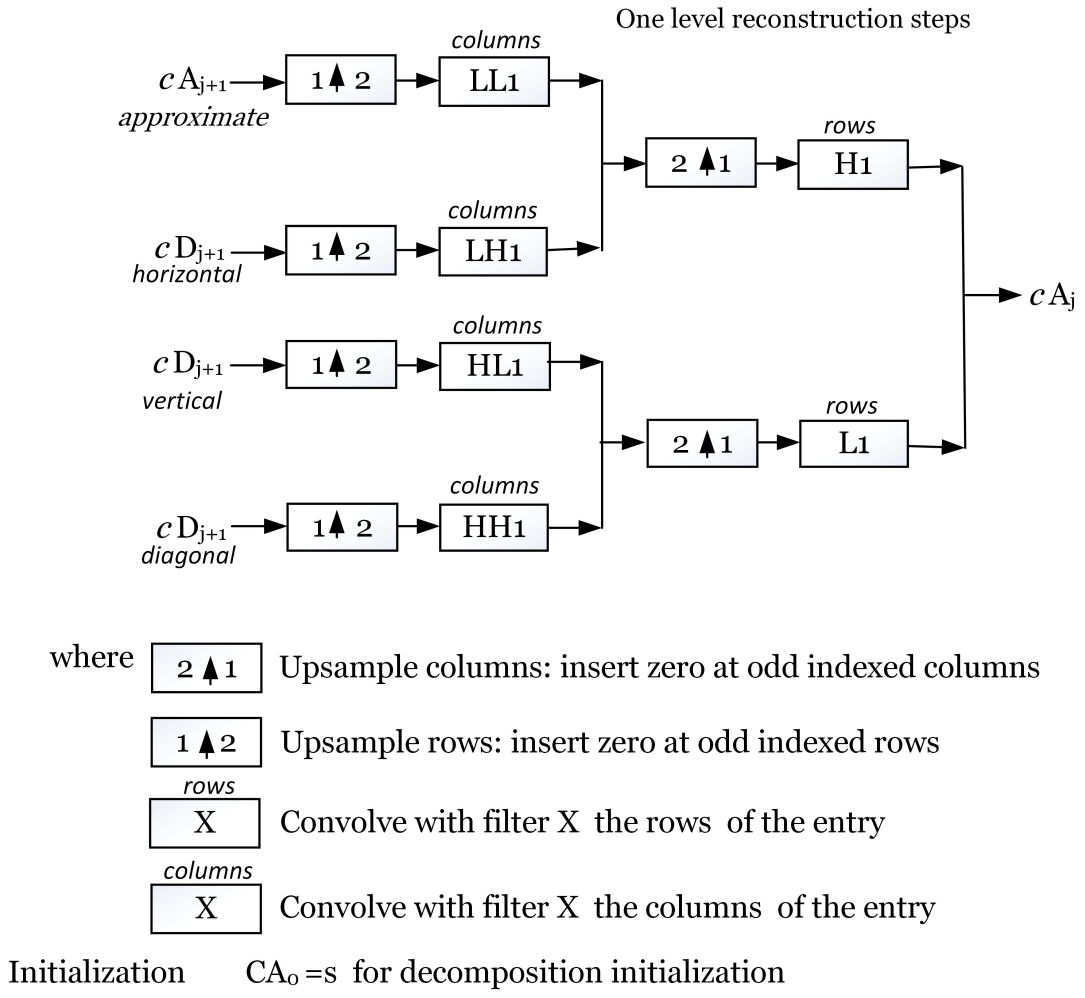

Figure 1.9: One-level 2D DWT Wavelet Reconstruction

ing a dual tree of real wavelet bank filters (Kumar et al. 2014).The reconstruction of CWT may be achieved in many ways. DT-CWT presents the perfect reconstruction properties and better computational efficiency by avoiding the extra redundancies.

The UDWT decomposes a noisy image into low-pass scaling coefficients approximation and high-pass wavelet details coefficients just like standard DWT but without down-sampling (Wang et al. 2010). The approximation subband of a decomposition level is used to compute the next level of scaling and wavelet coefficients. The down-sampling of wavelet coefficients is not discarded through decimation as in the traditional DWT but are instead retained with a redundancy. This type of wavelet transformation is better representation for noisy images with more wavelet coefficients, as the AWGN is spread over a small number of neighboring coefficients. UDWT is computed by two main algo-

rithms in the literature either by *à-trous* algorithm or by Beylkin's algorithm (Bhonsle and Dewangan 2012). These two algorithms proceed in different ways for the noisy image decomposition.

Kingsbury introduced a very elegant computational framework in wavelet domain that is known as DT-CWT (Kumar et al. 2014). Dt-CWT displays near-shift invariant properties and is more efficient tool for image denoising. It generates the real and imaginary parts of complex wavelet coefficients by using a dual-tree of real wavelet filters. A limited amount of redundancy is achieved by this method and also shift-invariance and directionally selectivity is achieved by the approximation filters. DT-CWT recovers the perfect reconstruction properties and computational efficiency. After the DT-CWT is performed on the noisy image, it is needed to do wavelet coefficients thresholding. The threshold is calculated using Bayesian estimator from the real part of DT-CWT.

1.4 Thesis Contribution

Chapter 1: This Chapter is introductory in nature and contains the noise models with their mathematical description and key foundation approaches from which image denoising evolved. Further, it analyzes the threshold selection criteria and its application for different image complexities. The Chapter discusses with image features preserving challenges, research contributions, and the organization of research work in different chapters.

Chapter 2: This Chapter provides the in-depth literature survey of existing IDAs. Firstly, a diagrammatic representation of the entire IDAs with their categorization and inter-relationship is given in year-wise sequence. Then the critical overview of each IDAs are given with their achievements and off-shorts. The gaps in the research image denoising and objectives to be achieved are covered in this chapter.

Chapter 3: In this Chapter, an adaptive image denoising with edge preserving using wavelets is proposed for grayscale and color images. The noisy image is decomposed using an appropriate wavelet type with vanishing moments. Then threshold value is calculated from the noise standard deviation of diagonal details subband by using the Bayesian estimator. As the edges of an image have less effect of noise than the flatten regions, a lower or reduced threshold value is applied on edge

region so that they can be avoided from over-smoothen. These threshold values are used to denoise the transformed image using soft thresholding. This Chapter also presents a comparison of the proposed algorithm with state-of-the-art existing IDAs.

Chapter 4: This Chapter contains an efficient edge preserving IDA using morphological operations in wavelets domain. In traditional DWT based image denoising, the image edges got-smoothen. In proposed IDA, morphological opening and closing are used to enhance the over-smoothened edges. The Chapter presents a comparison of the proposed algorithm with traditional wavelet based IDAs by PSNR values and denoised images for different noise densities in grayscale and color images.

Chapter 5: An adaptive and effective IDA using UDWT is proposed in this Chapter. The traditional DWT has lack of shift-invariance and directional selectivity due to which edges of an image are not handled properly. These lacks of standard DWT are covered by Undecimated DWT which has features of shift-invariant and direction selectivity. The efficiency of an IDA is improved by detecting the edge location and orientation using UDWT and then preserving them. The better results are achieved by hybrid thresholding scheme for different noise intensities. The experimental results of the proposed IDA is compared with traditional DWT based IDA and bilateral filtering in wavelet domain by PSNR values and visual perception.

Chapter 6: An edge preserving image denoising using DDT-CWT is proposed in this Chapter. The features of double-density and dual-tree are combinely used here to enhance the efficiency of proposed IDA. The pre-processing of noisy image before applying DDT-CWT based image denoising is preserving the image features more adaptively. The objective and subjective comparison of Wiener filtering in wavelet domain, traditional DT-CWT based IDA and a proposed IDA using DDT-CWT are presented for grayscale and color images.

Chapter 7: Conclusions and future scopes are discussed in this chapter so that in future research can be carried out in this area.

Chapter 2

Literature Survey

2.1 Introduction

The main objective of this Chapter is to study various existing standard IDAs, that are developed by researchers along with its relevant and recent applications. The literature survey of different IDAs is discussed here with their merits and limitations to achieve further improvement and enhancement. There are many IDAs originated from various mathematical disciplines such as linear and non-linear filtering, statistical modeling, probability theory, Partial Differential Equations (PDE), spectral and multiresolution analysis using wavelets *etc*. All the existing IDAs have been categorized into two groups: IDAs in spatial domain and IDAs in transform domain as shown in Figure 2.1.

2.2 Image Denoising Algorithms in Spatial Domain

In spatial domain, a neighborhood operation with pixels of a noisy image are operated directly. The magnitude of any required pixel of an output denoised image is computed by applying some denoising algorithms to the neighborhood pixel values of the input image. The spatial domain filtering may be linear and non-linear spatial filters (Beghdadi and Khellaf 1997).

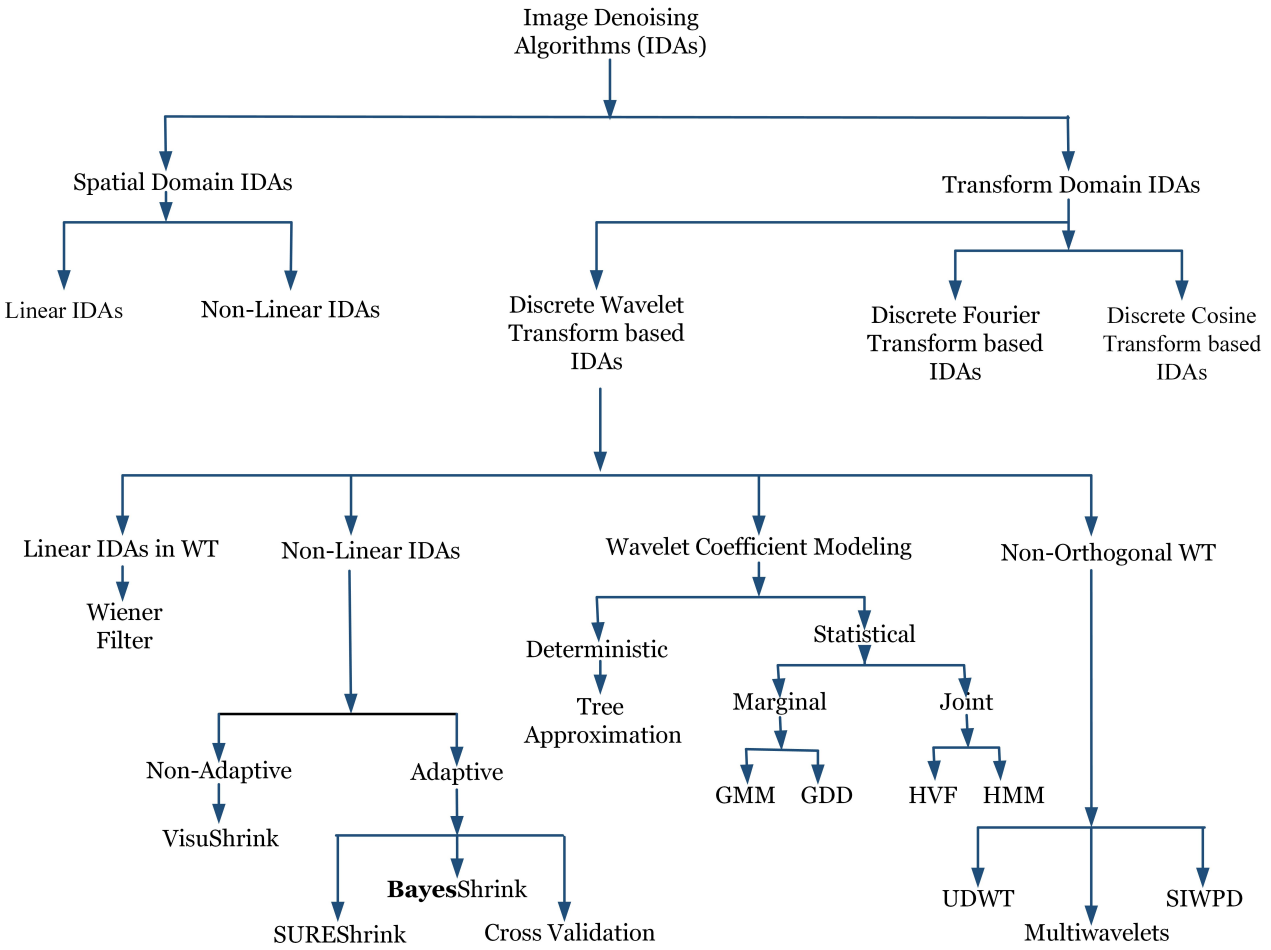

Figure 2.1: Tree structure of IDAs

2.2.1 Linear IDAs in Spatial Domain

The linear IDAs in spatial domain use the low-pass filters for noise reduction. The linear image filtering algorithms require the information about noise spectrum and original image spectrum in advance. Examples are: mean filtering and Wiener filtering.

Rank and Unbehauen (1992) proposed an edge preserving iterative low-pass filter for image denoising degraded by both Gaussian and non-Gaussian noise. A computationally efficient Wiener filtering for denoising an image by using N×N matrices by a cross-correlated multi-frame Wiener filter is achieved by Ozkan et al. (1992). Oten and de Figueiredo (2004) presented a fast adaptive alpha-trimmed mean filtering algorithm with optimal parameter α for images corrupted by AWGN.

Many a adaptive IDAs based on the NLM are investigated by many researchers. Buades et al. (2005b) proposed an efficient image denoising method at the crossing of functional analysis and

statistics using NLM algorithm based on asymmetrically optimal using a generic statistical image model. Brox et al. (2008) achieved a fast IDA using NLM filtering based on the arrangement of similar patches data of noisy image in a cluster tree. Efficient algorithm for image denoising based on Principal Component Analysis (PCA) in conjunction with the NLM using image neighborhood similarity weights is presented by Tasdizen (2009). Thaipanich et al. (2010) presented an adaptive IDA based on block classification in noisy images using method of Singular Value Decomposition (SVD) and clustering of the K-means.

A robust and iterative IDA for impulsive noise based on the set of patches of pixels in a noisy images as a union of low dimensional subspaces is proposed by Rehman and Wang (2011). Wiener filter based image denoising is enhanced by Chatterjee and Milanfar (2012) by using a geometrically and photometrically similar patch-based approach. Raghuvanshi et al. (2013) presented an efficient algorithm for image denoising based on NLM approach using the concept of self-similarity in the noisy image. Yoo and Ahn (2014) performed a blind-Wiener filter to denoise the noisy images with MMSE between restored image and the original image.

Verma and Pandey (2017) proposed an IDA by selecting a search window of optimal size for each pixel using the search region variance in the denoised images. Routray et al. (2018) presented an efficient hybrid denoising algorithm for gray image based on Support Vector Machine (SVM) classification designed and developed by a large number of overlapping patches followed by extraction of local features from each patches using scale invariant feature transform.

All linear filtering in spatial domain over-smoothen the fine details like edges of the noisy images and induced some artifacts in the denoised images. To overcome the weakness of linear filtering in spatial domain, non-linear filtering based IDAs are proposed by many researchers with better subjective and objective results.

2.2.2 Non-linear IDAs in Spatial Domain

The non-linear filters can reduce the additive noise without any attempts to explicitly identify the noise spectrum and original image spectrum. The popular non-linear filters are weighted median and rank-conditioned rank-selection *etc.*

Hamza and Krim (2001) provided an optimal non-linear filtering algorithm based on the robust estimation theory for Gaussian and heavy-tailed noise. An edge preserving non-linear IDA based on Bayesian formulation of edge stopping or diffusivity function under a marginal prior on noise-free gradient is presented by Pizurica et al. (2006). Chan and Chen (2006) performed an IDA based on patch-detection idea using fast multilevel method through an improved primal relaxations for the TV.

An efficient and adaptive bilateral filter based on the optimal unsharp mask for image noise reduction with enhancing edges and textures is presented by Zhang and Allebach (2008). Dabov et al. (2009) performed an efficient IDA using non-local image modeling, PCA and local shape-adaptive anisotropic estimation.

Liao et al. (2010) presented an adaptive edge preserving IDA by determining the stationary neighborhoods of the current pixel automatically using a non-linear time series observations. Bhujle and Chaudhuri (2014) proposed a fast IDA based on NLM filter using a dictionary for image edge patches as against to intensity patches of reducing the dictionary size. Meher and Singhawat (2014) achieved an improved and adaptive median filter for image denoising for impulse noise of higher density by replacing the current pixel value with current working window noise-free pixels and previously processed noisy pixels.

Rafsanjani et al. (2017) presented an algorithm for edge preserving image denoising based on adaptive selection of diffusion coefficient using the residual local power and the amount of the gradient magnitude. They also extended their work in the same year based on classical Perona-Malik diffusion coefficient using Perona-Malik flux for regions where the gradient magnitude is higher than smoothing threshold to avoid the undesirable blurring effect and edge displacement using the gradient magnitude as per threshold required.

After going the literature in-depth, it has been noted that spatial domain filtering based IDAs have some weaknesses and deficiencies. These IDAs disturb the sharp edges, lines and fine details of an image and perform weakly in the denoising of signal-dependent noise. Generally, non-linear spatial domain filters reduce the noise to a large extent but at the cost of image blurring due to which the edges get less visible in denoised images. To reduce their computational cost and quality enhancement, the researchers developed efficient IDAs in wavelet transform domain.

2.3 Image Denoising Algorithms in Wavelet Domain

Donoho and Johnstone presented the wavelet based denoising scheme to avoid the weakness of non-linear spatial domain filtering (Donoho and Johnstone 1994, Donoho 1995). The continuous wavelet transform is an alternative to Fourier transform of sinusoidal waves using a family function created by translations and dilatations of a mother wavelet. A spatial-frequency decomposition by wavelet transform gives more flexible multiresolution analysis of the images. From a decade, researchers have developed powerful wavelet based algorithms in applied mathematics and image processing for the multi-scale representation and analysis of images (Zhang and Desai 1998). These tools localize the information in the time-frequency plane differing from the domain provided by DFT and DCT. DWTs are capable to represent the resolution of one type to the other making them especially suitable for the image analysis.

2.3.1 Linear IDAs in Wavelet Domain

Linear filters like Wiener filter in wavelet domain produce an optimal result when the image is corrupted with AWGN. DWT of a noisy image produces one approximation subband and three details subbands. Wiener filter is applied on all the details subbands only and denoised image is reconstructed by applying the IDWT to approximation subband and filtered details subbands.

You and Crebbin (1995) proposed three algorithms namely the adaptive mean p-median filter, the minimum-maximum algorithm for reducing outlier noise and a robust adaptive mean p-median filter for restoring images corrupted by AWGN. Jansen and Bultheel (2001) investigated the IDA using wavelet-thresholding based on an optimal threshold without knowing the noise variance of the image. Zhang and Bao (2003) performed an efficient IDA using wavelet-based Linear MMSE (LMMSE) estimation based on a strong wavelet inter-scale dependencies in over-complete wavelet expansion.

Jin et al. (2003) achieved a Wiener filtering of noisy image and its sequences adaptively in the wavelet domain based on an adaptive weighted averaging technique to find the second-order statistics. Ray and Mallick (2003) developed a Bayesian estimator in wavelet shrinkage based on the linear model power transformation to represent a wide class of noise models common in medical imaging.

Lee and Rhee (2005) proposed an algorithm for image denoising based on the linear constrained filtering of least squares and thresholding scheme in DWT domain for AWGN. Shui (2005) performed an image denoising in wavelet domain using a full local Wiener filtering for low noise complexity based on the elliptic directional windows for different oriented subbands.

Blu and Luisier (2007) achieved a fast and efficient IDA using the image-domain based minimum estimate of the MSE-SURE based on the denoising procedure expressed as Linear Expansion of Thresholds (LET). Pragada and Sivaswamy (2008) presented an IDA for AWGN based on image-matched biorthogonal wavelet bases for natural, satellite and medical images. An efficient IDA based on the NLM with multiresolution Wiener filtering using the extensive self-similarity of natural images is proposed by Lin and Lingfu (2009). Yang et al. (2010) proposed a feature-preserving IDA based on NLM approach using Haar-like feature extraction in identifying weak particles. Verd-Monedero et al. (2011) proposed an adaptive grayscale IDA based on spatially variant dilation or erosion and opening or closing using diffusion process of the average square gradient field.

An edge preserving medical IDA using a Generalized Gaussian Mixture (GGM) model with edge information for modeling the noisy medical images is proposed by Cong-Hua *et al*. (2014). Bao *et al*. (2014) developed an efficient edge preserving strong image smoothing for high-contrast details using weighted-average filter by viewing pixel affinity in a probabilistic framework simultaneously.

Feng et al. (2014) presented an adaptive switching morphological filter for removing fixed-value impulse noise by identifies noise pixels using the two-stage morphological noise detector. Zhu et al. (2014) proposed an improved IDA using weak textured patches based single image noise estimation of input noisy image and two-stage NLM with adaptive smoothing parameter.

Shikkenawis et al. (2015) achieved an improved IDA based on the criteria of epitome using orthogonal locality preserving projection basis.

Linear IDAs in wavelet domain could be effective for slowly varying noises like speckle noise only, but not for rapidly varying noises. The non-linear wavelet thresholding is effective to denoise rapidly varying noisy images.

2.3.2 Non-linear IDAs in Wavelet Domain

The non-linear coefficient thresholding IDAs are perhaps maximum investigated domain in image denoising literature using DWT. After applying a selected DWT to a noisy image, two main parameters are utilized here: shrinkage rule and shrinkage function. The shrinkage rule calculates the threshold value from the noisy image data and shrinkage function applies the calculated threshold value to the noisy image data. Researchers have published different techniques to estimate the parameters for wavelet coefficients thresholding scheme and its application to various type of noises in a digital images (Dengwen and Wengang 2008).

In DWT representation, maximum image information with fine details are concentrated in few noteworthy coefficients and AWGN spreads throughout the wavelet coefficients uniformly. One straightforward scheme of separating the image information from AWGN in the wavelet domain is thresholding of DWT coefficients by a suitable threshold value. The selection of a suitable threshold value for all requirements is not finalized upto now for a wavelet-based IDA (Jung and Schacanski 2001). The unique threshold for all the wavelet coefficients is called universal threshold. The universal threshold is not capable to differentiate all the regions of an image *i.e.* the smooth (flat) and non-smooth (feature-based) region of the image and is applicable only when noise level is low. For a high noise densities of AWGN, the spatial local configuration and information of neighboring wavelet coefficients must be considered for noise-image classification. The threshold must be estimated adaptively based on scale and space of wavelet coefficients which is different for different region of image. All the important features and color components of the images may be preserved in this way. Various wavelet coefficients threshold techniques such as SUREShrink, VisuShrink and BayeShrink are explored by many researchers after Donoho and Johnstone (Donoho and Johnstone 1994) and the search towards a better one for image denoising is always continue.

The application of threshold to the wavelet transformed coefficients is known as thresholding (Donoho 1995). The hard thresholding or soft thresholding are mainly used in the literature. Hard thresholding follows the keep or kill trend and soft thresholding follows the keep or shrunk trend. A hybrid thresholding has also been applied in the literature Zhang and Feng (2014).

A non-linear spatial adaptive IDA using wavelet reconstruction of modified wavelet coefficients

based on the risk estimator is proposed by many researchers. Donoho (1995), Donoho et al. (1996) presented an IDA for reconstructing an unknown function on [0, 1] from noisy data with *i.i.d.* standard Gaussian random variables presented in Donoho (1995).

A spatially adaptive IDA for the noisy images using the pre-filtering through the least squares filtering based on optimal choices for the regularization parameter in wavelet domain is performed by Banham and Katsaggelos (1996). Abramovich and Benjamini (1996) suggested the choice of first decomposition level to construct a thresholding procedure based on the false discovery rate approach for adaptively IDA. Nason (1996) presented the estimation of images from noisy image using wavelet coefficients thresholding by modified version of two-fold cross-validation. An efficient non-linear IDA based on the entropy concept is proposed by Beghdadi and Khellaf (1997) and compared the well-known median filter with a central weighted median filter.

An adaptive IDA using SURE based on a class of thresholding functions is presented by Zhang and Desai (1998). Vidakovic (1998) proposed an adaptive IDA using the shrinkage of DWT coefficients based on Bayesian hypothesis test. Weyrich and Warhola (1998) achieved an IDA based on generalized cross validation on modified wavelet reconstruction using the shrinkage parameter vector without prior knowledge of the noise variance.

Basu (2002) reviewed several linear and non-linear Gaussian based edge detection methods using the various features of Gaussian operator. Bacchelli and Papi (2004) proposed a non-linear filtering algorithm for image denoising using a piecewise quadratic and an exponential function of the choice of thresholding parameter instead of the classical Donoho and Johnstone's soft thresholding filter. An adaptive and patch-based algorithm is developed by Kervrann and Boulanger (2006) for image denoising and of noisy images representation using a fixed size small image patches in the variable neighborhood of each pixel.

Zhang and Allebach (2008) proposed an algorithm for edge preserving image denoising using the multiresolution bilateral filter applied to the lower subbands of a decomposed noisy image using filter banks of a wavelet. Cho et al. (2009) presented the efficiently comparison of NeighShrink, NeighSure and NeighLevel wavelet shrinkage algorithms with higher PSNR and have less visual artifacts compared to other algorithms. Montefusco et al. (2011) performed a fast and efficient IDA based on

the convergence of the resulting two-steps iterative scheme using adaptive non-linear filtering in an recursive framework.

The wavelet coefficient thresholding based IDAs perform for low and medium level noise intensities but don't provide satisfactory results for higher noise intensities. These non-linear algorithms don't avoid over-smoothening of edges, artifacts and staircase like components in the denoised image, so unable in preserving the all type of edges which is the main component of an image for real visual perception.

2.3.3 Image Denoising Algorithms using Wavelet Coefficients Modeling

The orthogonal transform domain IDAs can also be sub-divided according to modeling of wavelet coefficients. DWT coefficient modeling technique is based on close correlation of image local information at different resolution. The deterministic or statistical type of wavelet coefficients modeling are mainly used in wavelet domain. A tree structure representation is used to represent the wavelet coefficients by nodes in the deterministic models. Statistical approach focuses on multi-scale and local correlation between the wavelet coefficients Portilla et al. (2001).

Some other denoising algorithms use the Gaussian Mixture Model (GMM) and Hidden Markov Model (HMM). The noisy image standard deviations is estimated by a Maximum Likelihood (ML) or a Maximum-a-Posteriori (MAP) estimator for every subband within a small region where standard deviations is assumed practically constant. Many denoising algorithms evaluate the denoised images by an MMSE estimator through calculating the variances of noisy coefficients and of original image.

Moulin and Liu (1999) explored various relationship between shrinkage methods and MAP estimation based on Rissanen's universal prior on integers using the heavy-tailed GGD expressions for the shrinkage rules. A simple spatially adaptive statistical model inspired by Estimation-Quantization (EQ) coder for image DWT coefficients is applied for image denoising using MAP by Mihcak et al. (1999). Chang et al. (2000) proposed a spatially adaptive IDA using DWT coefficient's context modeling with an unknown parameter random variable in a GGD . They also presented an adaptive algorithm using data-driven threshold value in a Bayesian framework via wavelet soft-thresholding in the same year.

Jung and Schacanski (2001) performed an adaptive edge preserving IDA for natural and artificial noise based on image multiresolution decomposition using the shrinkage functions of consecutive resolution and geometric constrains. Prudyus et al. (2001) developed an algorithm for image denoising using a MAP estimation scheme using DWT based on a new class of *i.i.d.* stochastic image priors. Zervakis et al. (2001) presented an efficient and robust IDA for Gaussian noise and impulse mixed with Gaussian noise in wavelet domain.

Hawwar and Reza (2002) proposed an algorithm for edge preserving image denoising in the wavelet transform domain for multiplicative noise using the standard deviations of the details diagonal subband wavelet coefficients to decide whether to smooth or to preserve these coefficients. Scharcanski et al. (2002) presented an algorithm for edge preserving image denoising using homogeneous regions separated by well-defined edges based on image multiresolution decomposition by a DWT. An IDA based on emerged geometrical Bayesian framework in wavelet domain using magnitudes of DWT coefficient and their spreading near image edges across scales and spatial clustering is presented by Pizurica (2002). Faghih and Smith (2002) performed an edge preserving image denoising based on image edges detection using spatial and scale representation.

A spatial-correlation thresholding scheme for image denoising using DWT by multiplying two adjacent scales of DWT to enhance important image structures like edges and dilute noise based on a spatial-correlation function is achieved by Zhang and Bao (2003). Ranta et al. (2003) presented an efficient wavelet-based IDA by revisited and interpreted an iterative denoising algorithm. Spatially adaptive medical images denoising algorithm in wavelet domain using the correlation of significant image features across the adjacent scales based on the coefficients statistical distributed empirically estimation is proposed by Pizurica (2002). Ge and Mirchandani (2003) presented an algorithm for image denoising using details coefficients direct correlation across the adjacent scales for the significant coefficients selection.

An effective algorithm for image denoising based on the multi-scale character of DWT for the noisy impulse response of the blind system is proposed by Shiguo et al. (2004). Scheunders (2004) presented an IDA for multivalued images exploiting inter-band correlations based thresholding of wavelet coefficients product at adjacent scales and from different bands analytically. Xie et al. (2004)

explored a spatially adaptive algorithm for image denoising based on a model of doubly stochastic process in a closed form of DWT coefficient using Minimum Description Length (MDL) principle.

Balster et al. (2005) presented an efficient selective IDA using the threshold value based on their absolute value, spatial and multiresolution scales regularity. Coupier et al. (2005) performed an efficient IDA using morphological filters for impulse noise by reducing small connected components within level sets based on any local pattern through a Poisson approximation. Voloshynovskiy et al. (2005) developed an efficient IDA for AWGN using a image stochastic model in DWT domain based on local correlation in image statistics and on geometrical priors. Chen et al. (2005) proposed an algorithm for image denoising to reduce the AWGN using wavelet thresholding scheme for Translation-invariant (TI) and non-TI neighboring coefficients. Azzalini et al. (2005) presented an efficient non-linear thresholding of wavelet coefficients using the quasi-optimal value of the threshold for image denoising with isolated singularities based on the sample size and on the standard deviation of noise.

An efficient edge preserving IDA for impulse noise based on new operator using a hybrid filtering by grouping four Central Weighted Median (CWM) filtering using Adaptive Neuro-Fuzzy Inference System (ANFIS) is presented by Yüksel (2006). Lian et al. (2006) proposed an algorithm for image denoising based on strong inter-color dependency in the form of means similarity between different color components of high-frequency using difference space projection of an optimal luminance/color.

Hirakawa and Parks (2006) presented an effective edge preserving IDA for additive, multiplicative and mixed noise based on image patches of a linear combination from the noisy image using the uncertainties in the measured data of image in Total Least Square (TLS). A reconfigurable system using the statistical modeling of Daubechies' 9/7 biorthogonal wavelet coefficients is presented for denoising images by Joshi et al. (2006) based on neighbourhood observations of the lifting wavelet transform and the windowing technique.

Liu and Ma (2006) presented an algorithm for image denoising by combining edge detection with denoising in which wavelet coefficients of edges are found by a wavelet edge detection. Gnanadurai and Sadasivam (2006) performed an efficient and adaptive threshold selection approach for image denoising using DWT based on subband coefficients GGD modeling. Dabov et al. (2006) presented an efficient IDA based on effective 3-*D* transform filtering by grouping sliding-window transform and

block-matching by similar searching for blocks with high level of correlation. Wang and Zhou (2006) explored an effective medical IDA with edge preserving based on a combination of TV minimization scheme in wavelet domain. Rabbani and Vafadoost (2006) presented an algorithm for image denoising using DWT coefficients modeling within each subband with Laplace random variables mixture better able to capture the heavy-tailed nature of DWT coefficients.

An algorithm for image denoising based on an inter-scale orthonormal wavelet using a sum of unknown weights of elementary non-linear processes is proposed by Luisier et al. (2007). Li et al. (2007) presented an adaptive IDA with edge preserving based on ANFIS classifier for local texture region identification using the subband-adaptive BayesShrink threshold. Lazzaro and Montefusco (2007) achieved an improved algorithm for image denoising for AWGN based on both deterministic regularization methods and stochastic MAP estimations in wavelet domain using a functional minimization of the sum of data fidelity term and a regularization term.

Hel-Or and Shaked (2008) proposed a IDA to reduce the AWGN using a Mapping Functions (MFs) set used for DWT coefficients of noisy image. Chen and Lien (2008) explored an IDA with edge preserving to remove the salt-and-pepper noise from noisy images using an efficient detector for impulse noise to find the noisy pixels. Raphan and Simoncelli (2008) presented an IDA using the minimization of MSE in the subband domain in over-complete representations using an estimator to subbands redundant through spatial replication of basis function. Rajpoot et al. (2008) performed an edge preserving IDA using non-linear diffusion of multiple scales from a wide range of an orthogonal and bi-orthogonal filter banks.

Edoh and Roop (2009) presented an edge preserving adaptive multilevel IDA using the multiresolution properties of wavelet is applied to the TV model in $2D$ inner products of Daubechies wavelets. Yu et al. (2009) developed an efficient IDA for noisy image corrupted with AWGN by including a tri-variate shrinkage wavelet filter with a joint bilateral filtering by preserving image fine details with small computational cost. Hongqiao and Shengqian (2009) presented an effective IDA based on narrow relativity of details wavelet coefficients and comparison with Donoho's threshold for soft-thresholding. Sadeghipour et al. (2009) proposed an algorithm for edge preserving image denoising to reduce AWGN using statistical properties of the noise in redundant transform based on a distinct

threshold for each noisy coefficient representation.

Wang et al. (2010) developed an edge preserving IDA using Least Square SVM (LS-SVM) training model formed by the spatial regularity in wavelet domain based on the excellent classification of noisy DWT coefficients as well as noise-free ones. Nikpour and Hassanpour (2010) proposed an algorithm for image denoising based on anisotropic diffusion used for the approximation subband to recover the lack of existing wavelet thresholding schemes.

Hassan and Saparon (2011) achieved an IDA for AWGN based on DWT using suitability wavelet thresholding due to sparsity property of DWT and TV methods. Hedaoo and Godbole (2011) presented an algorithm for efficient image denoising to reduce AWGN based on Rissanen's MDL principle using BayesShrink on the wavelet coefficients of GGD higher order moments in image. Kalavathy and Suresh (2011) proposed an edge preserving IDA based on a statistical model depending on the magnitude of wavelet coefficients by fusing and noise variance for each coefficient in a subband using ML estimator or MAP estimator.

Kumar and Saini (2012) performed an efficient image denosing using thresholding scheme based on the wavelet coefficients neighboring with distinct threshold for all details subbands using GGD modeling of all subbands coefficients. Raokhande and Marathe (2012) presented an algorithm for efficient image denoising to reduce AWGN from noisy image by including a trivariate shrinkage wavelet filter using GGD modeling with statistical dependencies. Hui et al. (2013) developed an algorithm for efficient image denoising using a threshold and analyzed that hard thresholding scheme is not continuous as well as soft thresholding scheme provides constant deviations and derivative discontinuity defects. Ho and Hwang (2013) proposed an IDA using a Bayesian network of DWT coefficients of image using MAP estimator to derive the wavelet coefficients with certain wavelet properties.

Sahu and Dewangan (2014) performed a computationally efficient edge preserving IDA based on the selection of coefficients according to their magnitude with a spatially regular behavior and applied the lower threshold value to edge region and normal threshold value for smoothen region. Huang et al. (2014) proposed an efficient IDA using a narrative image decomposition framework based on self-learning from the recent sparse representation success using an over-complete dictionary from the

high spatial frequency components of the noisy image. Khmag et al. (2015) presented an efficient denoising algorithm for AWGN using the clustering based on moment invariants and HMM for pre-classification to capture the dependencies among noisy coefficients in the transform domain. Jain and Tyagi (2015) explored an edge preserving IDA using multiple decomposition levels of the noisy image based on arbitrary shaped local windows and adaptive thresholding scheme.

These IDAs present effective results for additive noise but their performance gets degraded near the edges where noise variance is not varied regularly. Although these algorithms are effective in image denoising, they produce salient artifacts like noises of low-frequency and edge ringing effect due to the used standard wavelet function type. These wavelet coefficients based IDAs do not avoid the deficiencies of DWT like shift-invariant and TI, which are mandatory to preserve the image edges and color components.

2.3.4 Image Denoising Algorithms using Non-orthogonal Wavelet Transform

The UDWT can overcome the limitations of traditional DWT. When an UDWT is used for decomposing the noisy image then it keeps away visual artifacts like pseudo-Gibbs phenomenon. Thus UDWT is more feasible for many applications of the digital image processing. Multiwavelet have important properties like short support, symmetry, and vanishing moments with higher orders. Many mother wavelet function are applied to noisy image in multiwavelet domain. The performance and efficiency of an IDA is enhanced by using the multiwavelets but further increase the computation complexity. The Shift Invariant Wavelet Packet Decomposition (SIWPD) is the extension of normal hard/soft thresholding to obtain total count of basis functions. Then the best basis function was explored using MDL principle.

Lang et al. (1996) proposed a non-linear algorithm for image denoising similar to Donoho and Johnstone thresholding using DWT, but obeying a proposal by Coifman with different shifts that significantly improved noise reduction. Malfait and Roose (1997) developed an algorithm that relies on smoothness of the image and geometrical constraints for the reduction of noise in an image via DWT using a Bayesian probabilistic formulation based on a Markov Random Field (MRF) model for image. Bui and Chen (1998) presented an algorithm for image denoising using non-TI multi-

wavelet thresholding by extending the Coifman and Donoho's TI single wavelet denoising algorithm to multiwavelets.

Pan et al. (1999) performed an improved spatially selective algorithm for image denoising using a thresholding scheme based on UDWT. Starck et al. (2002) proposed an algorithm for edge preserving image denoising using tree-based Bayesian posterior mean method based on curvelet transform followed by component step ridgelet transform to achieve subbands of curvelet by a *à-trous* wavelet filter banks.

Tessens et al. (2006) presented an IDA for AWGN decomposed using curvelet transform into noise correlated in single direction and decorrelated in the perpendicular direction based on curvelet coefficients statistical analysis through a separation among the coefficient of important image content and noisy coefficients. Ranganathan and Von Borries (2006) explored an IDA to reduce AWGN using localized ridgelet transform based on the projection of each piece with a certain angle followed by a $1D$ wavelet transform to generate the ridgelet coefficients. A new wavelet transform for effective image denoising using the lifting paradigm using the lifting steps of an unidimensional wavelet along a local orientation minimizing the prediction error is performed by Chappelier and Guillemot (2006).

Chaux et al. (2007) presented an efficient IDA to reduce AWGN using an accurate property of the covariance of the DT-CWT coefficients through cross correlations among the primal and dual wavelets in theoretical analysis. Luisier and Blu (2007) proposed an IDA to reduce AWGN based on an UDWT coefficients thresholding using of a linearly parameterized pointwise thresholding function optimizing the parameters globally by minimizing the SURE. Bo et al. (2007) developed an algorithm for image denoising using the DT-CWT into simple ridgelet transform through the hard coefficients thresholding scheme. Chen and Kégl (2007) explored an edge preserving IDA for AWGN using the approximate shift-invariance property of the DT-CWT and high directional sensitivity of the ridgelet transform. Dai et al. (2007) proposed an IDA for color image with high texture information based on complex contourlet transform with effectively approximate the shift-invariance property of DT-CWT and directionality and anisotropy of contourlet transform.

Miller and Kingsbury (2008) presented an algorithm for efficient edge preserving image denoising to reduce the AWGN using statistical modeling of the coefficients of a redundant and oriented com-

plex multi-scale transform based on an adaptive Bayesian model selection framework by avoiding ringing artifacts. Mohideen et al. (2008) provided a comparative analysis of IDAs for AWGN using the suitability of different wavelet and multiwavelet basis and a different neighborhood size on the performance of IDA in terms of PSNR values. Dengwen and Wengang (2008) proposed an improved IDA of NeighShrink in wavelet domain by determining an optimal threshold value and neighboring window size for each subband by SURE in redundant DT-CWT domain.

Easley et al. (2009) performed a shearlet formulation of an TV method for effective image denoising based on shearlets mathematically proven representation of distributed discontinuities of an image like edges better than traditional DWT. Wu et al. (2009) proposed an adaptive edge preserving IDA by combining the non-subsampled contourlet transform and TV model based on SURE using the linear adaptive threshold function in each subband to avoid the pseudo-Gibbs artifacts. Ouarti and Peyré (2009) presented an algorithm for adaptive edge preserving image denoising based on a best basis search algorithm in a non-stationary wavelet packet dictionary using optimized labeled quad-tree filters.

Bhonsle and Dewangan (2012) achieved a comparative study of image denoising based on DT-CWT and double-density CWT techniques by exploiting the advantages and dis-advantages of applications of proper uses. Mohideen (2012) proposed an algorithm for image denoising to reduce AWGN using expansive CWT based on NeighSUREShrink wavelet coefficients thresholding scheme achieved better results than DWT. Verma and Mathur (2012) presented an algorithm for image denoising to reduce AWGN using multi-scale LMMSE estimation scheme based on UDWT applied to the image using two wavelet filters and generate two wavelet transformed images for each filter.

Liu et al. (2014) proposed a real-time image denoising using semi-soft shrinkage denoising algorithm using lifting wavelet transform to minimize computational complexity and hyperbolic threshold selection. Mahalakshmi and Anand (2014) performed an algorithm for efficient image denoising to reduce AWGN using adaptive Wavelet Packet (WP) decomposition to obtain optimum wavelet basis by utilizing Shannon entropy along with the improved neighboring window method based on SURE. Athira and George (2014) explored an algorithm for edge preserving image denoising using DT-CWT based on directional interpolation scheme using a model to find the noiseless and some missing sam-

ples within the similar framework of minimal estimation by LMMSE based proceeding. Shi et al. (2014) presented an algorithm for effective image denoising using a specific TI directional framelet transform for an efficient and sparse representation for images containing rich textures using an adaptive block-wise orientation MAP estimator for multivariate exponential distribution.

Naimi et al. (2015) developed an algorithm for efficient image denoising for noisy image using DT-CWT using coefficients thresholding with Wiener filter technique. Sethunadh and Thomas (2014) improved their work done significantly by spatially adaptive IDA using the application of multiresolution representations of noisy image with directional features in DT-CWT as an anisotropic.

However, designing an IDA based on multiresolution results in a denoised image that is more computationally power demanding than that of traditional DWT. All types of noisy images are denoised better by preserving their fine details and color components more. The denoising operation successfully reduces the MSE and can provide a better denoised images. The use of UDWT adds a large overhead of computations and the storage space requirements are three times bigger than that of standard DWT, for any number of decomposition levels , but it provides improved results objectively and subjectively. New version of CWT can avoid the pitfalls of standard DWT and gives better results.

2.4 Image Denoising Algorithms in Spatial-Frequency Domain

Fourier analysis (Fourier, 1822) is one of the most known signal processing tool to study stationary signals only. Fourier transform is a mathematical operation that decomposes a function according to its frequencies. Spatial-frequency filtering algorithms refer to the low-pass filters using FFT and the noise is removed by adapting a cut-off frequency.

Elad and Aharon (2006) presented an IDA based on sparse and redundant representations over trained dictionaries using the K-SVD algorithm for a global image prior that forces sparsity over patches in every location in the image. An adaptive non-linear approach for image denoising in the frequency transform is proposed and analyzed by Oktem and Ponomarenko (2007) for AWGN in the DCT domain using a small support expectation to approximate the Karhunen-Loeve decorrelating

transform in DCT. Oktem and Ponomarenko (2007) explored an effective IDA based on DCT using modified version of existing traditional algorithms. Foi et al. (2007) presented an algorithm for color edge preserving image denoising based on the shape adaptive DCT using the anisotropic local polynomial approximation—intersection of confirmed intervals technique for the local estimations using adaptive weights that depend on the region's statistics.

Shui (2009) proposed an efficient IDA based on the empirical subband energy distributions of the images using two sets of directional windows matching the direction–frequency selectivity of the subband filters of 2-*D* separable DFT modulated bases. Hu et al. (2012) proposed an effective IDA based on calculating the more accurate estimation of similarity weights in the DCT subspace of neighborhood. Abramov et al. (2013) presented an IDA based on quasi-optimal value of threshold parameters using simple statistics of DCT coefficients for different additive Gaussian noise levels and a set of grayscale test images. Shao et al. (2014) explored an IDA based on non-local representations using learned dictionaries for improved modeling of natural images.

These IDAs are more time consuming with more computation cost and also depend on the cut-off frequency and the filter function behavior. Their results are not so much visual friendly in denoised images and artifacts or induced stair free. Furthermore, they may produce artificial frequencies in the processed image.

2.5 Gaps

After doing in-depth survey of existing wavelet based IDAs, it has been noted that the selection of a wavelet type with vanishing moments and number of wavelet decomposition levels for image denoising are not finalized till now. Traditional IDAs only aim to suppress the noise without paying any attention to image fine details and color components. So edges of the image are not preserved and got over-smoothen.

Traditional DWT are not efficient in representing the location and orientation of image features like contours and edges. The shift invariance and directional selectivity is not supported by standard DWT. The efficiency of an IDA can be enhanced by deciding an appropriate wavelet type and its

number of decomposition levels so that important features and color components of the image are preserved. UDWT is shift-invariant and supports the directional selectivity. DT-CWT also provides phase information of edges in the images.

The threshold selection should be more adaptive so that local informations of the image are considered to preserve them. The spatial adaptive threshold selection may be better approach in enhancing the efficiency of an IDA. The threshold value may be applied based on selective adaptive approach for different region of image *i.e.* lower or reduced threshold value for edge region as noise is less visible here and normal calculated threshold value for flatten region. Wavelet coefficients thresholding schemes are mostly subband or level dependent and statistical modeling based in the literature. The over-smoothening of edges during traditional wavelet thresholding must be recovered by using morphological operations.

The use of non-orthogonal wavelet transform may avoid the lacks of standard DWT like approximate shift-invariance and directional selectivity. Different version of CWT may be the better choice for complex structural grayscale and color image denoising.

2.6 Objectives of the Research

The main focus of research work is on efficient development and analysis of adaptive denoising algorithms for digital images by incorporating spatially correlations of wavelet coefficients. The main objectives of the proposed research plan are summarized below:

- To analyze the wavelet based IDAs for grayscale and color images.
- To develop an efficient adaptive IDA using wavelets for grayscale and color images and to evaluate its performance with reference to existing state-of-art algorithms in terms of denoising quality.
- To analyze and enhance the results of the developed denoising algorithms against the existing wavelet based IDAs.

2.7 Methodology Used

The methodologies used to achieve these objectives are given as:

- First of all, the existing wavelet based adaptive IDAs have been studied as a part of in-depth literature survey. The relative performance and accuracy of these algorithms have also been analyzed. The study has focus on the development of wavelet-based adaptive denoising algorithms for grayscale and color images.
- The standard test images are considered for noise standard deviations started from 10 to 50 with the interval of 10.
- Input image is decomposed by using different families of DWTs with vanishing moments.
- A selective thresholding scheme is applied to preserve the fine details and color components of an image.
- Over-smoothen edges are recovered by using morphological operations.
- The lacking of traditional DWT is avoided by using shift-invariant and directional selectivity of UDWT.
- Phase information feature supported by DDT-CWT is used to enhance the performance.
- Performance parameters like PSNR and visual quality have been analyzed for the goodness of proposed IDAs. The verification and validation of the developed IDAs have been carried out using MATLAB.

Chapter 3

Edge Preserving Image Denoising using Discrete Wavelet Transform

3.1 Introduction

In this Chapter, an edge preserving denoising for grayscale and color images using selective thresholding in wavelet domain is proposed. As AWGN follows Gaussian distribution and spreads equally in the entire image so called white noise[1]. AWGN gets added to the original images to produce corrupted noisy images, as given by the expression (Xie et al. 2004):

$$\hat{I}(i,j) = I(i,j) + \eta(i,j) \tag{3.1}$$

where $\hat{I}(i,j)$ represents the noisy image, $I(i,j)$ represents the original image, $\eta(i,j)$ represents the induced noise.

Image denoising is an estimate of the original image by using some estimation procedure. While reducing the noise from noisy images, the main objective is to preserve the significant image features like edges, texture and other fine details. Noise reduction is a typical task as both AWGN and image features are in the high frequency range. An efficient IDA adapts to image discontinuities specially

[1]**The contents of this Chapter has been published in *International Journal of Imaging and Robotics*, 18(4), pp. 155-164, 2018**

edges which are necessary for the exact visual perception of the images. An image denoising process may cause blurring so it is a valid challenge to the researchers to search a more efficient edge preserving IDA (Routray et al. 2018, Brox et al. 2008).

The significant image features such as edges and textures are represented by a few small wavelet coefficients (Ray and Mallick 2003) due to compaction property of wavelet transform. For better visual perception of the image, each type of edges present in the image should be well detected before applying wavelet thresholding. Edges detection and localization is a critical task and have so many problems (Kaur and Kaur 2013). A true edge detection scheme is a challenging task to the researcher due to the presence of AWGN. An edge may be detected by the intensity changes due to the noise where edge does not exist. Another problem is due to edge location shifting by AWGN (Liu and Ma 2006). The performance of an edge detector is estimated by locating the true edges in noisy images. These issues are well covered by a better edge detector like Canny edge detector.

As the image edges have less effect of AWGN than the flatten region of the image. They require small threshold to be used to reduce the noise by preserving edges. If a single threshold value is applied for flatten region and edge region wavelet coefficients, then the edges may get over-smoothen. So the reduced threshold value is required for edge area and normal threshold value for smoothen area using the soft thresholding for the noisy coefficients. In its most basic form, each wavelet coefficient of the noisy image is compared with calculated threshold value, if a coefficient is smaller than the threshold value, then it is set to zero, otherwise slightly reduced coefficient magnitude by threshold itself (Donoho 1995, Balster et al. 2005). Then denoised image is recovered by wavelet reconstruction using the same wavelet function type with vanishing moments as used in wavelet decomposition.

3.2 Adaptive Thresholding for Image Denoising

Various IDAs have been proposed to deal with noise reduction from the images in wavelet domain. Most of the existing IDAs using DWT are not adaptive. Fine details of the images are not considered separately during the denoising operation and get blurred them abruptly. In this way, the quality of denoised images are not as per expectation. Local or spatial information of an image must be

considered for better results objectively and subjectively. These types of IDAs are following the adaptive approach for thresholding. These adaptive IDAs can consider the high frequency contents like noises and image edges separately.

The actual degradations of the images depend on the type of noise induced. The IDA must be chosen as per the percentage of image quality degradation as well as noise type. The traditional IDAs include NLM filter, TV method, shrinkage models in different wavelet transform (Bacchelli and Papi 2004). An ICA based IDA is a popular algorithm based on data-adaptive transform and used in low noise densities. It denoises images with non-Gaussian as well as Gaussian distribution of noises but it consumes the more computational cost. In some applications, it might be difficult to obtain the noise free training data (Zhu et al. 2014).

The motivation towards wavelets are due to their unique characteristics for visual information like images representation (Mittal and Kumar 2006, Banham and Katsaggelos 1996). Wavelet gives the excellent performance in field of image denoising because of sparsity and multiresolution property. They are briefly described below:

- **Sparseness**: A wavelet transform have a sparsity property and DWT of a noisy images yields a small number of larger wavelet coefficients (image and its features) and a large number of smaller wavelet coefficients (noise components) (Suresh and Lal 2017).

- **Spatial clustering:** The large magnitude coefficients in each subband form spatial clustering with strong dependencies for edges region and areas of texture (Krishnamoorthi 2007).

- **Persistence across scale:** The wavelet coefficients magnitudes in a subband are highly correlated *i.e.* large value of wavelet coefficients tends to propagate at same relative spatial locations across the different scales and at the neighboring spatial location at the same scale (the adjacent subband coefficients of next decomposition level). If a parent wavelet coefficient is of high magnitude, then its children will be of high magnitude and vice-versa (Lal and Chandra 2012)

Linear adaptive IDAs in transform domain are not so effective when transient non-stationary wide-band components are involved since their spectrum is similar to the spectrum of noise. Wavelet based non-linear IDAs rely on the basic idea that the energy of an image will often be concentrated in a

few coefficients in the transform domain while the energy of noise is spread among all coefficients of a subbands. The selection of a wavelet function type and number of decomposition level for image denoising are under improvement always for better results (Balster et al. 2005). There is a need to select the wavelet function type which can decompose the noisy image so that its important features are preserved. The preservation of an image features like edges are also dependent on the number of decomposition levels.

After finalizing the wavelet function type and its decomposition levels, DWT is applied to the noisy image to get its subbands (Abramovich and Benjamini 1996). The maximum noise exists in diagonal subband of first decomposition level. Thresholding of the wavelet coefficients also needs to be studied so that the important features of the image are preserved and artifacts after image denoising are avoided.

The noise standard deviation is calculated by using equation (1.16). This noise standard deviation is the basis for each type of threshold value calculation (Faghih and Smith 2002). The optimum threshold value is calculated using this noise standard deviation for each subband up to three decomposition levels separately. Two separate threshold values are computed by using the Bayesian estimator. These threshold values are used to denoise the transformed image using soft thresholding (Ray and Mallick 2003). The normal adaptive threshold value is used for flatten region and updated threshold value is used for edges region as the noise has low visual perception on the edges. Then these threshold values are applied using the soft thresholding approach adaptively to preserve the edges of an image.

In this way, all the wavelet coefficients smaller than threshold value are rejected and remaining are used to reconstruct the denoised image by using the inverse transform. The numeric results in the form of PSNR values are compared in the PSNR Table objectively.The subjective results are compared by visual perception of denoised images for different noise standard deviations.

A multiresolution bilateral filter is a state-of-the-art non-linear edge preserving IDA by avoiding blurring of edges (Jain and Tyagi 2015) and is used in this work for comparison. In bilateral filtering, one Gaussian filter works in spatial domain and another Gaussian filter works in intensity domain simultaneously (Shu et al. 2013). The weighted average are calculated based on a Gaussian distribu-

tion depending on the spatial distance and on the intensity of pixels. This filtering preserves the sharp edges better by adjusting the weights to adjacent pixels accordingly. The noisy image is decomposed into four frequency subbands using DWT. Bilateral filtering works in approximation subband only and soft thresholding is applied on all three details subbands. In this way, multiresolution bilateral filtering is eliminating the low-frequency noise components also. This IDA combines both bilateral filtering and wavelet thresholding with preserving the distinct edges (Voloshynovskiy et al. 2005).

In particular, BM3D filtering can be considered state-of-the-art in IDAs literature. As the image data is locally highly correlated, so similar data patches from different locations of an image are considered in this type of filtering. It exploits a specific non-local modeling of image data through grouping of mutually similar patches (Dabov et al. 2006). Grouping of non-local image data finds mutually similar 2-*D* image blocks and stacks them together in 3-*D* arrays to improve the denoised image quality more significantly. So BM3D filter relies both on non-local and local characteristics of an images in the form of mutually correlated similar patches (Dabov et al. 2009). These results improve the denoising performance by preserving the image fine details in the local estimates of the matched blocks. So BM3D introduces very few artifacts in the filtered images.

3.2.1 Bayesian Estimation in Image Processing

The Bayesian approach is based on probability theory that makes it possible to rank a continuum of possibilities on the basis of their relative likelihood or preference. The Bayesian framework provides a means to incorporate prior knowledge in the data analysis. Bayesian analysis is based on the posterior probability, which summarizes the degree of one's certainty concerning a given situation. Bayes's law states that the posterior probability is proportional to the product of the likelihood and the prior probability. The likelihood encompasses the information contained in the new data. The prior presents a degree of certainty concerning the situation before data are taken.

Although the posterior probability completely describes the state of certainty about any possible image,it is often necessary to select a single image as the 'result' or reconstruction. A typical choice is that image that maximizes the posterior probability, which is called the MAP estimate. Other choices for the estimator may be more desirable, for example, the mean of the posterior density function. The

single set of any is not sufficient to specify a unique solution to the problem. The prior is one of the most critical aspects of Bayesian analysis and can provide a preferred solution. Different priors like Maximum-a-posteriori (MAP) and the maximum likelihood (ML) are used in literature.

A digital image is represented as an array of discrete values. The Bayesian method provides a way to solve image reconstruction problems that would otherwise be insoluble. Viewing it as a stochastic problem, however, leads one to estimate the digital restored image (statistical) knowledge of the noise. We adopt the latter view, which leads directly to the concept of conditional estimates: to estimate f conditioned on a knowledge of g. Baye's law leads immediately to the description of the a posteriori conditional density:

$$pf|g = \frac{p(f)|(g)p(f)}{p(g)} \tag{3.2}$$

where $p(g|f)$, the probability of the observed data given f, is the likelihood and $p(f)$ is the prior probability of f.

3.2.2 Edge Preserving Adaptive Thresholding based Algorithm

As the wavelet decomposition level increases, the SNR of a subband usually become smaller *i.e.* the noise density in all the subbands is higher (Coupier et al. 2005). For example, the subband LH_3 has higher noise density than the corresponding subband in the previous level LH_2 which appears in the edges more, so the threshold value for edges region of LH_3 should be estimated high to reduce more noisy coefficients than the corresponding lower subband LH_2.

In this Chapter, an adaptive IDA is proposed, which can preserve each edge structure well. In this proposed algorithm, edge pixels are detected in the image by using the Canny edge detector which is superior edge detector in the image processing literature (Basu 2002). To improve the image denoising, two threshold values are used within a subband of each decomposition level. A normal threshold value is calculated and applied for flatten region of each subband of different decomposition levels based on Bayesian estimator as usual and a updated (lower) threshold value is used for edge regions as the noise appears less in these regions. In this way, an edge dependent thresholding scheme

is used to threshold the wavelet coefficients within each subband for preserving them.

Algorithm 3.1 Proposed IDA using Adaptive Thresholding in DWT:-

1: Input image is corrupted with AWGN using the standard MATLAB function.

2: The corrupted image is decomposed into four subbands namely, LL_1, LH_1, HL_1 and HH_1, where LL_1 represents the approximation coefficients, while LH_1, HL_1 and HH_1 are the details coefficients over which thresholding are applied.

3: The noise standard deviation and the image standard deviation for each details subband are computed. The threshold value is computed with these two standard deviations using Bayesian estimator.

4: Thresholding of the details wavelet coefficients is computed by two ways:

- the calculated normal threshold value is used for flatten region and
- a lower threshold value is used for edges region by detecting the edges.

5: This is repeated for next higher decomposition level by taking the previous level approximation subband as an input image.

6: Inverse DWT is applied on the modified wavelet coefficients to get the denoised image.

3.3 Experimental Results and Analysis

Proposed adaptive wavelet coefficients thresholding scheme has been implemented in MATLAB. Different grayscale and color images of size 512×512 are considered for experiment purpose. The results are analyzed subjectively and objectively for different values of noise standard deviation from 10 to 50 for each noisy image in considered and proposed IDAs.

3.3.1 Objective Analysis

All the algorithms implemented are compared by finding the MSE and then PSNR in dB using wavelet types 'Haar' and Daubechies wavelet function with eight vanishing moments ($Db8$), as they are more suitable in image denoising. PSNR Table 3.1 illustrates the comparison among bilateral filtering in wavelet domain, BM3D filtering and Edge Preserving Adaptive Thresholding (EPAT) on the basis of

PSNR values for the grayscale and color images of different structures. Further, output PSNR have been compared and analyzed for these thresholding algorithms at different noise standard deviations 10, 15, 20, 25, 30, 35, 40, 45 and 50 respectively (low, medium and high), as shown ahead in Table 3.1. An IDA which results in higher PSNR values is better IDA than those having lower PSNR values.

Table 3.1: PSNR values for various noise standard deviations of different images

Noise Std σ_n	Wavelet Type	Bilateral Filtering	BM3D Filtering	Proposed Algorithm
Child				
10	Haar	31.6221	31.8236	32.6911
	db8	32.3102	33.2928	34.5614
15	Haar	30.2313	30.4702	30.6381
	db8	31.1821	32.0527	33.3961
20	Haar	28.7039	29.1021	29.4287
	db8	29.8313	30.9106	31.9381
25	Haar	27.3861	27.9492	28.3752
	db8	28.6739	29.5173	30.6287
30	Haar	26.2253	26.9273	26.8287
	db8	27.3861	28.3905	29.5752
35	Haar	25.1879	25.4923	25.9104
	db8	26.1253	26.9371	28.0987
40	Haar	24.0835	24.5634	24.9395
	db8	24.9379	25.7276	26.8624
45	Haar	23.1952	23.8104	24.0216
	db8	23.6035	24.4843	25.7911
50	Haar	22.0536	22.7057	23.1482
	db8	22.1823	23.3502	24.6118
	Peppers			
10	Haar	30.2267	32.1381	33.2189

	db8	31.4637	32.6348	33.8278
15	Haar	28.9832	30.1562	31.0134
	db8	29.8592	30.9541	32.1932
20	Haar	27.8826	29.5157	30.2773
	db8	28.5135	29.7723	30.8829
25	Haar	26.1767	28.4104	28.6903
	db8	26.7254	28.5327	28.9974
30	Haar	25.5242	26.3832	27.2676
	db8	25.7791	26.9428	27.8707
35	Haar	24.6506	25.6377	26.1736
	db8	24.6452	25.8152	26.7175
40	Haar	23.6222	24.5211	24.9624
	db8	23.5915	24.7046	25.8633
45	Haar	23.0414	23.8108	23.8926
	db8	22.4227	23.3721	24.4372
50	Haar	22.1533	22.7231	22.9620
	db8	21.1743	22.0841	23.1652
	Lena			
10	Haar	31.7095	32.2702	32.9034
	db8	32.0618	33.3051	34.8087
15	Haar	29.3436	30.4175	31.6339
	db8	30.8112	31.9731	33.5143
20	Haar	28.6357	29.4325	30.2274
	db8	29.4126	30.6412	32.1896
25	Haar	26.6533	27.4214	28.5804
	db8	27.4829	28.9146	30.6374
30	Haar	25.5785	26.1451	26.7827

	db8	26.0437	27.6865	28.9561
35	Haar	24.1549	24.9613	25.8365
	db8	24.7809	26.0505	27.4037
40	Haar	23.0135	23.8271	24.9176
	db8	23.3122	24.5096	26.0804
45	Haar	22.0210	22.5327	23.7256
	db8	22.1414	23.1835	24.7129
50	Haar	21.0345	21.6267	22.6538
	db8	21.2347	22.2059	23.6413
	Parrot			
10	Haar	30.5810	31.6273	33.0143
	db8	32.3487	33.9327	35.7182
15	Haar	28.6904	29.1125	31.3323
	db8	30.6477	31.7660	33.8413
20	Haar	27.8856	28.8524	30.3703
	db8	29.1351	30.4256	32.2820
25	Haar	26.8802	27.3205	28.5208
	db8	27.3507	28.7481	29.9694
30	Haar	25.7692	26.0754	26.8135
	db8	26.1459	27.2836	28.9842
35	Haar	24.2775	24.6117	25.3894
	db8	24.7478	25.8864	26.8937
40	Haar	23.0423	23.9782	25.1137
	db8	23.7522	24.2347	25.8304
45	Haar	22.2502	22.9631	23.7573
	db8	22.1409	23.1831	24.5235
50	Haar	21.1225	21.9352	22.6136

	db8	21.2512	22.2381	23.7766
	color ***Peppers***			
10	Haar	31.0403	33.1240	34.2271
	db8	32.3618	34.3051	36.3925
15	Haar	29.4162	31.0231	32.3721
	db8	30.8346	32.3742	34.2143
20	Haar	27.9198	28.9512	29.7692
	db8	29.5128	30.8204	32.3896
25	Haar	26.8638	27.2423	28.5230
	db8	27.4869	28.9096	30.4378
30	Haar	25.2682	26.4710	27.4831
	db8	26.1437	27.4861	29.1559
35	Haar	23.2532	24.8211	25.9861
	db8	24.7809	26.2505	28.0038
40	Haar	22.1020	23.5282	24.7751
	db8	23.3122	24.5096	26.3810
45	Haar	21.1289	22.5288	23.6285
	db8	22.1366	23.3817	25.0176
50	Haar	21.0051	21.6258	22.9881
	db8	21.3629	22.2652	23.9617
	color ***Lena***			
10	Haar	33.1161	34.6723	35.0128
	db8	32.3810	34.1130	36.7864
15	Haar	31.7911	32.1246	33.2289
	db8	30.8455	32.3749	34.2084
20	Haar	27.8945	28.5904	30.3328
	db8	29.5126	30.6402	32.3903
25	Haar	26.8766	27.6455	29.0458

	db8	27.4834	28.8165	30.6411
30	Haar	25.9531	26.1374	27.7723
	db8	26.1437	27.4858	29.0064
35	Haar	24.2907	25.1252	26.1782
	db8	24.7809	26.2505	27.9037
40	Haar	23.1903	23.9880	24.4711
	db8	23.3237	25.4968	26.1805
45	Haar	22.0023	22.9723	23.4562
	db8	22.1501	23.1821	24.8129
50	Haar	21.0826	21.9471	22.7416
	db8	21.2219	22.1712	23.7173

3.3.2 Subjective Analysis

The results of the proposed EPAT based IDA are shown for low, medium and high noise standard deviations for grascale and color images with their PSNR values. The denoised images from the proposed IDA are shown with their PSNR values for corresponding noise standard deviation. The EPAT scheme restores the most of fine details and color components of images at the high noise standard deviations and avoids the artifacts in images of different structures.

(i) Original Image (ii) Noisy Image (iii) Denoised Image

Figure 3.1: Noise standard deviation = 10, Value of PSNR = 34.5614

(i) Original Image

(ii) Noisy Image

(iii) Denoised Image

Figure 3.2: Noise standard deviation = 20, Value of PSNR = 31.9381

(i) Original Image

(ii) Noisy Image

(iii) Denoised Image

Figure 3.3: Noise standard deviation = 30, Value of PSNR = 29.5752

(i) Original Image

(ii) Noisy Image

(iii) Denoised Image

Figure 3.4: Noise standard deviation = 40, Value of PSNR = 26.8624

3.4 Performance Analysis

Wavelet provides localization information of an image in time-frequency domain therefore leads to less loss of image information. Each of these IDAs are compared in terms of PSNR values and visual perception. The comparative graphs for all type of IDAs among the noise standard deviations and corresponding PSNR values are given here. The performance graphs for each type of image confirm


(i) Original Image


(ii) Noisy Image


(iii) Denoised Image

Figure 3.5: Noise standard deviation = 10, Value of PSNR = 33.8278


(i) Original Image


(ii) Noisy Image


(iii) Denoised Image

Figure 3.6: Noise standard deviation = 20, Value of PSNR = 30.8829


(i) Original Image


(ii) Noisy Image


(iii) Denoised Image

Figure 3.7: Noise standard deviation = 30, Value of PSNR = 27.8707

that proposed EPAT based IDA provide better results for all noise standard deviations.

As shown in performance graphs, the bilateral filtering in wavelet domain is performing better for lower and medium noise standard deviations than that of BM3D filtering. The proposed EPAT base IDA performs much better than the bilateral filtering in wavelet domain for higher noise standard deviations. The proposed EPAT scheme is better than traditional schemes which provides higher PSNR values and better edges as well as color components preserving as seen in denoised images and

(i) Original Image (ii) Noisy Image (iii) Denoised Image

Figure 3.8: Noise standard deviation = 40, Value of PSNR = 25.8633

(i) Original Image (ii) Noisy Image (iii) Denoised Image

Figure 3.9: Noise standard deviation = 10, Value of PSNR = 34.8087

(i) Original Image (ii) Noisy Image (iii) Denoised Image

Figure 3.10: Noise standard deviation = 20, Value of PSNR = 32.1896

shown PSNR values comparison using $Db8$ wavelet. It produces the better PSNR values for higher noise standard deviations (greater than 35) and image sharpness compared to multiresolution bilateral filtering and BM3D filtering algorithms. The denoised images from proposed adaptive thresholding scheme are much closer to the real images and there is no blurring in the denoised images. The $Db8$ provides better results for all noise densities and complex image structures. Some other wavelet types with different vanishing moments are also analyzed but $Db8$ gives better results for every type of


(i) Original Image


(ii) Noisy Image


(iii) Denoised Image

Figure 3.11: Noise standard deviation = 30, Value of PSNR = 28.9561


(i) Original Image


(ii) Noisy Image


(iii) Denoised Image

Figure 3.12: Noise standard deviation = 40, Value of PSNR = 26.0804


(i) Original Image


(ii) Noisy Image


(iii) Denoised Image

Figure 3.13: Noise standard deviation = 10, Value of PSNR = 35.7182

images and noise standard deviations.

(i) Original Image (ii) Noisy Image (iii) Denoised Image

Figure 3.14: Noise standard deviation = 20, Value of PSNR = 32.2820

(i) Original Image (ii) Noisy Image (iii) Denoised Image

Figure 3.15: Noise standard deviation = 30, Value of PSNR = 28.9842

(i) Original Image (ii) Noisy Image (iii) Denoised Image

Figure 3.16: Noise standard deviation = 40, Value of PSNR = 25.8304

(i) Original Image (ii) Noisy Image (iii) Denoised Image

Figure 3.17: Noise standard deviation = 10, Value of PSNR = 36.2925

(i) Original Image (ii) Noisy Image (iii) Denoised Image

Figure 3.18: Noise standard deviation = 20, Value of PSNR = 32.3896

(i) Original Image (ii) Noisy Image (iii) Denoised Image

Figure 3.19: Noise standard deviation = 30, Value of PSNR = 29.1529

(i) Original Image (ii) Noisy Image (iii) Denoised Image

Figure 3.20: Noise standard deviation = 40, Value of PSNR = 26.3810

(i) Original Image (ii) Noisy Image (iii) Denoised Image

Figure 3.21: Noise standard deviation = 10, Value of PSNR = 35.7864

(i) Original Image (ii) Noisy Image (iii) Denoised Image

Figure 3.22: Noise standard deviation = 20, Value of PSNR = 32.3903

(i) Original Image (ii) Noisy Image (iii) Denoised Image

Figure 3.23: Noise standard deviation = 30, Value of PSNR = 29.0064

(i) Original Image (ii) Noisy Image (iii) Denoised Image

Figure 3.24: Noise standard deviation = 40, Value of PSNR = 26.1805

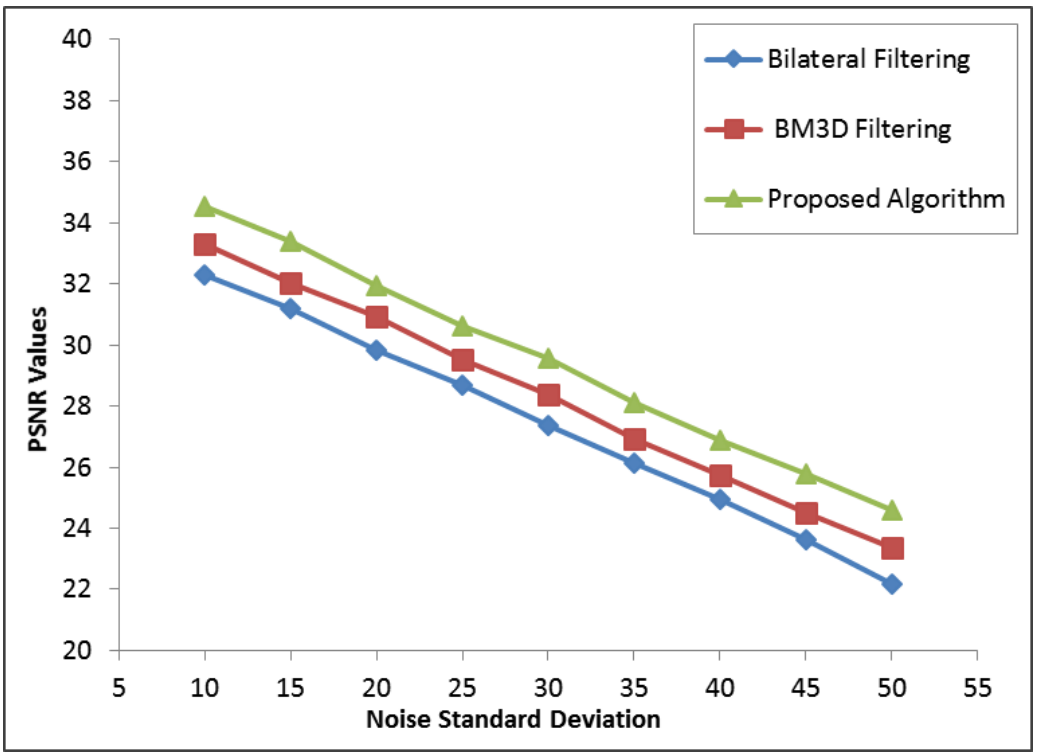

Figure 3.25: PSNR performance graph for *Child* image

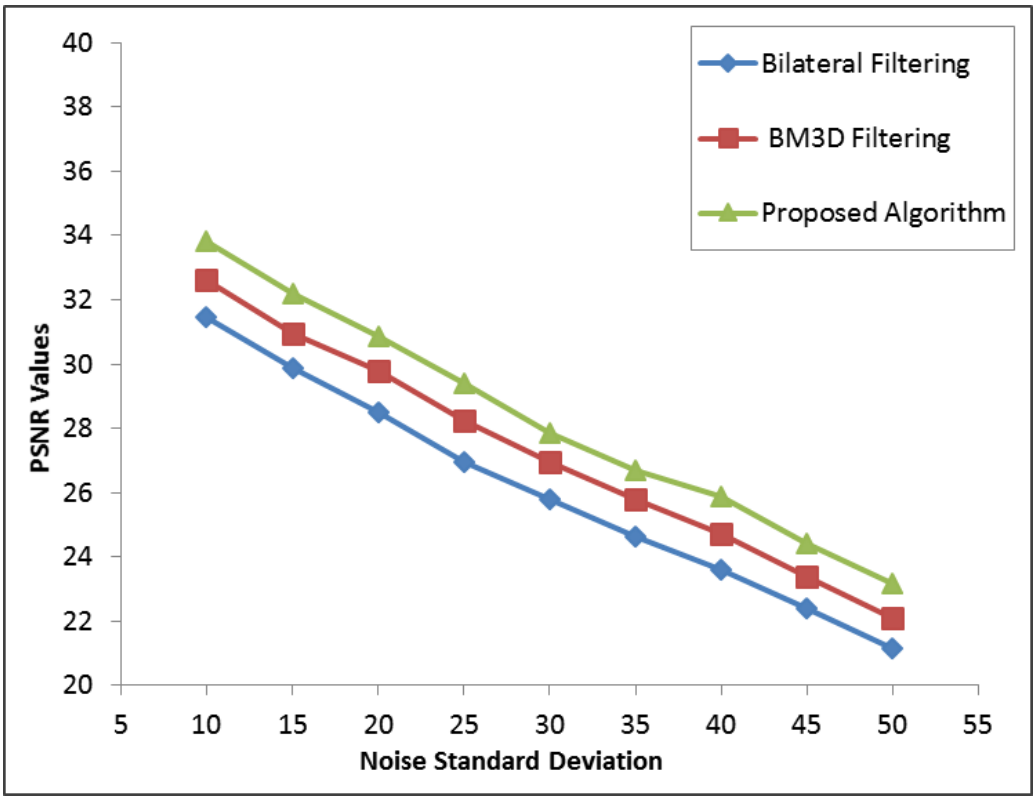

Figure 3.26: PSNR performance graph for *Peppers* image

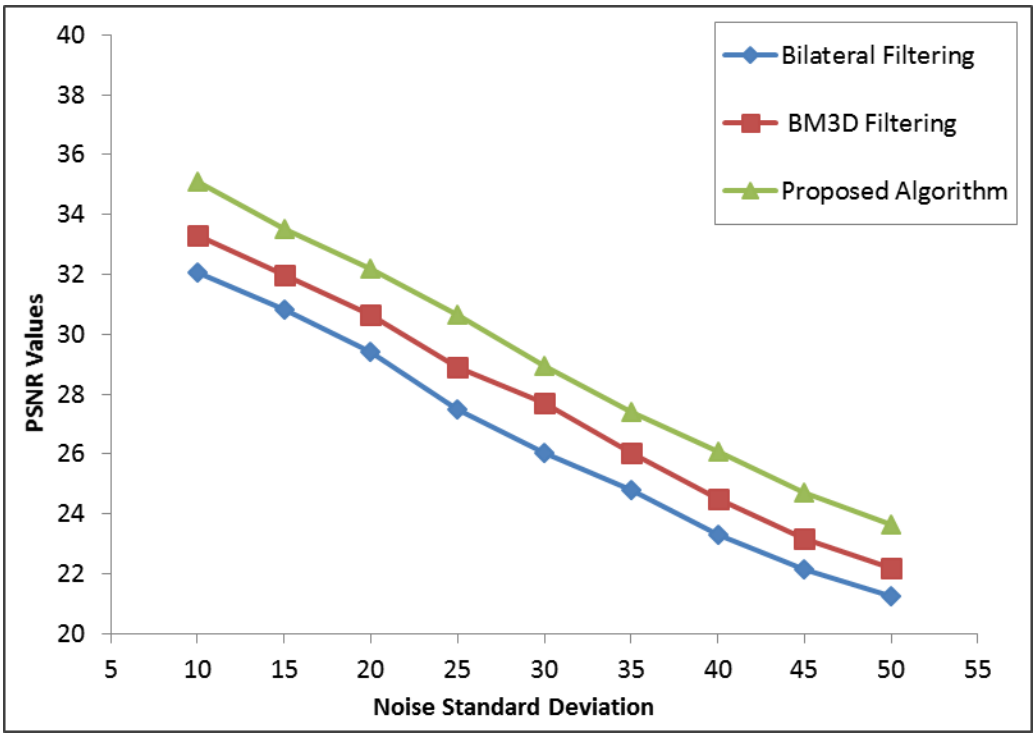

Figure 3.27: PSNR performance graph for *Lena* image

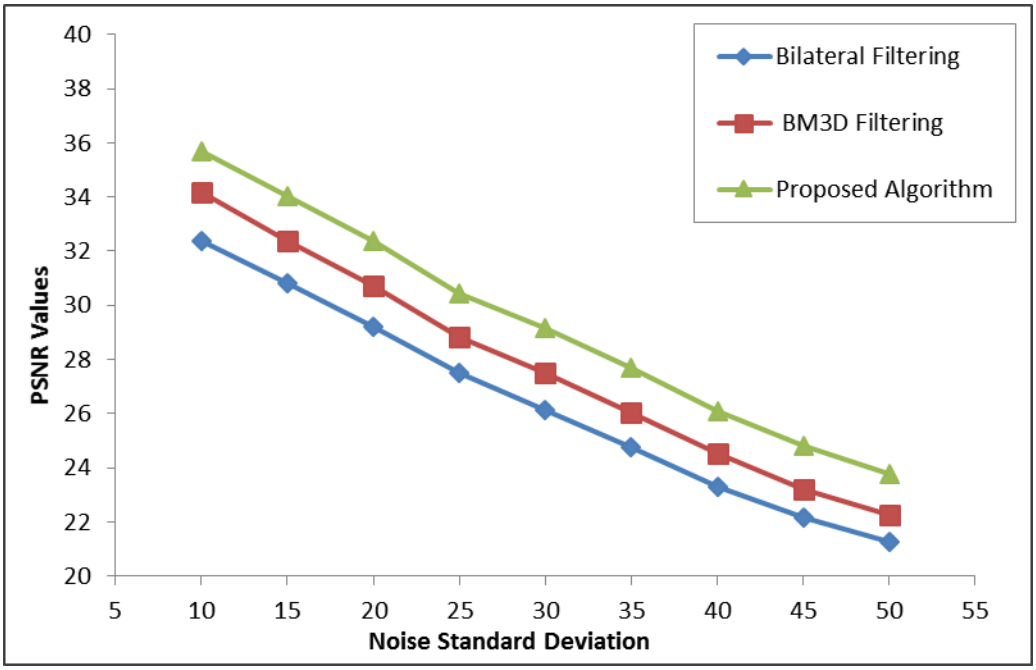

Figure 3.28: PSNR performance graph for *Parrot* image

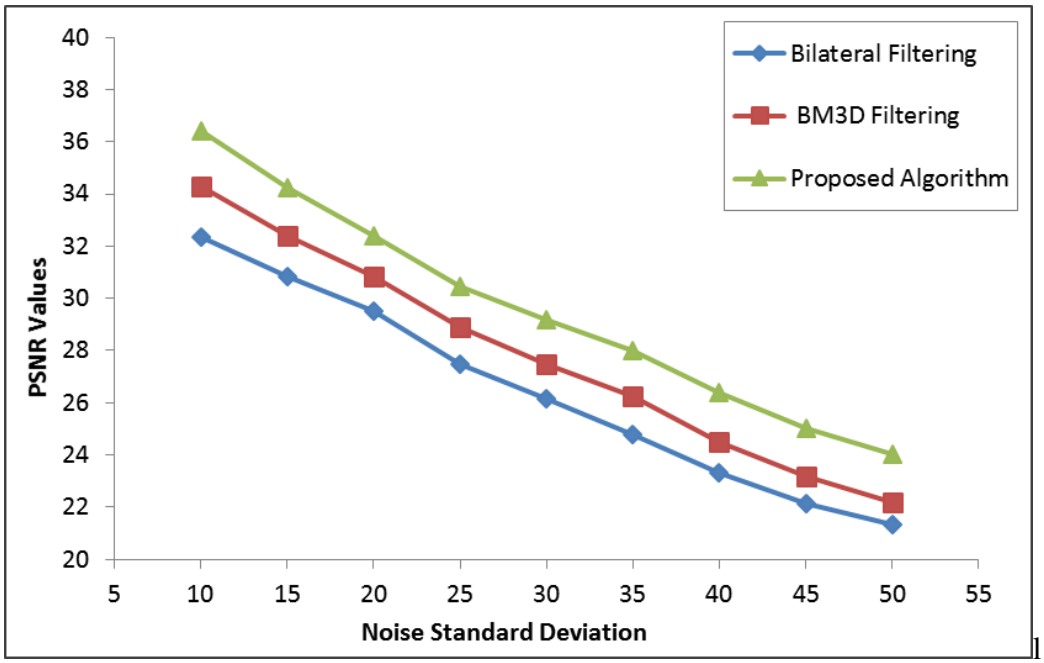

Figure 3.29: PSNR performance graph for *Peppers* color image

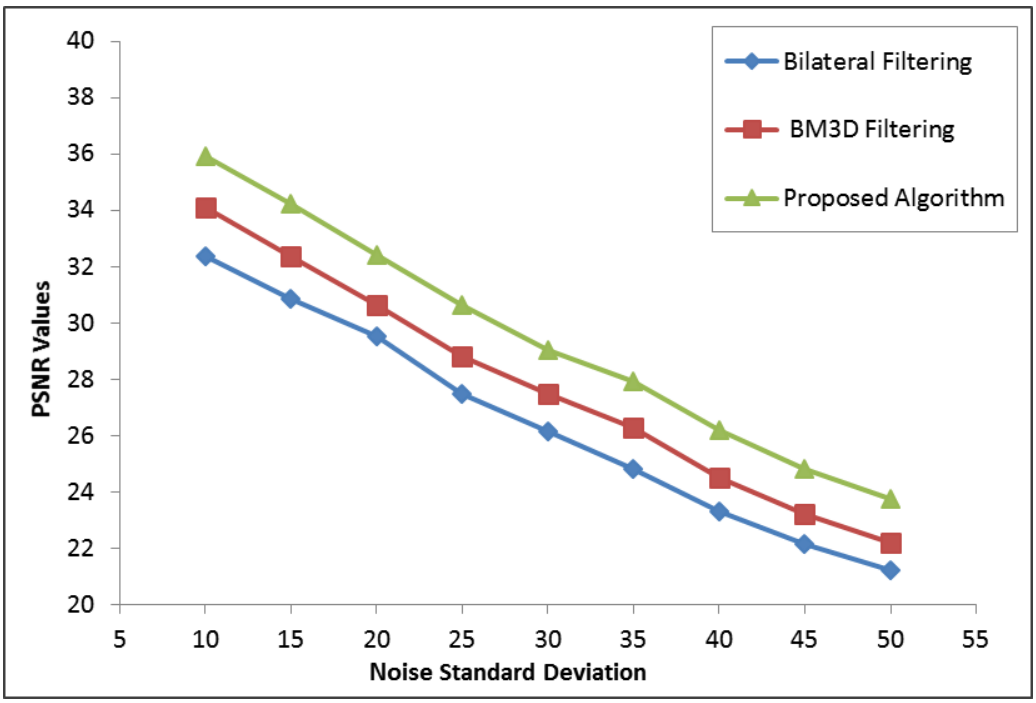

Figure 3.30: PSNR performance graph for *Lena* color image

3.5 Conclusions of the Chapter

All these algorithms are analyzed for different intensities of AWGN in the images of different structures. The noise intensities from the standard deviation 10 to 5o with the interval of 5 are taken in consideration. The image of simple structure like a snap of *Child* and more complex image like *Peppers* is taken for all the algorithms. Different types of wavelet families with different vanishing moments are analyzed for all type of the IDAs. The selective thresholding in proposed IDA provides better results objectively and subjectively. It has been observed that proposed IDA is also effective for higher noise standard deviations. The $Db8$ provides better results for all noise densities and complex image structures.

In the experimental analysis given above, it is experimented to determine the best adaptive thresholding scheme which preserve the image edges more. Spatially adaptive thresholding scheme is able to improve the performance for wavelet coefficients thresholding because it allows additional local information of the images. This thresholding scheme may also be extended to next generation of wavelets. Similar bodies of research work may be conducted for other kinds of non-grayscale (color) images. Future work shall address novel shrinkage criteria based on more local information of images.

Chapter 4

Efficient Edge Preserving Adaptive Image Denoising using Morphological Operations in Wavelet Domain

4.1 Introduction

A digital image get noisy during its major operations like its compression and transmission from one place to another through any medium. The interference in the transmission channel induces the noise in an image (Hosseini et al. 2016). This type of noise is mainly additive in nature and is of two types namely AWGN and salt-and-pepper noise. These noises degrade the image quality and must be removed before further image processing. During the image denoising, the important features like edges, textures *etc.* are also disturbed (Chen and Lien 2008). This may also degrade the visual quality as well contents of the original image[1].

The characteristic of fine details specially edges have the great significance for the real visual perception of an image (Voloshynovskiy et al. 2005). The image features preserving during the image denoising is necessary for exact restoring the images. So the problem of image denoising and edge preserving using the mathematical tools attract attention in image processing computer vision

[1]**The contents of this Chapter have been published in *International Journal of Applied Engineering Research,*, 13(16), pp. 12941-12949, 2018**

research. The first reason is the wide range of commercial applications and the second is the availability of improved technologies for image processing.

The AWGN and image fine details like edges are always of high frequency components in the frequency spectrum. During the image denoising the fine details like edges get disturbed more. So it is difficult to reduce AWGN from the images without blurring the edges of the image (Donoho et al. 1996). Now question arises that how can edges be preserved during image denoising. For better edge preserving, it is necessary to detect the position and orientation of the edge. To detect the presence and location of edges is a critical task and have so many problems (Jain and Tyagi 2015). A true edge detection is a challenging task to the researcher due to the presence of AWGN. An edge may be detected by the intensity changes due to noise where edges do not exist. Another problem is due to the edge location shifting by the AWGN. The performance of an edge detector is estimated by locating the true edges in a noisy image.

A wavelet is a mathematical function used in image denoising and image compression. Image denoising for AWGN using wavelets is very effective because of advance features of wavelet in representing the non-stationary signals like images. The wavelet has the ability to capture the energy of a image in few energy transform values. For two decade there has been a great amount of research on wavelet coefficients thresholding for image denoising (Abramovich and Benjamini 1996, Chen et al. 2005, Blu and Luisier 2007). DWT based image denoising using the wavelet coefficients thresholding are gaining popularity from decades. DWT is also capable to present the real spatial information of an image by providing the good time resolution at high frequency and good frequency resolution at low frequency. DWT can reveal the local characteristics of the input image more precisely and compactly as its great time and frequency localization ability (Kalavathy and Suresh 2011).

Generally all the IDAs in wavelet domain do not consider an edge direction and location primarily. This is due to the hidden edges in the wavelet transform domain (Lal and Chandra 2012) and it is not easy to detect their location and orientation. So it is difficult to accommodate these edges exactly during the image denoising process (Ho and Hwang 2013). It is important that edges present in the image should not be missed and false edge detection should be avoided. These issues motivated the researchers to design a novel approach for efficient edge preserving image denoising in wavelet

domain. Thus, during the image denoising, the first thing that should be cared about is trying to retain edge information.

A new adaptive and efficient IDA is proposed here: first of all, the noisy image is decomposed using a desired wavelet basis function with appropriate vanishing moments. The standard deviation of noise is calculated using the first level diagonal subband using equation (1.16) and is used to estimate the noise standard deviation for each subband of desired decomposition levels (Hel-Or and Shaked 2008). Then this noise standard deviation is utilized to find the optimal threshold for each subband by Bayesian estimator.

Then the edges are detected using the Canny edge detector. The Canny edge detector is optimal for a certain class of edges by detecting the real edge with maximum possibility. The selective thresholding is applied here to avoid the edge over-smoothing (Chang et al. 2000). For this wavelet coefficients that are detected edges will be protected from the ensuing denoising process. For this two types of threshold values are required here, lower one for edge region as the noise has less visibility effect in edges and exact threshold value for flatten region. If a single threshold is applied for both types of the wavelet coefficients, then the edges got over-smoothing.

Small wavelet coefficients are trimmed using the coefficients thresholding, *i.e.* after removing the noisy wavelet coefficients from all the details subbands, image reconstruction is performed using the same wavelet function type and version as used at the time of decomposition of the noisy image (Pizurica et al. 2006). During the wavelet thresholding, the edges get over-smoothened due to not well handled separately. Then the edges can be improved by using morphological operations like opening and closing. Closing smooths the contour of an image and fills small gaps and holes. Opening also smoothes the contour, breaks narrow isthmuses, and eliminates thin protrusions. Removal of small holes and narrow branches can be accomplished by concatenating opening with closing. In this way, degraded edges can be enhanced and preserved by using these morphological operations (Verd-Monedero et al. 2011).

The image reconstruction is achieved by finding the inverse DWT of approximation subband of first decomposition level and modified and enhanced details coefficients of each decomposition level. This process is continued through the same number of decomposition levels as in the decomposition

process to obtain the original image (Scharcanski et al. 2002). In this way, the AWGN gets reduced with better edge preservation. The experimental results are presented for different type of noise standard deviations in the form of PSNR and visual perception as given in the PSNR Table 3.1 and denoised images. The subjective and objective analyses of results demonstrate that the proposed IDA is more efficiently preserving the edges than traditional edge preserving IDA for high noise intensities also.

4.2 Mathematical Preliminaries

Basic important mathematical concepts are discussed in this section which are used in this Chapter.

4.2.1 Discrete Wavelet Transform

Recently, various wavelet based algorithms using DWT have been proposed for the image denoising. The wavelet transform coefficients within the subbands can be locally modeled as *i.i.d* random variables with GGD. In wavelet based denoising, DWT on the noisy image is applied to find the wavelet coefficient subbands. Let W and W^{-1} denotes the two dimensional DWT and its inverse respectively. The input image and transform coefficients relationship is given as:

$$X = Wx \qquad and \qquad x = W^{-1}X \tag{4.1}$$

In DWT, a noisy image can be decomposed into a sequence of four frequency subbands namely, LL_1, HL_1, LH_1 and HH_1 as shown in Figure 4.1. The low pass band (LL_1) of decomposed image represents a coarse approximation image in the lowest resolution, and three detail images in higher bands (HL_1, LH_1 and HH_1) (Scharcanski et al. 2002). The next level of DWT is applied to the low frequency subband image LL_1 only and it can be further decomposed into four subbands namely LL_2, HL_2, LH_2, and HH_2 and continue in this way upto desired decomposition levels.

DWT is continued until a desired decomposition level is achieved but it depends more on noise standard deviation as well as image structures. In DWT, the magnitude of DWT coefficient varies

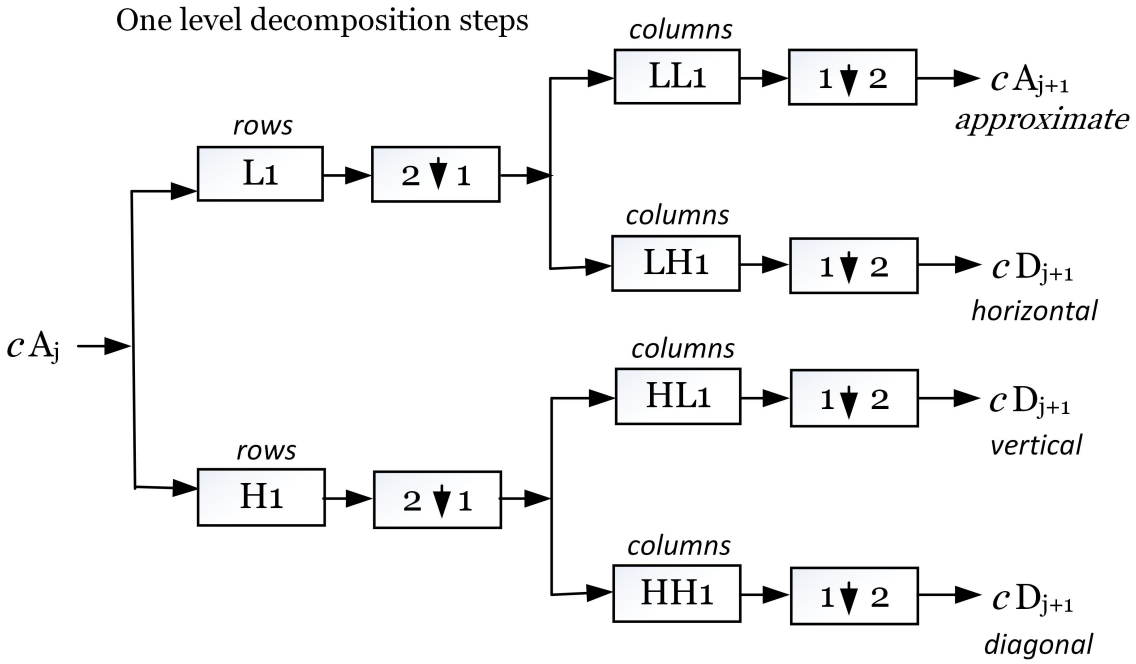

Figure 4.1: 2D DWT Wavelet Decomposition

depending on the decomposition level. The wavelet coefficients become smoother as the level of decomposition increases. Thus the subband HL_2 is smoother than the adjacent subband in the first level (HL_1) and so the threshold value for HL_2 should be smaller than that of HL_1. After forth decomposition level, there is no more image details information are left in the decomposition subbands, only a severer noise remains.

After DWT is performed on the noisy images, the wavelet coefficients thresholding is needed to reduce the noise. It has mainly two parameters: shrinkage rule and shrinkage function. The shrinkage rule is how to calculate the threshold and shrinkage function is how to apply the calculated threshold. Researchers published different ways to estimate the parameters for thresholding of wavelet coefficients and its application.

4.2.2 Multiscale Mathematical Morphology

Now a days image processing and analysis use a powerful mathematical tool known as Mathematical Morphology (MM). MM is an appropriate and effective tool for visual information like natural images. Different components of images are considered as set of distinguish points in MM. The com-

ponents of images as an object and the Structuring Element (SE) are considered two set of data to which MM are applied (Feng et al. 2014). SE is a base set for any MM operations and shape as well as size of it are defined as per the requirement or purpose of the application. There are four morphological operations like erosion, dilation, opening and closing. Opening is the sequential combination of erosion and dilation. In the same way, closing is the sequential combination of dilation followed by erosion.

A high level operation is performed by concatenation of two basic operations like dilation and erosion in different orders, including *closing* and *opening*. The closing basic operation is performed as dilation followed by erosion and mathematically given below:

$$(A \bullet B) = (A \oplus B) \ominus B = \{z|(B)z \cap A\} \neq \emptyset \tag{4.2}$$

Closing morphological operation fills the foreground holes smaller than SE, smoothen the contour, fuses narrow breaks and long thin gulfs *etc.* (Verd-Monedero, Angulo and Serra 2011).

The opening operation is erosion followed by dilation as given below:

$$(A \circ B) = (A \ominus B) \oplus B = \cup\{(B)z \,|(B)z\} \subseteq A \tag{4.3}$$

In opening operation, the structures that are smaller than the SE will disappear and larger structures will remain. It smoothes the contour, breaks narrow isthmuses, and eliminates thin protrusions

The fine details of an image can be well handled by the same shape and size of the SE B (Verd-Monedero, Angulo and Serra 2011). A scalable SE in morphological operations with appropriate shape and size can extract image features like edges very well. A sequence of morphological operations can improve the presence of edges by concatenating opening with closing and used in this work.

4.3 Adaptive Thresholding for Image Denoising

This section covers the details regarding the adaptive algorithms of image denoising along with their theory. The wavelet coefficients thresholding schemes discussed here are bilateral filtering in wavelet domain, BM3D filtering and efficient EPAT (Dabov et al. 2009). A robust estimate of noise variance is calculated from noise standard deviation using the median absolute value of the wavelet coefficients of first decomposition level diagonal subband HH_1. A universal threshold value is calculated using the noise standard deviation for each subband and is applied for all desired decomposition levels (Donoho 1995). The standard deviation of noise is calculated and used to calculate the threshold value using Bayesian estimator.

The processed image may be overly smoothened due to the larger threshold value so that sufficient information preservation is not possible and the image gets blurred. So an adaptive thresholding is required for image features preservation especially edges. For this, an adaptive threshold is calculated for each subband at each level separately.

4.3.1 Proposed Image Denoising Algorithm

A noisy image is decomposed after finalizing the wavelet basis and number of decomposition levels in advance. As the wavelet decomposition level increases, then SNR of a subband usually becomes smaller *i.e.* the noise intensity is higher in higher decomposition level and after fourth decomposition level, only severe noise exists. For example, the subband LH_3 has higher noise than the corresponding subband in the previous level LH_2 which appears in the edge's region more, so the threshold value for edge's region of LH_3 should be applied higher to remove more noisy coefficients than that applied for LH_2.

In this way, edge pixels are detected in the image by Canny edge detector which is superior edge detector in image processing literature. To improve the image denoising, two threshold values are used within all details subband of each decomposition level. A normal calculated threshold value is applied using soft thresholding for flatten region of each details subband as usual and a lower threshold value is used for edge's regions as the noise appears less in these regions (Chang et al. 2000). In this way, an

edge dependent thresholding scheme is used to threshold the wavelet coefficients of the edges within that subband for preserving them. So the wavelet coefficients are thresholded adaptively according to their local statistics and better results are achieved (Cho et al. 2009) objectively and subjectively.

After wavelet thresholding, many details features (edges and texture) of an image are disturbed more which are significant for the image quality and visual perception. There is a need to restore these features for further image processing operations. This can be achieved by applying the morphological operations like opening and closing to the thresholded wavelet coefficients of each details subband at each decomposition level. Closing smooths the contour of a denoised images and fill small gaps and holes induced during thresholding process. Opening also smooths the contour, breaks narrow isthmuses, and eliminates thin protrusions. Removal of small holes and narrow branches can be both accomplished by concatenating morphological opening with closing. The degraded edges can be enhanced and preserved by using these morphological operations to the thresholded wavelet coefficients.

4.4 Experimental Results and Analysis

Proposed IDA has been implemented using MATLAB. Different structure images of size 512×512 corrupted with all noise intensities of AWGN are considered for this work. The results are analyzed subjectively by visual perception and objectively by PSNR for different values of noise standard deviations.

4.4.1 Objective Evaluation

All the IDAs implemented are compared by calculating the PSNR values using wavelet types $db3$ and $db8$, as they are more suitable in image denoising.PSNR Table 4.1 illustrates the comparison among bilateral filtering in wavelet domain, edge preserving IDA and proposed efficient EPAT based IDA on the basis of PSNR values for different image structures. Further, output PSNR values have been compared and analyzed for these IDAs at different noise standard deviations from 10 to 50 respectively (low, medium and high), as shown in this Table. The IDA which results in higher PSNR

Algorithm 4.1 Proposed IDA using Morphological Operations in DWT:

1: An sample image is corrupted with AWGN first.

2: The noisy image is decomposed using DWT with different vanishing moments of Daubechies wavelet.

3: There are four subbands namely, LL_1, LH_1, HL_1 and HH_1, where LL_1 represents the approximation coefficients, while LH_1, HL_1 and HH_1 are the details coefficients over which thresholding is applied.

4: The noise standard deviation is calculated from the diagonal subband of first decomposition level. It is used to compute the noise variances for each details subband of desired decomposition levels.

5: The standard deviation of noise and image for each details subbands are computed. These standard deviations are used to compute the threshold value by using Bayesian estimator.

6: Thresholding of the details wavelet coefficients is achieved by applying the selective threshold value to the flatten and non-flatten regions.

7: This is repeated for next higher decomposition level by taking the previous level approximation subband as an input image.

8: The morphological opening and closing operations with a appropriate SE are applied to the thresholded wavelet coefficients for edge enhancement.

9: Inverse DWT is performed on the modified wavelet coefficients to obtain the denoised images.

value is better denoising approach compared to those having lower PSNR value for the same noise standard deviation.

Table 4.1: PSNR values for various noise standard deviations of different images

Noise Std. σ_n	Wavelet Type	Bilateral Filtering	Edge Preserving IDA	Proposed Algorithm
	Lena			
10	db3	32.0017	34.4636	35.7821
	db8	32.0618	34.8087	36.4975
15	db3	30.1323	32.6932	33.8381
	db8	30.8112	33.5143	34.8974
20	db3	28.8041	31.3643	32.4764
	db8	29.4126	32.1896	33.3499
25	db3	27.0861	29.7365	30.6852
	db8	27.4829	30.7374	31.7521
30	db3	25.8543	28.0568	29.4687
	db8	26.0437	28.9561	30.5917
35	db3	24.2869	26.7537	28.2104
	db8	24.7809	27.4037	29.3126
40	db3	23.0625	25.5730	26.9395
	db8	23.3122	26.0804	27.7915
45	db3	22.0031	24.1465	25.4217
	db8	22.1414	24.7129	26.5053
50	db3	21.0210	23.1128	24.2256
	db8	21.2347	23.6413	25.4534
	Parrot			
10	db3	31.9634	33.3758	34.9189
	db8	32.3487	35.7182	36.2303
15	db3	29.6792	31.9731	33.0134

	db8	30.6477	33.8413	34.5015
20	db3	28.5126	30.4720	31.9673
	db8	29.1351	32.2820	32.6571
25	db3	26.8867	28.4536	29.6903
	db8	27.3507	29.9694	30.9953
30	db3	25.7342	27.8915	28.7646
	db8	26.1459	28.9842	29.7421
35	db3	24.1506	25.8245	27.6760
	db8	24.7478	26.8937	28.5463
40	db3	23.2222	24.4721	25.9624
	db8	23.7522	25.8304	27.3627
45	db3	22.0014	23.5472	24.8426
	db8	22.6409	24.5235	26.2439
50	db3	20.9502	22.3782	23.9871
	db8	21.2512	23.7766	25.1507
	Peppers			
10	db3	31.1095	32.7170	34.9034
	db8	31.4637	33.8278	36.2206
15	db3	29.0436	31.2653	33.2391
	db8	29.8592	32.1932	34.2431
20	db3	28.0057	30.0217	31.8274
	db8	28.5135	30.8829	32.3883
25	db3	26.0533	28.1900	29.5875
	db8	26.7254	28.9974	30.6389
30	db3	24.8785	26.4909	27.9827
	db8	25.7791	27.8707	29.1672
35	db3	23.8549	25.6027	26.5365

	db8	24.6452	26.7175	28.0142
40	db3	22.9035	24.8528	25.2376
	db8	23.5915	25.8633	26.3873
45	db3	21.5210	23.4048	24.0256
	db8	22.4227	24.4375	25.1108
50	db3	20.6210	22.4176	23.7261
	db8	21.1743	23.1652	24.0212
	Child			
10	db3	31.6810	33.4093	35.0143
	db8	32.3102	34.5614	36.1534
15	db3	30.0904	31.7125	32.9136
	db8	31.1821	33.3961	34.3372
20	db3	28.8856	30.3524	31.5988
	db8	29.8313	31.9361	32.4193
25	db3	26.8771	28.3205	29.8208
	db8	28.6739	30.3287	31.0374
30	db3	25.6692	26.8744	28.6137
	db8	27.3861	28.5752	29.4561
35	db3	24.7175	25.9769	27.0967
	db8	26.1253	27.4987	28.0126
40	db3	23.0423	24.8789	25.8136
	db8	24.9379	26.8624	27.5832
45	db3	22.1502	23.7782	24.6571
	db8	23.6035	25.5911	26.3129
50	db3	21.0385	22.1705	23.8126
	db8	22.1823	24.6118	25.0536

4.4.2 Subjective Evaluation

The different grayscale images of size 512×512 are used as test images with different noise standard deviations. The kind of noise is AWGN with standard deviations from 10 to 50 for each IDA with proposed one. Here PSNR values are given for three level of noise standard deviations *i.e.* the low, medium, high values respectively. The subjective results show that the proposed algorithm performs better edge preserving image denoising using morphological operations and gives better results as seen by visual perception of denoised images.

(i) Original Image (ii) Noisy Image (iii) Denoised Image

Figure 4.2: Noise standard deviation = 10, Value of PSNR = 36.4975

(i) Original Image (ii) Noisy Image (iii) Denoised Image

Figure 4.3: Noise standard deviation = 20, Value of PSNR = 33.3499

4.5 Performance Analysis

The proposed IDA is compared subjectively and objectively with adaptive edge preserving thresholding algorithms to present its denoising effectiveness. A combined graph of bilateral filtering in


(i) Original Image


(ii) Noisy Image


(iii) Denoised Image

Figure 4.4: Noise standard deviation = 30, Value of PSNR = 30.5917


(i) Original Image


(ii) Noisy Image


(iii) Denoised Image

Figure 4.5: Noise standard deviation = 40, Value of PSNR = 27.7915


(i) Original Image


(ii) Noisy Image


(iii) Denoised Image

Figure 4.6: Noise standard deviation = 10, Value of PSNR = 36.2303

wavelet domain, edge preserving IDA and proposed efficient edge preserving IDA are plotted with noise standard deviation at x-axis and PSNR value at y-axis for all level of noise standard deviation from **low** to **high** *i.e.* from 10 to 50.

In the performance analysis of the proposed algorithm, the major factor is the application of selective thresholding on all details subbands and further improving the edges using morphological

(i) Original Image (ii) Noisy Image (iii) Denoised Image

Figure 4.7: Noise standard deviation = 20, Value of PSNR = 32.6571

(i) Original Image (ii) Noisy Image (iii) Denoised Image

Figure 4.8: Noise standard deviation = 30, Value of PSNR = 29.7421

(i) Original Image (ii) Noisy Image (iii) Denoised Image

Figure 4.9: Noise standard deviation = 40, Value of PSNR = 27.3627

operations. It helped in preserving edges and other details in images more. This adds power to the proposed algorithm as noise components can be eliminated better in details subbands as compared to traditional subbands thresholding.

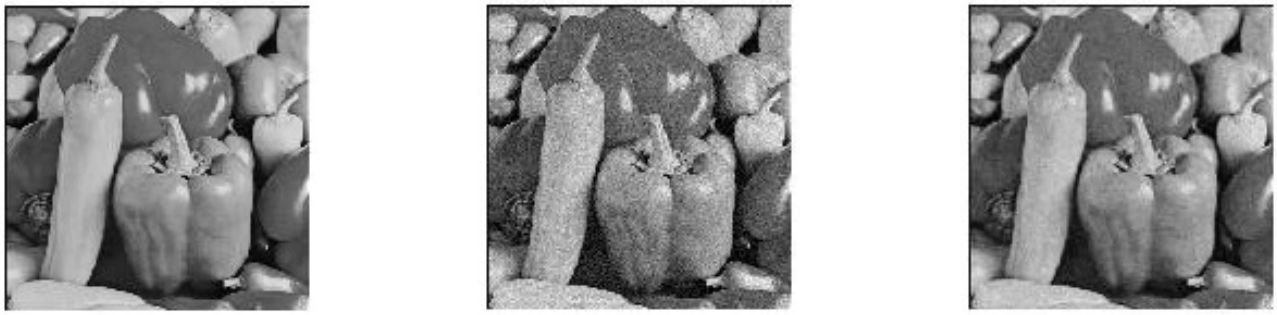

(i) Original Image (ii) Noisy Image (iii) Denoised Image

Figure 4.10: Noise standard deviation = 10, Value of PSNR = 36.2206

(i) Original Image (ii) Noisy Image (iii) DenoisedImage

Figure 4.11: Noise standard deviation = 20, Value of PSNR = 32.3883

(i) Original Image (ii) Noisy Image (iii) Denoised Image

Figure 4.12: Noise standard deviation = 30, Value of PSNR = 29.1672

(i) Original Image (ii) Noisy Image (iii) Denoised Image

Figure 4.13: Noise standard deviation = 40, Value of PSNR = 26.3873

(i) Original Image (ii) Noisy Image (iii) Denoised Image

Figure 4.14: Noise standard deviation = 10, Value of PSNR = 36.1534

(i) Original Image (ii) Noisy Image (iii) Denoised Image

Figure 4.15: Noise standard deviation = 20, Value of PSNR = 32.4193

(i) Original Image (ii) Noisy Image (iii) Denoised Image

Figure 4.16: Noise standard deviation = 30, Value of PSNR = 29.6561

(i) Original Image (ii) Noisy Image (iii) Denoised Image

Figure 4.17: Noise standard deviation = 40, Value of PSNR = 26.5832

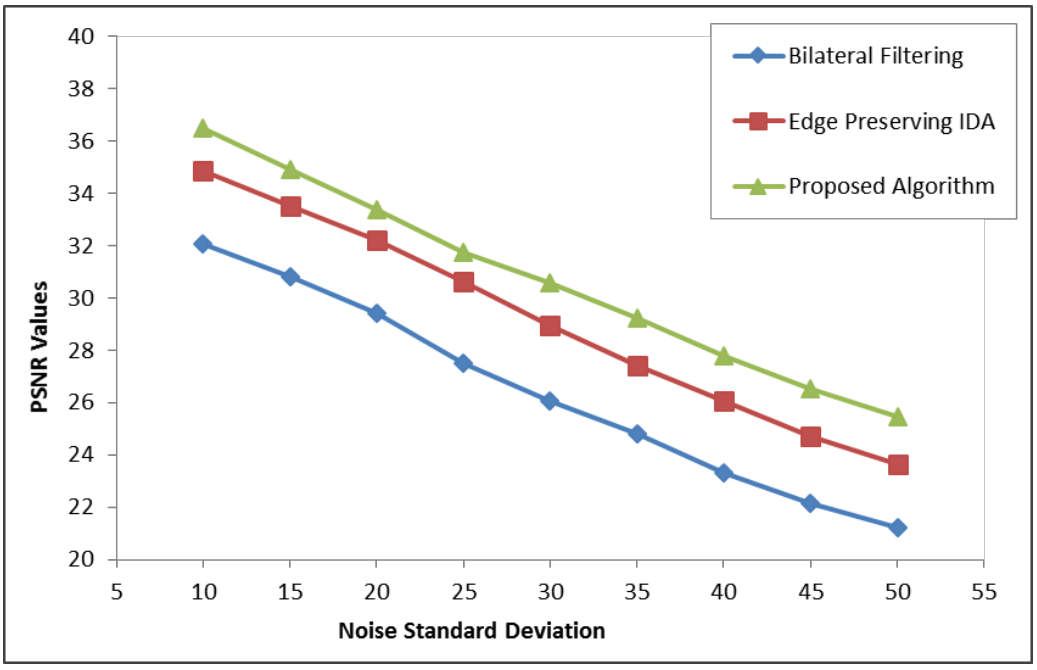

Figure 4.18: PSNR performance graphs for *Lena* image

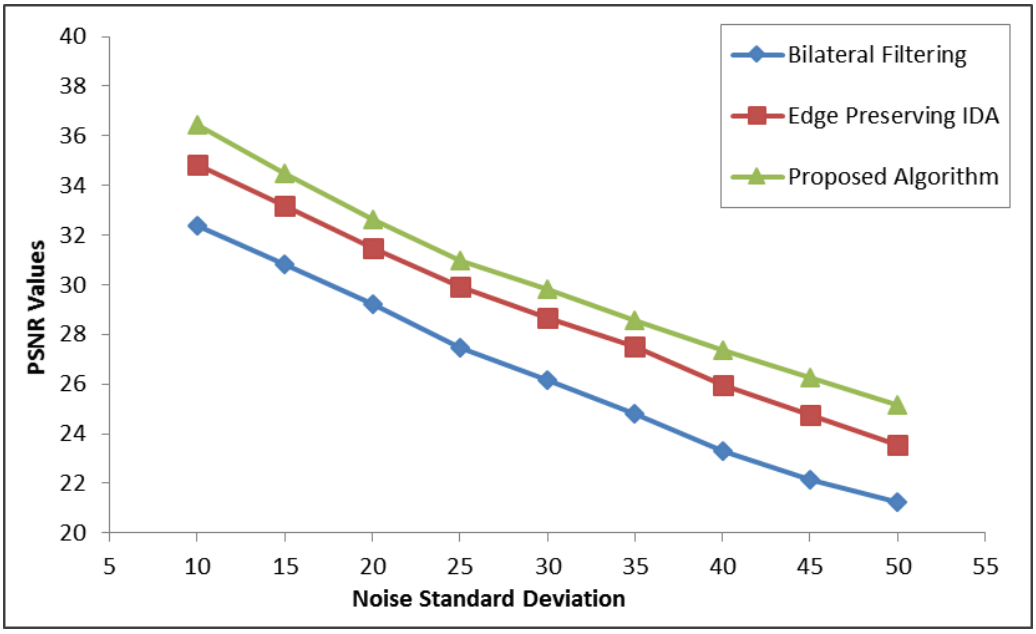

Figure 4.19: PSNR performance graphs for *Parrot* image

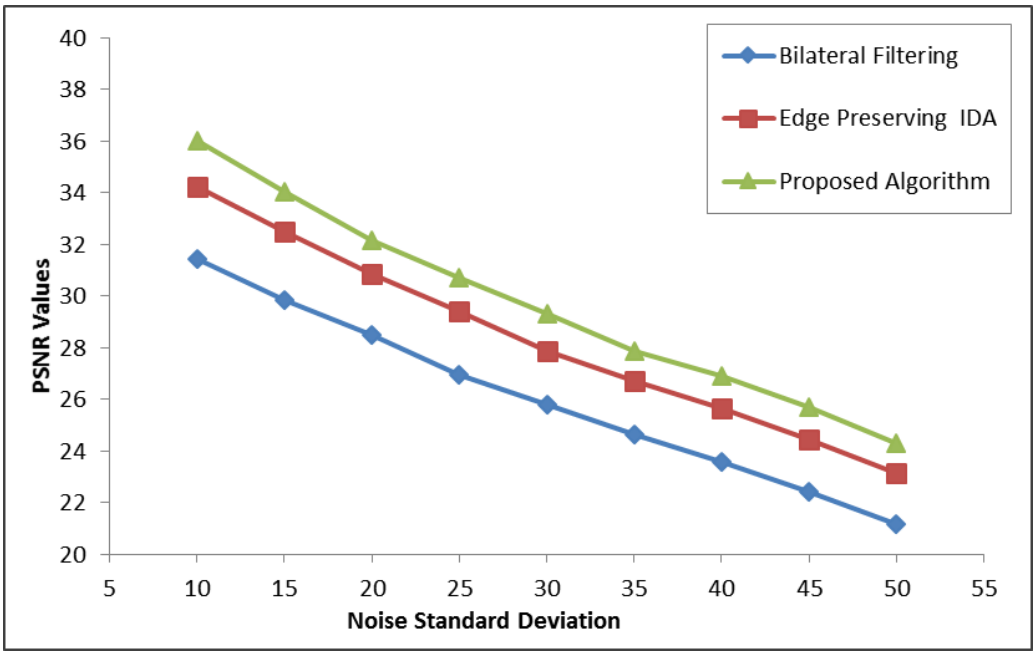

Figure 4.20: PSNR performance graphs for for *Peppers* image

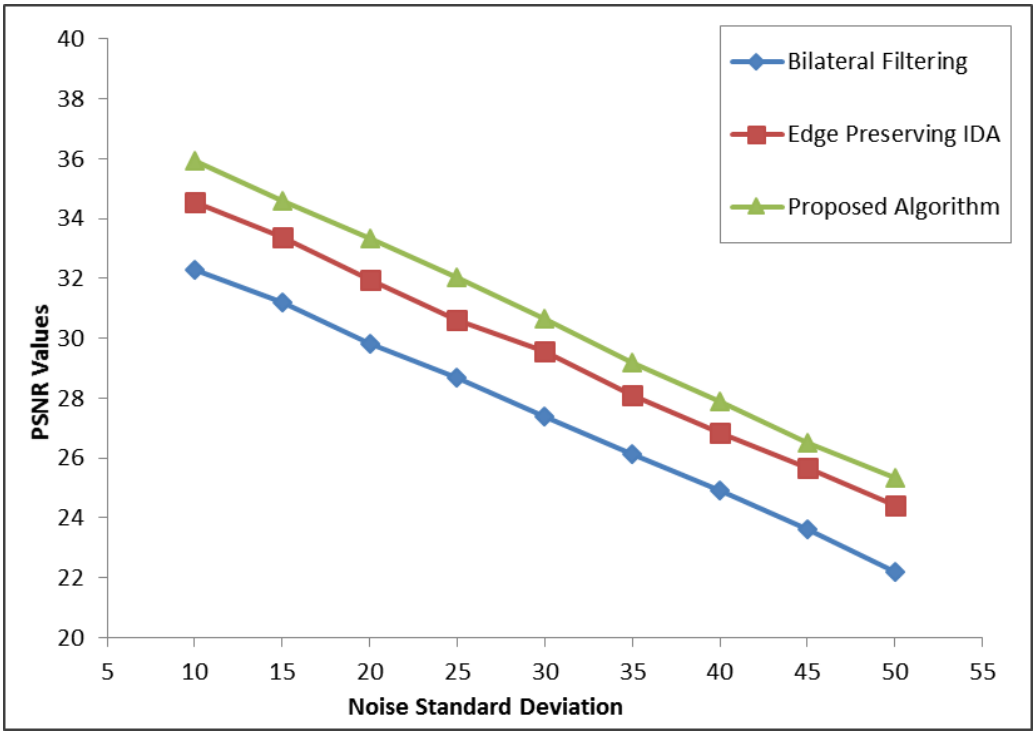

Figure 4.21: PSNR performance graphs for *Child* image

4.6 Conclusions of the Chapter

Wavelet analysis is widely used in many applications because it provides localization in both time and frequency domain therefore leads to avoid the loss of information. When an image is corrupted with AWGN, the wavelet shrinkage denoising has proved to be nearly optimal. All these IDAs are adaptive in nature. Each of these IDAs are compared in terms of the PSNR values and visual perception.

Morphological operations are used for recovering the over-smoothening of edges or other features during the traditional IDAs in wavelet domain. The concatenating morphological opening with closing can improve the experimental results more efficiently. Subjective and objective results of the proposed IDA shows that edges of the test images are more preserved with enhanced sharpness than the traditional EPAT based IDA given Chapter 3 both in terms of PSNR values and visual perception.

The proposed efficient EPAT algorithm is efficient that provides higher PSNR and better edge preserving as seen in denoised images and PSNR comparison using Daubechies ($Db3$ and $Db8$) wavelet as shown in performance graphs. It produces the better image sharpness for higher noise standard deviations compared to multiresolution Bilateral filtering and edge preserving IDA. The output denoised images from proposed IDA are much closer to the real images and there is no blurring or step-chairs in them.

Most of the Duabechies wavelets perform well in an IDA but $Db8$ provides better results for higher noise standard deviations and complex image structures. Some other wavelet types with different vanishing moments are also analyzed but $Db8$ gives better results for every types of image structures.

The limitations of bilateral filtering in wavelet domain and edge preserving IDA are eliminated by proposing an efficient EPAT based IDA using the morphological operations. The adaptive wavelet coefficients thresholding scheme allows additional local information like identification of smooth or edges regions of an image to be incorporated into the algorithm. This enhances the visual quality of the denoised image and it looks like original image. The proposed algorithm is extendable to various other wavelet families such as Symlets, and Coiflets, depending upon the number of vanishing points. This algorithm can be extended to undecimated wavelet domain and for next generation of wavelets.

Chapter 5

Improved Color Image Denoising using Spatially Adaptive Statistical Dependency in Undecimated Wavelet Transform Coefficients

5.1 Introduction

Image denoising is an important and mandatory pre-processing step in image processing pipeline. Main features of DWT are sparsity and multiresolution analysis are used in an efficient IDA. Since the early use of the classical orthonormal DWT for reducing AWGN through wavelet coefficients thresholding (Athira and George 2014) is a powerful image processing platform. A lot of image denoising literature has been reported using DWT based thresholding scheme (Abramovich and Benjamini 1996, Azzalini et al. 2005, Hedaoo and Godbole 2011), but standard DWT has two severe disadvantages: [1].

- Lack of shift-invariance in DWT,
- DWT causes poor directional selectivity for diagonal features since the wavelet filters are separable and real.

[1] **The contents of this Chapter has been communicated in *Ain Shams Engineering Journal, SCI* Indexed.**

Standard DWT is shift-variant as the transform coefficients behave un-predictably under shifts of input image signal, a problem that has been treated by introducing large amounts of redundancy into the transform to make it shift-invariant. DWT has also poor directional selectivity because it can only differentiate three different spatial-feature orientations. These two features are of great importance when color image is processed.

Shift-invariance implies that a minor changes in an input image signal causes an unpredictable major changes in the output wavelet coefficients (Chaux et al. 2007). This is an undesirable property of DWT due to which DWT are not well suited for preserving the color components and others fine details of color image during denoising more accurately. The shift-sensitivity of DWT is due to the down-samplers followed by up-samplers from filter banks implementation of DWT.

When using DWT, the translations of an image signal lead to different wavelet coefficients with down-sampling (Athira and George 2014). Two main objectives are achieved in order to overcome this problem and to get more complete characteristic of the denoised image:

- Improved performances can be achieved by wavelet transform with shift-invariant property such as UDWT (Lang et al. 1996)
- Further improvements can be obtained with spatially adaptive thresholding functions with interscale and intrascale dependencies.

The use of UDWT doesn't decimate the noisy color image during decomposition. The first objective is achieved by suing UDWT of noisy images and a threshold value is calculated based on Bayesian estimator. This redundant and translation-invariant transform is especially useful for denoising the color image of higher noise intensity with preserving the color components (Beghdadi and Khellaf 1997).

Color images are built of stacked grayscale channels. For example, RGB images are composed of three independent channels for red, green and blue primary color components; CMYK images have four channels for cyan, magenta, yellow and black ink plates, *etc*. Three Components of color in the color images are:

- **Hue**: the dominant wavelength, the redness of red, greenness of green, etc.

- **Saturation**: the purity of the color, or how much white is contained in the color. For example, red and royal blue are more saturated than pink and sky blue, respectively.
- **Luminance** (intensity, value): the intensity of the light.

The characteristic of edges and color components have the great significance for the visual perception of a color image. So the color image features as well as color components preserving is necessary during its denoising. The fine details of a color image and AWGN exist in the same high frequency spectrum. The color image denoising requires more care to preserves the color components as well as fine details like edges, lines, *etc.* (Lian et al. 2006). The exact presence and location of edges in wavelet coefficients are not easily found in color images and have so many problems. One major problem is due to edge location shifting by AWGN. A true edge detection scheme is a challenging task in the traditional DWT in the presence of AWGN but can be easily detected in spatially correlated coefficients as the noise decays level to level but edges are not.

The UDWT decomposes data into low-pass scaling coefficients (approximation) and high-pass wavelet coefficients (details) to obtain a projective decomposition of the noisy color image into different subbands just like DWT without down-sampling (Shensa 1992). This transform is good for denoising the color images, as the full samples of the decomposed images are considered for better handling the complete fine details of color images.

In image processing literature, there are two main algorithms for computing UDWT of a noisy image. The *à-trous* algorithm and Beylkin's algorithm (Shensa 1992) may be used for decomposition. The Beylkin's algorithm is used in this work due to its better achievement (Ray and Mallick 2003) in image restoration. The non-decimation approach is one way to think about UDWT and another way is to think about the shift invariance. The wavelet coefficients from all shifts are not necessary for image denoising. The shift by one to any odd and even number is achieved here. Generally, this means that computing DWT for a noisy image and its shift by one in horizontal, vertical and diagonal direction and repeating this for each decomposition level, gives all possible wavelet coefficients.

The inverse of UDWT is not unique because of redundant information due to shifts. The UDWT have approximately $N(log_2 N)$ wavelet coefficients during its decomposition. The denoised image can be reconstructed from corresponding set of odd or even shifted wavelet coefficients. The inverse

UDWT of N coefficients may be achieved by using a rule to decide which coefficient to throw away and which coefficient is kept to eliminate the redundancy. This independent inverses UDWT for each shift is then used to average the separate results into one (Wang et al. 2010). If the coefficients are not changed the reconstructed image will be exactly the same as the original.

The repetition of number-of-shifts have made more work for better results. However, if the coefficients have been changed before the inverse transform, the reconstructed shifts differs from each other. In image denoising case, different parts of the noise is reduced in the different shifts and noise is also further reduced by getting the average of shift. This approach has nice properties that it is very simple to compute and it does not introduce artifacts (Bala and Ertüzün 2005). That is why the averaging approach is used in this work.

(Zhang and Bao 2003) presents a spatial-correlation thresholding scheme for noise reduction using DWT. This denoising algorithm multiplies the wavelet coefficients of corresponding subbands of adjacent decomposition level to amplify instantaneous fine details of the test image and then applies coefficients thresholding to the multiplication. This algorithm is able to distinguish edges and other fine details of image from noise more effectively and achieve better experimental results in PSNR measurement and the visual perception compared with standard DWT based thresholding schemes.

5.2 Color Image Denoising in Wavelet Domain

This section presents the required details regarding the considered and proposed adaptive algorithms of color image denoising along with their theoretical description. The color IDAs using wavelet coefficients thresholding considered are bilateral filtering in wavelet domain, spatially correlation thresholding using DWT and proposed is spatially correlation thresholding using UDWT.

In UDWT, there is no decimation when a noisy image is decomposed. The UDWT of color image is carried out as follows: The application of UDWT decomposes the input noisy color image into different frequency subbands without down-sampling, The lowest frequency subband LL_1, created by low-pass filtering along the rows and columns yields to a coarse approximation of the color image with same size of input image. LH_1, HL_1 and HH_1 subbands are known as horizontal, vertical and

diagonal details subbands of the image. These subbands present all the information about color image and they are of same size of the original image (Wang et al. 2010).

The size of coefficients array in UDWT does not reduce from one decomposition level to next level as in case of DWT. This means that reduction of the noise only can be achieved at the real places of its existence, without disturbing the neighboring pixels. It gives the best experimental results in terms of visual quality with less blurring for larger noise reduction (Lang et al. 1996). The diagonal subband of first decomposition level can contain a significant amount of noise distribution. A robust estimate of noise standard deviation is computed using the median absolute value of the highest diagonal correlated subbands HH_1 and HH_2 and is given in equation (1.16).

The denoised image may be over-smoothened by applying a similar larger threshold value to all the wavelet coefficients of a subband and also sufficient information preservation is not possible and denoised image gets blurred. So an adaptive thresholding is required for image features preservation especially edges (Voloshynovskiy et al. 2005). For this, an adaptive threshold is calculated for each subband at each decomposition level separately.

5.2.1 Spatial Correlation using DWT Coefficients

This algorithm presents a noise reduction technique based on spatial-correlation thresholding scheme in DWT domain. The edge structures and other fine details of a color image are of high magnitude across decomposition levels but noise decays rapidly (Zhang and Bao 2003). The spatial correlation is computed by multiplying two adjacent wavelet scales to enhance significant structures of the color image and to dilute noise. As the decomposition level increases, the SNR of subband usually become lower i.e. the noise density is higher.

The wavelet decomposition of a noisy color image is achieved by finalizing the choice of wavelet function with required vanishing moments and number of decomposition levels. The application of DWT decomposes the input noisy color image into four different subbands and are labeled as LL_J, HL_k, LH_k and HH_k, $k = 1, 2, ...J$, where the subscript indicates the k-th decomposition level of DWT and J is the largest scale in the decomposition (Chang et al. 2000). Each subband contains special information about the noisy color image. The lowest subband LL_J corresponds to

a coarse approximation and contains the maximum basic information of a color image. The LH_k, HL_k and HH_k subbands are known as horizontal, vertical and diagonal details of input color image respectively. The diagonal subband HH_1 of first decomposition level contains a significant amount of AWGN. The first LL_J subband can be decomposed to form the LH_{k-1}, HL_{k-1} and HH_{k-1} subbands.

DWT is a greatly successful technique of image decomposition, as it effectively separates image components and noise component in the wavelet domain. DWT exploits scarcity property and the fact that DWT maps AWGN in the image domain to AWGN in the wavelet transform domain. Thus, maximum image energy is concentrated into fewer coefficients in the transform domain, noise energy spreads over all coefficients equally. So, it is an important property of wavelet transform that separates image components from the induced noise.

After the wavelet decomposition is performed on a noisy color image, it is needed to achieve the wavelet coefficients thresholding. Wavelet coefficients thresholding has two parameters: shrinkage rule and shrinkage function. The shrinkage rule is how to calculate the threshold value and shrinkage function is how to apply the calculated threshold value to noisy DWT coefficients. Different thresholding schemes are used in the literature for threshold value estimation and its application to noisy wavelet coefficients.

The threshold value is calculated from the noise standard deviation computed from the correlated coefficients and thresholding is applied to the resultant correlated coefficients.

5.2.2 Proposed Image Denoising Algorithm

In this work, a color IDA using UDWT is suggested, which preserves edges and major color components well. To avoid the limitation of standard DWT due to down-sampling step, UDWT is used here so that every subband has same number of coefficients as input image. In this proposed algorithm, edge pixels are enhanced by spatial correlation of two adjacent decomposition levels. To improve the color image denoising, the threshold value is calculated from the correlated coefficients of each details subbands based on Bayesian estimator and applied to each correlated subbands by using the soft thresholding. In this way, fine details and color components of a color image are more preserved as edges are amplified by correlation. So wavelet coefficients are thresholded adaptively according to

their local statistics.

UDWT of a color image is computed by using the same filter bank as in the standard DWT and it also gives three details subbands namely horizontal, vertical and diagonal. In UDWT, all the subbands have same size as the original color noisy image. UDWT decomposes data into low-pass scaling approximation coefficients and high-pass wavelet details coefficients to obtain a decomposition of noisy color image into different scales like standard DWT (Wang et al. 2010). The scaling coefficients of a decomposition level are used to compute the next level of scaling and wavelet coefficients. This type of transform is better representation for denoising the images, as the AWGN is spread over a small number of neighboring coefficients. UDWT is computed by two main algorithms in the literature: *à-trous* algorithm and Beylkin's algorithm (Bhonsle and Dewangan 2012). These two algorithms proceed in different ways for the noisy color image decomposition. Beylkin's algorithm is used in this work due to its efficiency in image representation.

This IDA is based on the idea of no decimation in each decomposition level. The color noisy image is decomposed using the standard DWT without down-sampling in the forward DWT here (Verma and Pandey 2017). In other words, it applies DWT at each point of the color image and saves details coefficients. Then approximation coefficient subband is used as an input image for next decomposition level. The size of wavelet coefficients does not diminish from decomposition level to level. No up-sampling is used in the inverse wavelet transform. So shift-invariance and direction selectivity are achieved here. It was shown that wavelet coefficients thresholding using an UDWT improves the experimental results rather than a traditional DWT (Wang et al. 2010).

The proposed color IDA produces better denoising results objectively and subjectively than the traditional DWT. The results are improved by shifting computation at the first decomposition level only. In the proposed algorithm, DWT is applied independently to the noisy color image and its shifting by one is achieved in vertical, horizontal and diagonal directions. So in this case the storage space requirements get reduced and more improvement is achieved than the standard UDWT based algorithm. The inverse UDWT is also achieved independently and the four thresholded results are averaged into one denoised image at the end. Hence, the proposed color image denoised algorithm has very straight forward implementation improved.

To improve the color image denoising, three thresholds for each color channel are used within all details subband of each decomposition level. A calculated threshold value is applied using soft thresholding for each details subband as usual. An adaptive thresholding scheme is used to threshold the noisy wavelet coefficients of an edge's region and flatten region within a subband for preserving the fine details of images. So the adaptive thresholding is applied on wavelet coefficients according to their local statistics and better results are achieved for color images. After wavelet coefficients thresholding, detail features (edges and texture) of color image are not disturbed more and well preserved.

Algorithm 5.1 Proposed Color IDA using Spatial Correlation in UDWT:

1: The color images are loaded into the workspace by using MATLAB input function.

2: The color images are corrupted with AWGN to obtain noisy color image.

3: The obtained images are subjected to NDWT using Daubechies, Coiflets and Symlets.

4: There are four subbands namely, LL_1, HL_1, LH_1 and HH_1, where LL_1 represents the approximation coefficients, while HL_1, LH_1 and HH_1 are the details coefficients over which thresholding is applied.

5: The noise standard deviation is calculated from the correlated diagonal subband of first decomposition level. The noise variance is computed for each correlated details subband of desired decomposition levels.

6: The noise and image standard deviations for each correlated details subbands are computed first and then used to calculate the threshold value based on Bayesian estimator.

7: The correlated details wavelet coefficients thresholding is achieved as follows:

a) the above calculated threshold (normal) is applied for flatten region and

b) a two-by-three threshold (reduced) is applied for edges region after detecting them.

8: This is repeated for next higher decomposition level by taking the previous level approximation subband as an input image.

9: Inverse NDWT is performed on the modified wavelet coefficients to obtain the reconstructed images.

5.3 Analysis of Experimental Results

Proposed IDA for color images has been implemented using MATLAB. Different structure color images of size 512×512 corrupted with all noise intensities of AWGN are considered for this work. The results are analyzed subjectively by visual perception of color denoised images and objectively by PSNR values for different values of noise standard deviations. UDWT is widely used in many applications because it provides the solution of each drawback of traditional DWT. Specially, the UDWT based spatially correlated coefficients thresholding provides better results for a color images corrupted with AWGN.

5.3.1 Objective Evaluation

All the color IDAs implemented are compared by calculating PSNR values for different values of noise standard deviations ranging from 10 to 50. PSNR Tables 5.1 illustrates the comparison among bilateral filtering in wavelet domain, spatial correlation thresholding using DWT and spatially correlation thresholding using UDWT on the basis of PSNR values for the color images of different structures. The color IDA which preserves more color components like hue, saturation and luminance with higher PSNR values is better denoising approach as compared with those having lower PSNR values.

Table 5.1: PSNR values for various noise standard deviations of different color images

Noise Std. σ_n	Bilateral Filtering	Sp. Corr. using DWT	Proposed Algorithm
	Barbara		
10	32.9102	34.7892	36.5087
15	31.5256	32.8907	34.7143
20	29.8613	31.3293	32.8896
25	28.4294	29.9428	31.1374
30	27.0291	28.4615	29.8561
35	25.9062	27.2269	28.5137
40	24.6061	25.8417	26.9404

45	23.5104	24.6816	25.8629
50	22.1815	23.3083	24.7507
	Peppers		
10	32.7214	34.6751	36.2807
15	31.3401	32.7982	34.3611
20	29.8372	31.3329	32.6742
25	28.8295	30.2352	31.4893
30	27.7095	29.3591	30.4762
35	26.8116	28.1592	29.3247
40	25.6531	27.2416	28.6322
45	24.7223	26.3725	27.8042
50	23.6417	25.4782	26.6593
	Lena		
10	33.6127	35.0636	36.5821
15	32.4323	33.6932	34.8781
20	31.0541	32.2643	33.4764
25	29.6861	30.7365	31.9752
30	27.8954	28.9568	30.2687
35	26.3869	27.4536	28.9104
40	25.0362	25.9870	27.3395
45	23.7510	24.9265	26.2816
50	22.2513	23.4428	25.1526
	Mandrill		
10	33.8634	35.3758	36.7189
15	32.4792	33.6731	34.8203
20	31.1126	32.0720	33.4773
25	29.1767	30.5535	31.8894

30	27.5242	28.7915	29.9646
35	26.0506	26.9745	28.3463
40	24.5222	25.7721	26.7304
45	23.0414	24.2372	25.5426
50	22.0502	23.0782	24.4235

5.3.2 Subjective Evaluation

The different color images of size 512×512 are used as test images with different noise standard deviations. The kind of noise is AWGN with noise standard deviations from 10 to 50 for each color IDA with proposed one. Here, PSNR values are given for three levels of noise standard deviations *i.e.* including the low, medium, and high values respectively. These experimental results show that the proposed color IDA performs better edge and color components preserving by using UDWT and gives better results in terms of PSNR values as given in the Table 5.1 and visual perception as shown in denoised color images. All the color components and fine details of different structural images are well preserved.

(i) Original *Barbara* Image (ii) Noisy *Barbara* Image (iii) Denoised by Bilateral filtering (iv) Denoised by Edge Preserving IDA (v) Denoised by proposed algorithm

Figure 5.1: Noise standard deviation=15, PSNR=31.5256, PSNR=32.8907 and PSNR=34.7143

5.4 Performance Analysis

The proposed color IDA is compared subjectively and objectively with bilateral filtering in wavelet domain and spatially correlated coefficients thresholding algorithms using DWT to present its denois-

(i) Original *Barbara* Image | (ii) Noisy *Barbara* Image | (iii) Denoised by Bilateral filtering | (iv) Denoised by Edge preserving IDA | (v) Denoised by proposed algorithm

Figure 5.2: Noise standard deviation=25, PSNR=28.4294, PSNR=29.9428 and PSNR=31.1374

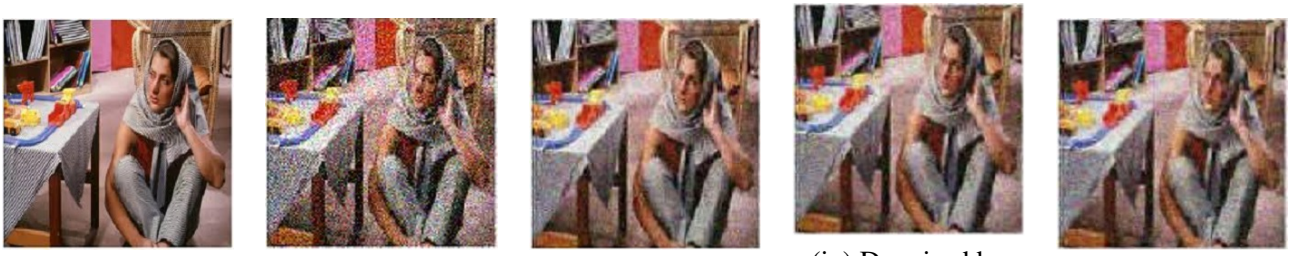

(i) Original *Barbara* Image | (ii) Noisy *Barbara* Image | (iii) Denoised by Bilateral filtering | (iv) Denoised by Edge preserving IDA | (v) Denoised by proposed algorithm

Figure 5.3: Noise standard deviation=35, PSNR=25.9062, PSNR=27.2269 and PSNR=28.5137

(i) Original *Peppers* Image | (ii) Noisy *Peppers* Image | (iii) Denoised by Bilateral filtering | (iv) Denoised by Edge preserving IDA | (v) Denoised by proposed algorithm

Figure 5.4: Noise standard deviation=15, PSNR=31.3401, PSNR=32.7982 and PSNR=34.3611

(i) Original *Peppers* Image | (ii) Noisy *Peppers* Image | (iii) Denoised by Bilateral filtering | (iv) Denoised by Edge preserving IDA | (v) Denoised by proposed algorithm

Figure 5.5: Noise standard deviation=25, PSNR=28.8295, PSNR=30.2352 and PSNR=31.4893

(i) Original *Peppers* Image | (ii) Noisy *Peppers* Image | (iii) Denoised by Bilateral filtering | (iv) Denoised by Edge preserving IDA | (v) Denoised by proposed algorithm

Figure 5.6: Noise standard deviation=35, PSNR=26.8116, PSNR=28.1592 and PSNR=29.3247

(i) Original *Lena* Image | (ii) Noisy *Lena* Image | (iii) Denoised by Bilateral filtering | (iv) Denoised by Edge preserving IDA | (v) Denoised by proposed algorithm

Figure 5.7: Noise standard deviation=15, PSNR=32.4323, PSNR=33.6932 and PSNR=34.8781

(i) Original *Lena* Image | (ii) Noisy *Lena* Image | (iii) Denoised by Bilateral filtering | (iv) Denoised by Edge preserving IDA | (v) Denoised by proposed algorithm

Figure 5.8: Noise standard deviation=25, PSNR=29.6861, PSNR=30.7365 and PSNR=31.9752

(i) Original *lena* Image | (ii) Noisy *Lena* Image | (iii) Denoised by Bilateral filtering | (iv) Denoised by Edge preserving IDA | (v) Denoised by proposed algorithm

Figure 5.9: Noise standard deviation=35, PSNR=26.3869, PSNR=27.4536 and PSNR=28.9104

(i) Original *Mandrill* Image | (ii) Noisy *Mandrill* Image | (iii) Denoised by Bilateral filtering | (iv) Denoised by Edge preserving IDA | (v) Denoised by proposed algorithm

Figure 5.10: Noise standard deviation=15, PSNR=32.4792, PSNR=33.6731 and PSNR=34.8203

(i) Original *Mandrill* Image | (ii) Noisy *Mandrill* Image | (iii) Denoised by Bilateral filtering | (iv) Denoised by Edge preserving IDA | (v) Denoised by proposed algorithm

Figure 5.11: Noise standard deviation=25, PSNR=29.1767, PSNR=30.5535 and PSNR=31.8894

(i) Original *Mandrill* Image | (ii) Noisy *Mandrill* Image | (iii) Denoised by Bilateral filtering | (iv) Denoised by Edge preserving IDA | (v) Denoised by proposed algorithm

Figure 5.12: Noise standard deviation=35, PSNR=26.0506, PSNR=26.9745 and PSNR=28.3463

ing effectiveness and efficiency. A combined graph of all these color IDAs are plotted with noise standard deviation at x-axis and PSNR value at y-axis for all levels of noise standard deviations from **low** to **high** *i.e.* from 10 to 50.

In performance graphs of the proposed algorithm, the major factor is the application of correlated coefficients thresholding on all details subbands. It helped in preserving edges as well as color components in color images more. The comparative graphs confirm that proposed IDA effectively

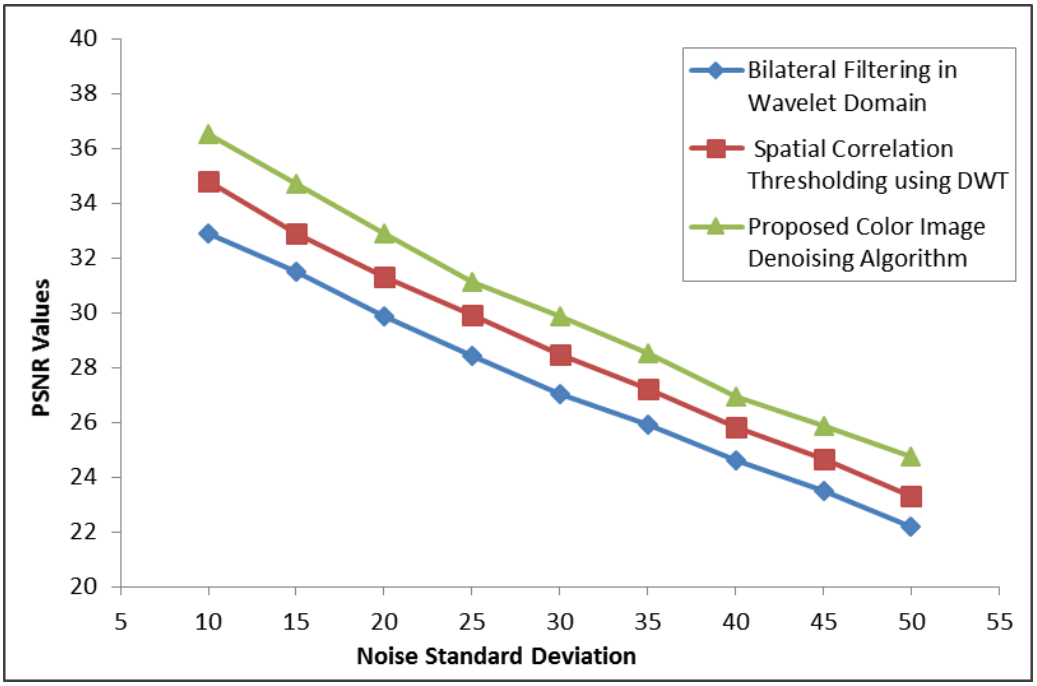

Figure 5.13: PSNR performance graphs for *Barbara* color image

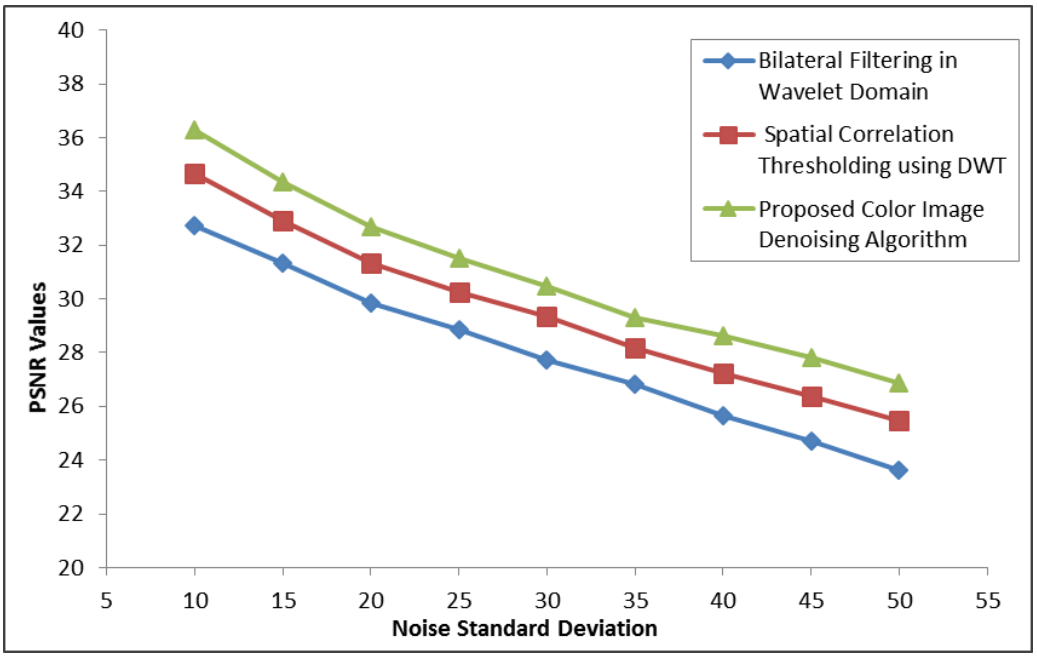

Figure 5.14: PSNR performance graphs for *Peppers* color image

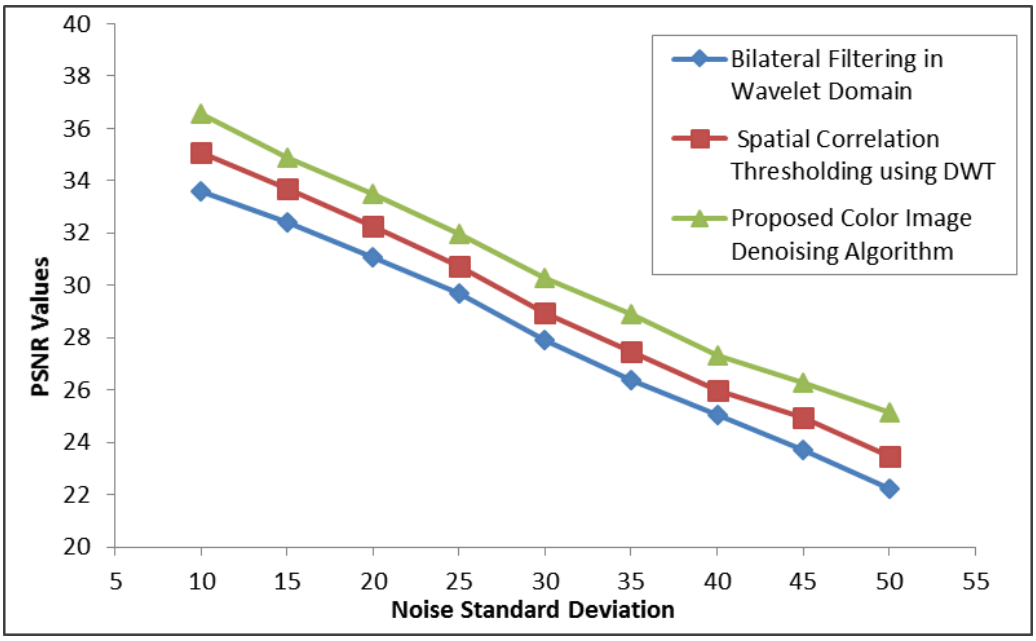

Figure 5.15: PSNR performance graphs for *Lena* color image

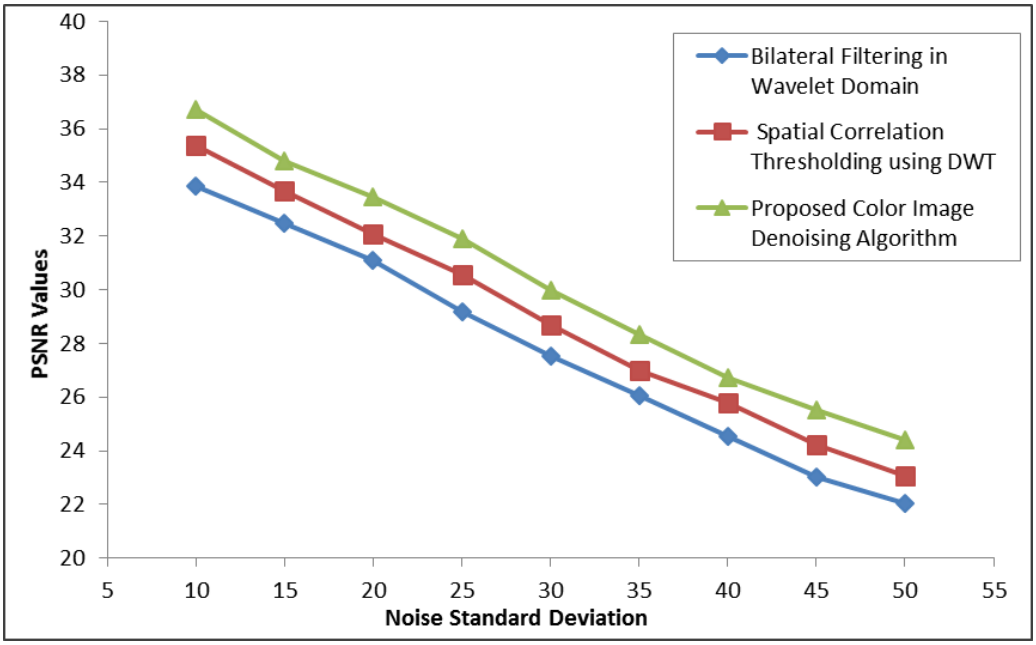

Figure 5.16: PSNR performance graphs for *Mandrill* color image

eliminates the higher noise components in details subbands without disturbing the images realness as compared to spatially adaptive coefficients thresholding scheme based IDAs in standard DWTs.

5.5 Conclusions of the Chapter

The traditional wavelet shrinkage denoising has been proved to be nearly optimal for grayscale images, but they have some limitations due to decimation when used for color image denoising. These may be recovered by undecimated DWT with selective thresholding scheme.

The proposed spatial correlation of UDWT coefficients thresholding algorithm is efficient which provides higher PSNR values and better preservation of edges and color components as seen in denoised color images. It produces the higher PSNR values and color image sharpness as compared to bilateral filtering in wavelet domain and spatial correlation of DWT coefficients thresholding scheme. The denoised images from proposed spatially adaptive thresholding algorithm are much closer to the real color images and there is no blurring in the denoised color images. Subjective and objective results of the proposed IDA confirms that fine details and color components of the color images are more preserved with enhanced sharpness than the traditional EPAT both in terms of PSNR values and visual perception.

In the experimental result analysis for color image denoising given above, it is tried to determine the best spatial adaptive algorithm which preserves the image edges and color components more. Spatially correlation of wavelet coefficients using UDWT improves the performance and efficiency because it allows additional local information of the color images to be incorporated into the algorithm. This spatial correlated thresholding will be extended to various other generation of wavelet families. Similar bodies of research work may be conducted for other kinds of grayscale and color medical images.

Chapter 6

An Adaptive Image Denoising using Prefiltering in Double-density Dual Tree Complex Wavelet Transform Domain

6.1 Introduction

A image gets noisy during its acquisition and transmission process mostly. In image acquisition using a camera, the amount of noise is induced due to the intensity levels and sensor temperature. The transmission channel interference also induces the noise in an image during its transmission (Gnanadurai and Sadasivam 2006). This type of noise is mainly additive in nature and is called AWGN (Zhang and Desai 1998). The induced noise in image poses degradations in the visual quality and automated analysis operations. It must be removed before further processing of the image[1]. Noise reduction or image denoising is a very important and necessary pre-processing in image processing era. The multiresolution analysis achieved by DWT has been confirmed to be efficient proceeding in image denoising and compression. The early application of the classical orthonormal wavelet transform for reducing AGWN through wavelet coefficients thresholding is a powerful image processing tool (Bolster et al. 2003). The AWGN and image edges are always represented by high frequencies components. So it

[1]**The contents of this Chapter has been communicated in *International Journal of Signal and Imaging System Engineering*, *SCOPUS* Indexed**

is difficult to reduce AWGN from the images without blurring the edges of image. How can edges be preserved during image denoising in wavelet domain motivates for further researches. For better edges preserving, it is necessary to detect the position and orientation of the edge.

From two decade there has been a great amount of research on wavelet coefficients thresholding for image denoising (Coupier et al. 2005). A wavelet is a mathematical tool useful in digital image denoising and compression. DWT based IDAs follow the non-linear thresholding of noisy DWT coefficients. These algorithms are promoted by the sparseness property of wavelet coefficients and ignore the clustering properties. The main goal of DWT based image denoising is to suppress low amplitude wavelet coefficients which are more likely to constitute the noise, and retain high amplitude wavelet coefficients which contain the real information of the desired image. Standard DWT based image denoising using the wavelet coefficients thresholding are gaining popularity now-a-days but they are not able to represent the local information of an image. A lot of work has been done (Donoho and Johnstone 1995, Balster et al. 2005, Fodor and Kamath 2001) using DWT, it has following severe disadvantages:

- **Shift-invariance lacking:** A small shifts in the input image can generate a major variations in the output image information as a distribution of wavelet coefficients energy,
- **Lack of directional selectivity:** Poor or weak selectivity of directions for diagonal features of an image due to the separable and real wavelet filters.
- **Absence of phase information:** The details subbands don't have any idea about the phases and orientation of edges, so it does a unexpected job of separating orientations.

Actually DWT has the property of shift-variant in which transform coefficients provide un-predictably results under minor shifts of input image. Standard DWT also has weak directional selective due to three different spatial-feature orientations, but the edges in an image can have multiple orientations.

Shift sensitivity implies that an input image changes cause an unpredictable changes in the output DWT coefficients. A minor shifts in the input image can cause major variations in the output image information as a distribution of energy between DWT coefficients at different scales. This is an undesirable property, making DWT not suited for some applications like image denoising more accurately.

The shift-sensitivity of standard DWT is avoided by the down-samplers followed by up-samplers from DWT's filter-bank implementation.

DT-CWT is a very elegant computational structure given by Kingsbury, which displays near-shift invariant properties. The DT-CWT generates the real and imaginary parts of complex wavelet coefficients using a dual tree of real wavelet filters (Kumar et al. 2014). A limited amount of redundancy is achieved by DT-CWT. An approximate shift-invariance and directional selectivity is provided by this filter for preserving the image fine details through the perfect reconstruction.

The same filters at all decomposition levels are used in double-density wavelet transform. Double-density DT-CWT (DDT-CWT) performs better than the standard DWT and DT-CWT in terms of results enhancement and efficiency. A dominant spatial orientation is provided by the DDT-CWT by utilizing more wavelets and it combines the better characteristics of both the Double-density DWT and the DT-CWT. Basically DDT-CWT used two scaling functions and four distinct wavelet functions in the form of two pairs. Two wavelet functions of the first pair are offset and an approximate Hilbert transform pair is performed by other pair of wavelets (Chaux et al. 2007). Two wavelet are generated in the same dominating orientations.

The input image is corrupted with AWGN of zero mean and noise variance ${sigma_n}^2$. Since the DDT-CWT follows a linear transform, the coefficients of noisy image can be written as:

$$\tilde{I}(x, y) = I(x, y) + \eta(x, y) \tag{6.1}$$

where $\tilde{I}(x, y)$ represents the noisy image, $I(x, y)$ is the original image and $\eta(x, y)$ is the induced noise. Mainly two type of noises follow this noise model AWGN and salt-and-pepper noise.

After the DDT-CWT is performed on the noisy image, it is needed to do thresholding. The wavelet coefficients thresholding is achieved by shrinkage rule and shrinkage function. The shrinkage rule is how to calculate the threshold and shrinkage function is how to apply the calculated threshold value to the noisy DWT coefficients. Researchers published different thresholding schemes for the threshold estimation and its application. The noisy coefficients are retained by selecting small threshold value and the fine details of images are smoothened by large threshold value. The threshold value may be

adaptive and non-adaptive approach across the wavelet scales and locations.

In the DDT-CWT domain, the image information is wholly directed in few significant coefficients but the noise is uniformly spread within all other coefficient subbands. The noise standard deviation of a noisy image is computed from the real part of first decomposition level using standard formula given in Chapter 1. This noise standard deviation is used for each type of threshold value calculation. Bayes Shrink is a guided adaptive threshold for image denoising and used in this work. The threshold value is calculated here by minimizing the Bayesian Risk (Ertuzun and Bala 2002). The threshold application is called shrinkage function.

The wavelet coefficients less than the calculated threshold are removed and remaining are left unchanged in hard thresholding scheme. But this scheme causes over-smoothen of fine details of the images due to removing the wavelet coefficients larger than threshold. Soft thresholding based on DDT-CWT is used here to recover the demerits of hard thresholding (Athira and George 2014). The wavelet coefficients smaller than the threshold value are removed while larger wavelet coefficients are reduced by the absolute threshold value itself using soft thresholding scheme. After removing the small DDT-CWT noisy coefficients from all the details subbands, image reconstruction is performed using the same wavelet function type and version as used at the time of decomposition of the noisy image. In this way, the image reconstruction is the exact reverse process of wavelet decomposition by finding the inverse.

During the image denoising, the important features like edges, textures etc are also well preserved due to shift-invariance and directional selectivity features of DDT-CWT. The characteristic of edges has the great significance for the visual perception of an image. So the edge preserving during the image denoising is the necessary pre-processing for further image processing.

6.2 Wiener Filtering using DWT

In this section, Wiener filtering using DWT and image denoising using different versions of CWT are discussed here with their theory background and applications. The Wiener filter is a minimum MSE filter. The multiresolution Wiener filter reduces the noise very well in the smooth and non-smooth

regions like edges and textures. It is used to reduce the AWGN with zero-mean from a corrupted images. Wiener filtering is based on the noise power *i.e.* variance of noise in a corrupted images. When the noise variance is large, the Wiener filter performs little smoothing *i.e.* less noise reducing. For small noise variance, more smoothing is performed by this filter and reduces the sharpness of the image. The drawback of traditional Wiener filtering is covered by multiresulation Wiener filtering (Athira and George 2014).

The noisy image is decomposed using DWT which gives one approximation subband and three details subbands. The Wiener filtering is applied on the approximation subband only. All the details subbands are thresholded using the soft thresholding. It reduces the AWGN very well and achieves the deblurring simultaneously. The overall MSE is minimized by Wiener filtering through the operations of smoothing noise and inverse filtering . The original image is a linearly estimated to the original image corrupted with AWGN.

The Wiener filter simplifies the images denoising corrupted with AWGN and no blurring:

$$G(u,v) = \frac{P_s(u,v)}{P_s(u,v) + \sigma_n^2} \tag{6.2}$$

where σ_n^2 represents the variance of noise.

Wiener filters are able to reconstruct images degraded by AWGN. Wiener filters in wavelet domain is comparatively provides the better results as compared its traditional version in frequency domain filtering. Wiener filter requires to estimate the covariance matrix of the image. It can be proved that if both the image and noise follow the Gaussian distribution then Winer filtering is the best possible MSE estimator .

The above expression for a Wiener filter is applied over the whole image in general. Standard Wiener filter does a good job in deblurring and denoising. The Wiener filter gives the better results for a noisy image with same local statistics within the image. The first order statistics in most natural images vary from one part of an image to another and hence traditional Wiener filter performs poorly in the presence of large noise in spatial domain.

6.3 Image Denoising using Dual Tree Complex Wavelet Transform

Kingsbury also introduced the DT-CWT, with additional properties of perfect reconstruction with approximate shift-invariance. Two unique sets of separable 2*D* wavelet bases are utilized to implement the 2*D* DT-CWT. The shift-invariance and directionally selectivity are the main features of DT-CWT in two and higher dimensions and so it is considered as one of the recent improvement of the standard DWT. Normally it is achieved with a factor of redundancy of 2*D* for *D*-dimensional images, which is more lower than the UDWT. A computationally efficient multidimensional DT-CWT with separable filter bank are used (Kumar et al. 2014).

The subband images associated with the DT-CWT. Since the energy with each subband image at any given decomposition level remains constant despite of shift, the DT-CWT is therefore shift-invariant. Unlike DWT which combines positive and negative frequencies and produces three subband images at each decomposition level, the DT-CWT treats positive and negative frequencies separately and produces six subband images at each level. Each subband contains wavelet coefficients whose magnitudes are proportional to one of the ± 15 degree, ± 45 degree, ± 75 degree directional orientations of the input signal. Because positive and negative orientations are taken into account individually, the DT-CWT provides greater directional selectivity than that of DWT.

6.4 Proposed Image Denoising Algorithm

By introducing CWT concept, DDT-CWT is achieved by combining the double-density DWT and DT-CWT. The images are decomposed into real and imaginary parts using CWT. The amplitude of coefficients is calculated by real coefficients and phase information is computing by imaginary coefficients. The real part is represented by first wavelet and an imaginary part is represented by second wavelet in each direction. Total four 2*D* double-density DWTs are used in parallel with each filter set for the rows and columns for DDT-CWT implementation. Then 32 oriented wavelets are achieved by the different subband images sum and differences.

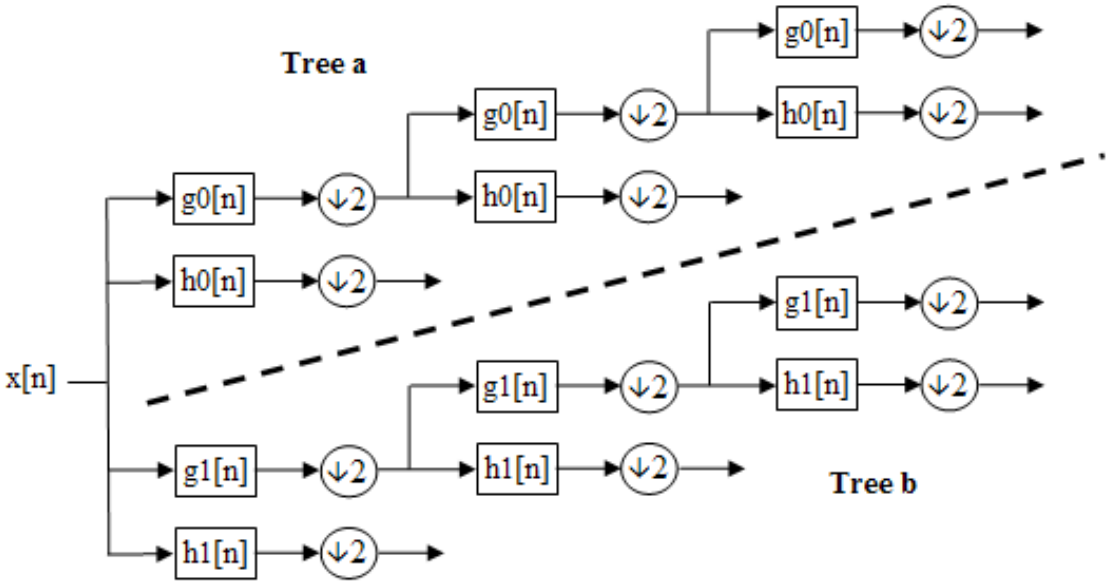

Figure 6.1: 2D DT-CWT Decomposition

Figure 6.2 shows that design implementation of DDT-CWT with details. The DDT-CWT is an over-complete DWT with the characteristics of DWT with double-density and with the dual-tree form. As the decomposition level increases, SNR of the subband usually become smaller *i.e.* the noise becomes higher. The edges and texture of an image are disturbed more after coefficients thresholding which are significant for the image quality and visual perception.

Kingsbury introduced a very elegant computational structure known as DT-CWT, which displays near-shift invariant properties (Kumar et al. 2014). The DT-CWT generates the real and imaginary parts of complex wavelet coefficients by using a dual tree of real wavelet filters. A limited amount of redundancy is achieved by this and also it provided shift-invariance and directionally selectivity approximate filters. DT-CWT recovers the perfect reconstruction properties and computational efficiency. After the DT-CWT is performed on the noisy image, it is needed to do thresholding. The threshold is calculated using Bayesian estimator from the real part of DT-CWT.

The other decomposition types may also be used for a complex wavelet transforms. One scaling and two wavelet filters for row and column filtering can create a double-density wavelet transform. Same filters at all stages are used by the traditional double-density wavelet transform (Bhonsle and Dewangan 2012). The real part 'realdt' and imaginary part 'cplxdt' provide the oriented dual-tree

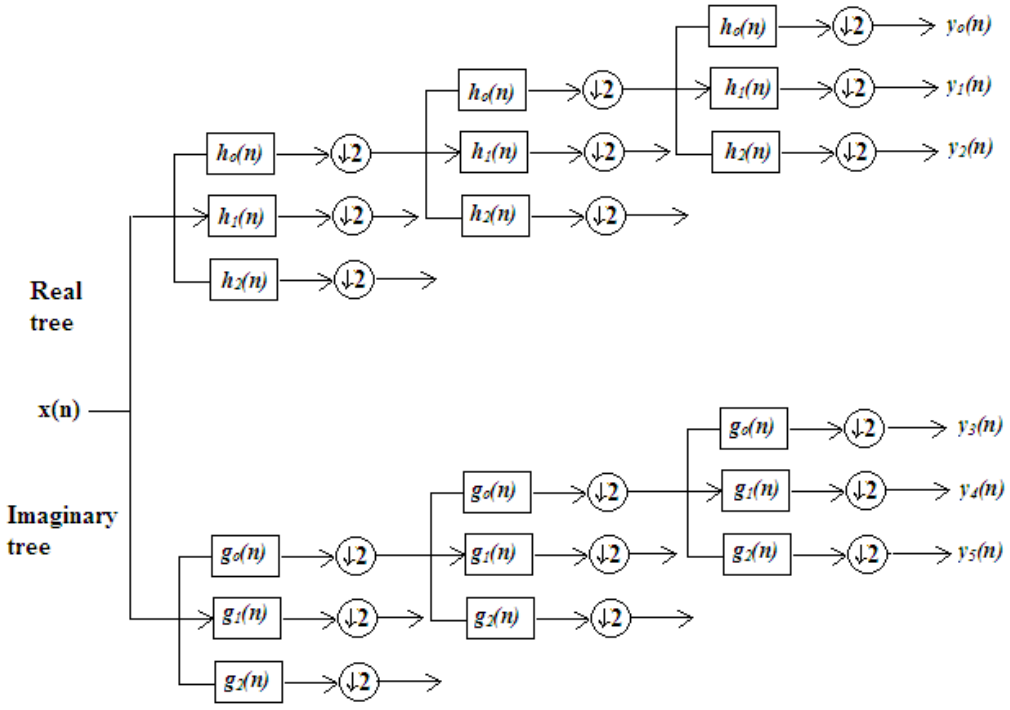

Figure 6.2: Double-density DT-CWT

wavelet transforms using two scale and four wavelet transforms separately. Similarly the real part 'realdddt' and imaginary part 'cplxdddt' provide a type of DDT-CWT. Different filters are used for the first decomposition level to implement the DDT-CWT for noisy images.

The DDT-CWT has higher redundancy than standard DWT but lower than DT-CWT implementation. A redundancy of 2-*D* is provided by the *D*-dimensional DT-CWT (Bhonsle and Dewangan 2012). When the structure is repeated indefinitely, the rate of oversampling is achieved $8/3$ for a critically sampled 2-*D* filter banks. The steerable pyramid is also used to achieve an over-complete image decomposition (Bo et al. 2007). These filter banks are specially designed to give orientation information of image components.

6.5 Experimental Results and Their Analysis

This proposed denoising algorithm for different structural images has been implemented using MATLAB. In this work, different gray scale images of size 512×512 are considered with all noise densities of AWGN induced in the images. The results are analyzed subjectively by visual perception and ob-

Algorithm 6.1 Proposed IDA using Adaptive Thresholding in DDT-CWT:

1: Load the test image and make it corrupted with AWGN to obtain a noisy image.
2: The noisy image is first prefiltered using standard Wiener filtering.
3: Then filtered image is decomposed using DDT-CWT which gives real and imaginary parts:
    a) The double-density DWT of noisy images are obtained first,
    b) Then obtain the DT-CWT of above double-density wavelet transformed images.
4: There are six subbands presented by two scaling functions and four unique wavelets of the approximation coefficients.
5: The noise standard deviation is calculated using the equation (1.16). This is used to compute the noise variance for each details subband of current decomposition level.
6: The threshold value is computed based on these variances by using Bayesian estimator.
7: Soft thresholding is applied with all of the details wavelet coefficients.
8: This is repeated for next higher decomposition level.
9: Inverse DDT-CWT is performed on the thresholded wavelet coefficients to obtain the reconstructed image.

jectively by PSNR for different values of noise standard deviation.

6.5.1 Objective Evaluation

The objective analysis of all the algorithms is given by comparing the calculated PSNR in dB, as it is more suitable in image denoising. The PSNR table for all algorithms illustrates the comparison of six images of different structure among Wiener filtering in wavelet domain, image denoising using DT-CWT and image denoising using pre-processing in DDT-CWT domain on the basis of PSNR values. Further, output PSNR have been compared and analyzed for these IDAs at different noise standard deviation from 10 to 50 respectively (low, medium and high), as shown ahead in Tables. The IDA which results in higher PSNR values is better IDA compared those having lower values of PSNR.

Table 6.1: PSNR values for various noise standard deviations of different images

Noise Std. σ_n	Wiener Filtering in WD	DT-CWT based Denoising	Proposed Algorithm
	Barbara		

10	32.4626	34.3050	36.5303
15	30.8038	32.5710	34.3013
20	29.5128	30.8402	31.5471
25	27.8862	29.3705	30.7353
30	26.6742	28.1565	29.7411
35	25.5809	27.2405	28.6460
40	24.3122	26.0896	27.5627
45	23.1414	25.7308	26.3426
50	22.2502	24.8178	25.4507
	Peppers		
10	33.8177	35.2693	36.5372
15	32.0203	33.4632	34.9174
20	30.6729	31.8965	33.2499
25	29.5718	30.7390	31.9521
30	28.5186	29.6802	**30.8917**
35	27.3892	28.7034	**29.6104**
40	26.1516	27.5993	**28.5915**
45	25.0013	26.2310	**27.3516**
50	23.4088	24.7864	**26.2056**
	Lena		
10	32.7352	34.3134	36.1087
15	30.8312	32.3733	34.2146
20	29.2126	30.8402	32.3896
25	27.4903	29.2165	31.0314
30	26.1437	27.4865	29.4561
35	24.7809	26.2505	28.0037
40	23.3122	24.8096	26.4805

45	22.3414	23.7813	25.3129
50	21.4718	22.5878	24.1509
	Mandrill		
10	31.5314	33.2756	35.3543
15	30.3448	32.0359	33.4364
20	28.9613	30.4672	31.8478
25	27.7767	29.2935	30.4834
30	26.6242	27.9715	**29.2116**
35	25.7063	26.8050	**28.0255**
40	24.6213	25.7093	**27.2657**
45	23.5464	24.6932	**26.1439**
50	22.6012	24.8882	**25.3508**
	Child		
10	32.8583	34.6431	36.3429
15	31.3734	33.0321	34.7306
20	29.3875	31.2307	32.8041
25	27.9863	29.8923	31.2367
30	26.5506	28.5695	29.9650
35	25.4982	27.4320	**29.0928**
40	24.3316	26.8028	**27.8570**
45	23.2772	26.4372	**26.9961**
50	22.1923	25.9594	**25.6365**
	Bird		
10	32.3401	34.2751	35.9807
15	30.8720	32.8932	33.3621
20	29.8382	31.2329	32.5742
25	28.5095	30.3352	31.5141

30	27.3656	29.1591	30.6762
35	26.7531	28.0592	**29.5247**
40	25.6223	27.2327	**28.8322**
45	24.4410	26.3725	**27.6042**
50	23.3527	25.2782	**26.7593**

6.5.2 Subjective Evaluation

The different grayscale images of size 512×512 are taken as sample noisy images with different noise standard deviations. The kind of noise is AWGN with standard deviations from 10 to 50 for each IDA with proposed one. The denoised images with PSNR values from all the IDAs are shown for three level of noise standard deviations *i.e.* the low, medium, high values respectively. The experimental results confirm about the better performance of proposed IDA in edge preserving image denoising using prefiltering and gives improved results in form of PSNR values as given in the Table 6.1 and visual perception as shown in denoised images.

(i) Original *Barbara* Image | (ii) Noisy *Barbara* Image | (iii) Denoised by Wiener filtering | (iv) Denoised by DT-CWT | (v) Denoised by proposed algorithm

Figure 6.3: Noise standard deviation=15, PSNR=30.8038, PSNR=32.5710 and PSNR=34.3013

6.6 Performance Analysis

This proposed IDA is compared subjectively and objectively with state-of-art algorithms to present its denoising effectiveness. A combined graph of all these IDAs are plotted with noise standard deviation at x-axis and PSNR value at y-axis for all level of noise standard deviation from **low** to **high** *i.e.* from

(i) Original *Barbara* Image | (ii) Noisy *Barbara* Image | (iii) Denoised by Wiener filtering | (iv) Denoised by DT-CWT | (v) Denoised by proposed algorithm

Figure 6.4: Noise standard deviation=25, PSNR=27.8862, PSNR=29.3705 and PSNR=30.7353

(i) Original *Barbara* Image | (ii) Noisy *Barbara* Image | (iii) Denoised by Wiener filtering | (iv) Denoised by DT-CWT | (v) Denoised by proposed algorithm

Figure 6.5: Noise standard deviation=35, PSNR=25.5809, PSNR=27.2405 and PSNR=28.6460

(i) Original *Peppers* Image | (ii) Noisy *Peppers* Image | (iii) Denoised by Wiener filtering | (iv) Denoised by DT-CWT | (v) Denoised by proposed algorithm

Figure 6.6: Noise standard deviation=15, PSNR=32.0203, PSNR=33.4632 and PSNR=34.9174

(i) Original *Peppers* Image | (ii) Noisy *Peppers* Image | (iii) Denoised by Wiener filtering | (iv) Denoised by DT-CWT | (v) Denoised by proposed algorithm

Figure 6.7: Noise standard deviation=25, PSNR=29.5718, PSNR=30.7390 and PSNR=31.9521

10 to 50.

(i) Original *Peppers* Image | (ii) Noisy *Peppers* Image | (iii) Denoised by Wiener filtering | (iv) Denoised by DT-CWT | (v) Denoised by proposed algorithm

Figure 6.8: Noise standard deviation=35, PSNR=27.3892, PSNR=28.7034 and PSNR=29.6104

(i) Original *Lena* Image | (ii) Noisy *Lena* Image | (iii) Denoised by Wiener filtering | (iv) Denoised by DT-CWT | (v) Denoised by proposed algorithm

Figure 6.9: Noise standard deviation=15, PSNR=30.8312, PSNR=32.3733 and PSNR=34.2148

(i) Original *Lena* Image | (ii) Noisy *Lena* Image | (iii) Denoised by Wiener filtering | (iv) Denoised by DT-CWT | (v) Denoised by proposed algorithm

Figure 6.10: Noise standard deviation=25, PSNR=27.4792, PSNR=29.2165 and PSNR=31.0314

(i) Original *Lena* Image | (ii) Noisy *Lena* Image | (iii) Denoised by Wiener filtering | (iv) Denoised by DT-CWT | (v) Denoised by proposed algorithm

Figure 6.11: Noise standard deviation=35, PSNR=24.7809, PSNR=26.2505 and PSNR=28.0037

In the performance of the proposed algorithm, the major factor is the application of pre-processing in DDT-CWT based IDA. It helped in preserving edges and other fine details in denoised images

(i) Original *Mandrill* Image | (ii) Noisy *Mandrill* Image | (iii) Denoised by Wiener filtering | (iv) Denoised by DT-CWT | (v) Denoised by proposed algorithm

Figure 6.12: Noise standard deviation=15, PSNR=30.3448, PSNR=32.0359 and PSNR=33.4364

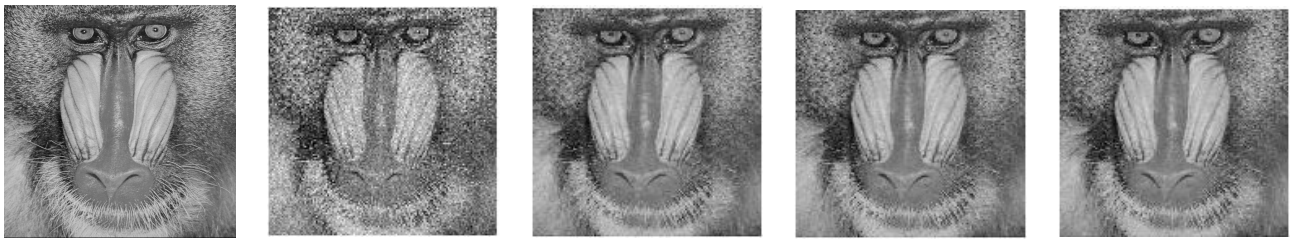

(i) Original *Mandrill* Image | (ii) Noisy *Mandrill* Image | (iii) Denoised by Wiener filtering | (iv) Denoised by DT-CWT | (v) Denoised by proposed algorithm

Figure 6.13: Noise standard deviation=25, PSNR=27.7767, PSNR=29.2935 and PSNR=30.4834

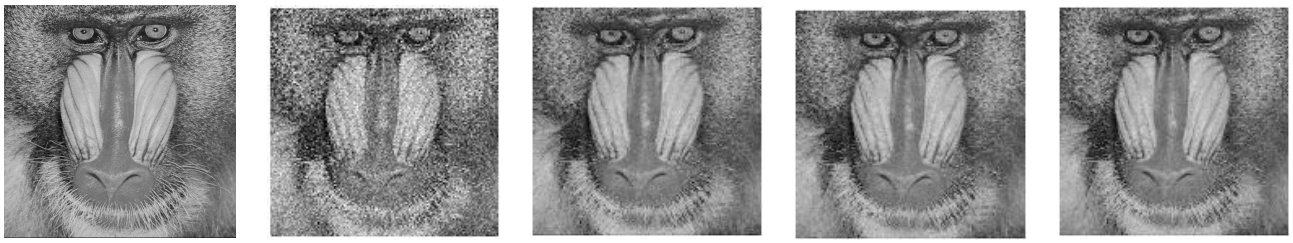

(i) Original *Mandrill* Image | (ii) Noisy *Mandrill* Image | (iii) Denoised by Wiener filtering | (iv) Denoised by DT-CWT | (v) Denoised by proposed algorithm

Figure 6.14: Noise standard deviation=35, PSNR=25.7063, PSNR=26.8050 and PSNR=28.0255

(i) Original *Child* Image | (ii) Noisy *Child* Image | (iii) Denoised by Wiener filtering | (iv) Denoised by DT-CWT | (v) Denoised by proposed algorithm

Figure 6.15: Noise standard deviation=15, PSNR=31.3734, PSNR=33.0321 and PSNR=34.7306

more. This adds strength in the proposed algorithm as the components of additive noise can be reduced better in all details subbands as compared to traditional DWT domain and DT-CWT domain

(i) Original *Child* Image | (ii) Noisy *Child* Image | (iii) Denoised by Wiener filtering | (iv) Denoised by DT-CWT | (v) Denoised by proposed algorithm

Figure 6.16: Noise standard deviation=25, PSNR=27.9863, PSNR=29.8923 and PSNR=31.2367

(i) Original *Child* Image | (ii) Noisy *Child* Image | (iii) Denoised by Wiener filtering | (iv) Denoised by DT-CWT | (v) Denoised by proposed algorithm

Figure 6.17: Noise standard deviation=35, PSNR=25.4982, PSNR=27.4320 and PSNR=29.0928

(i) Original *Bird* Image | (ii) Noisy *Bird* Image | (iii) Denoised by Wiener filtering | (iv) Denoised by DT-CWT | (v) Denoised by proposed algorithm

Figure 6.18: Noise standard deviation=15, PSNR=30.8720, PSNR=32.8932 and PSNR=33.3621

(i) Original *Bird* Image | (ii) Noisy *Bird* Image | (iii) Denoised by Wiener filtering | (iv) Denoised by DT-CWT | (v) Denoised by proposed algorithm

Figure 6.19: Noise standard deviation=25, PSNR=28.5095, PSNR=30.3352 and PSNR=31.5141

IDAs. The Wiener filter in wavelet domain performs better in flatten image like *Lena*, but not for more complex image like *Peppers* as shown from the graphs.

(i) Original *Bird* Image | (ii) Noisy *Bird* Image | (iii) Denoised by Wiener filtering | (iv) Denoised by DT-CWT | (v) Denoised by proposed algorithm

Figure 6.20: Noise standard deviation=35, PSNR=26.7531, PSNR=28.0592 and PSNR=29.5247

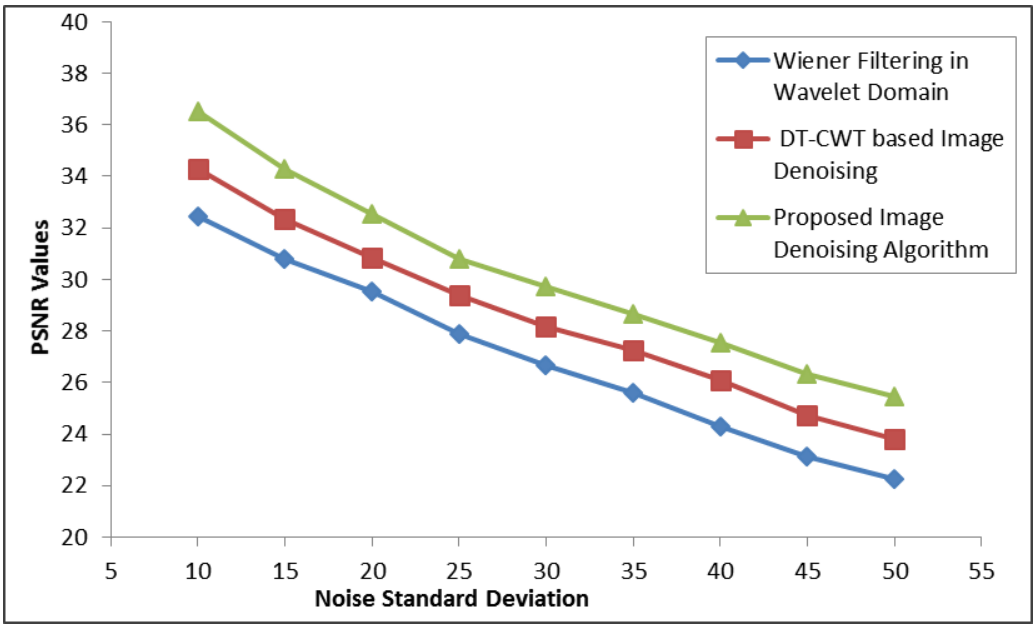

Figure 6.21: PSNR performance graphs for *Barbara* image

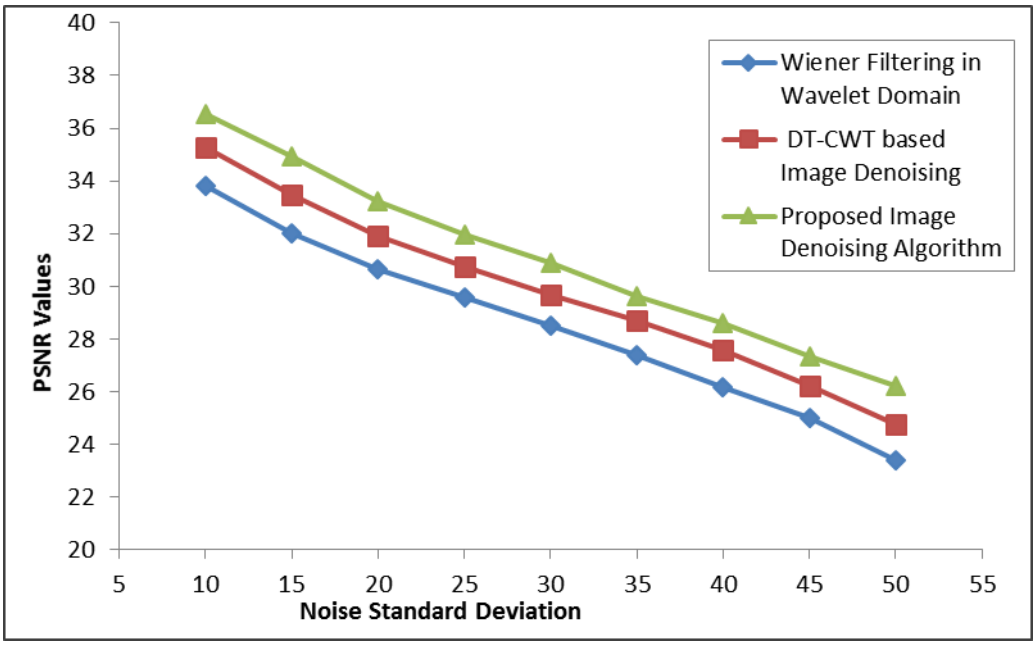

Figure 6.22: PSNR performance graphs for *Peppers* image

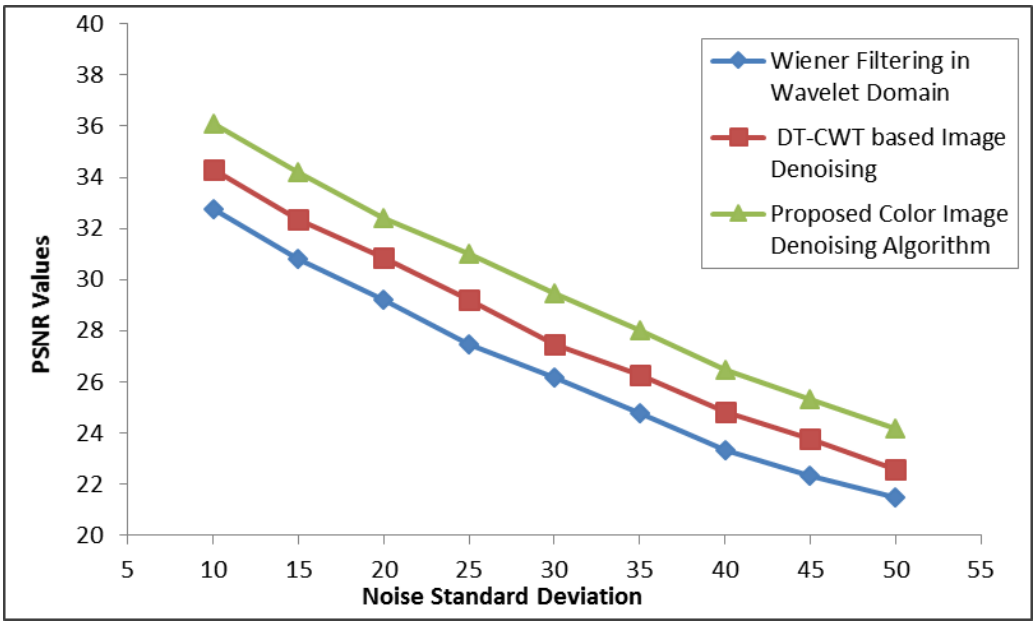

Figure 6.23: PSNR performance graphs for *Lena* image

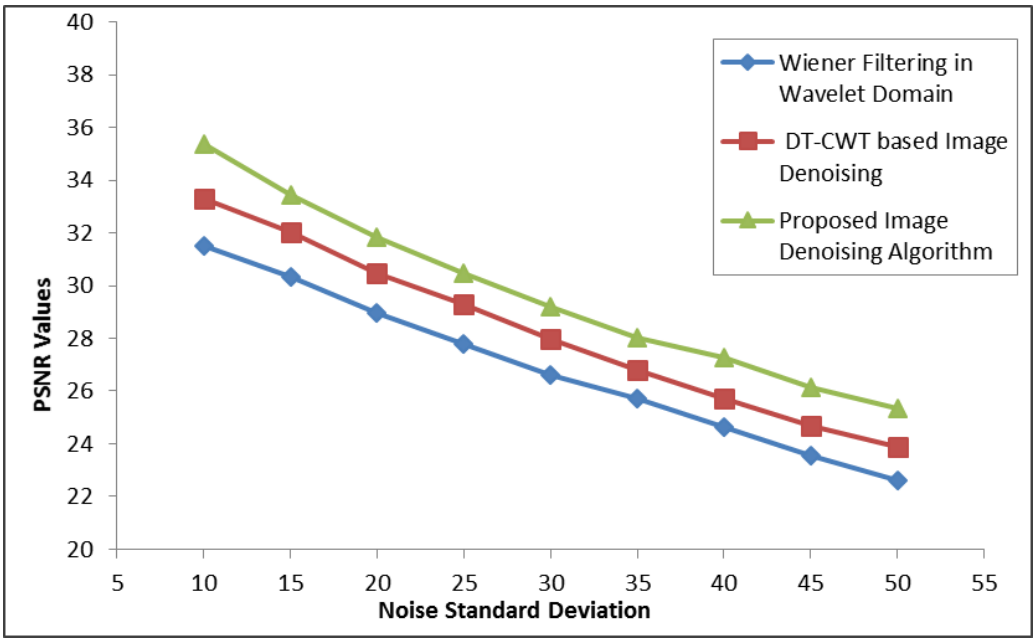

Figure 6.24: PSNR performance graphs for *Mandrill* image

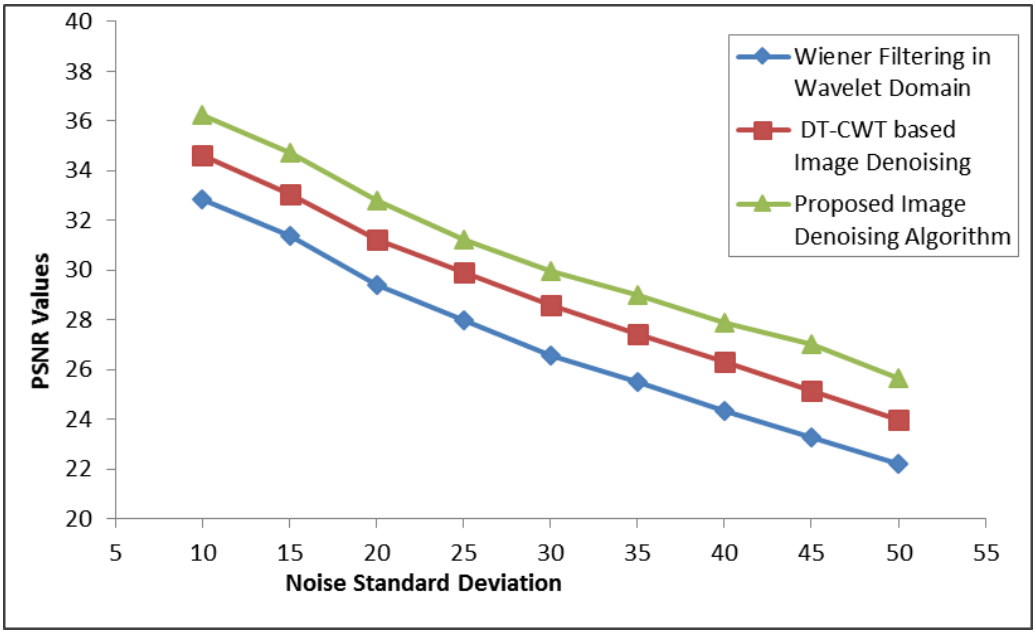

Figure 6.25: PSNR performance graphs for *Child* image

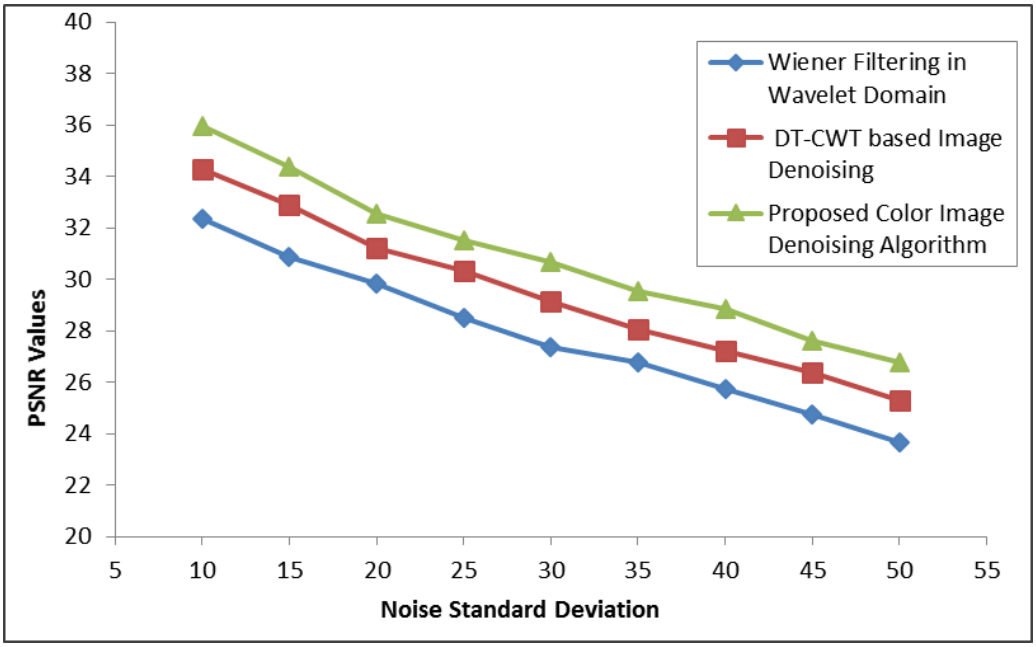

Figure 6.26: PSNR performance graphs for *Bird* image

6.7 Conclusions of the Chapter

The objective of this work is to provide a comparative results analysis between newly proposed complex wavelet transform IDA with the existing IDAs. Traditional DWT does not provide satisfactory results due to the absence of shift-invariance and weak selectivity of directions. The Wiener filter using DWT reduces the noise vary well in the smooth regions of an image but performs poorly near the image edges and corners.

In this work, DDT-CWT based IDA has been proposed which minimizes drawbacks of IDAs in wavelet domain and Wiener filtering in wavelet domain. Selection of wavelet coefficients thresholding is adaptive which allows additional local information like identification of smoothen or edge regions of the image to be included into the proposed algorithm. This enhances the visual quality of the denoised image and it looks like original image. This algorithm can be extended to wavelet packet domain and multichannel images.

Chapter 7

Conclusions and Future Scope

7.1 Conclusions

Thesis entitled **Efficient Algorithms for Image Denoising using Wavelets** focuses on the efficiency enhancement of IDAs for grayscale and color images corrupted. In an efficient image denoising, the fine details and color components must be preserved as much as possible as these are normally disturbed by image denoising process as the frequency spectrum of image fine details and noise are same.

Spatial domain IDAs operate directly on noisy pixels. All the linear IDAs in spatial domain over-smoothen the fine details of the noisy images and may induce some artifacts in the denoised images. The limitations of linear IDAs in spatial domain have been improved through non-linear IDAs by many researchers with better subjective and objective results. The non-linear IDAs reduce the noise without any attempts to identify the spectra of noise and the original image structure explicitly.

All adaptive IDAs are analyzed for different densities of AWGN in the images of different structures. The noise densities from the standard deviations of 10 to 50 are taken in consideration in this work. The grayscale and color images of simple structure like a snap of Child, Lena *etc.* and more complex images like Peppers, Mandrill *etc.* are taken for all the reported in literature and proposed IDAs. Different types of wavelet families with different vanishing moments are analyzed for all the IDAs for grayscale and color images.

The proposed EPAT scheme is superior which provides higher PSNR as given in PSNR comparison Table 3.1 and better edge preserving as shown in denoised images using Daubechies wavelet with eight vanishing moments ($Db8$). It provides the better PSNR value for higher noise standard deviations and image sharpness compared to multiresolution bilateral filtering and BM3D filtering algorithms. The denoised images from EPAT scheme are much closer to the real images and there is no blurring in the denoised images for both grayscale and color. It has been observed that EPAT scheme is also effective for noise standard deviations higher than 35 as shown in the performance analysis graphs given in Figures 3.1 to 3.6. Different wavelet types with different vanishing moments are analyzed, out of these, $Db8$ gives better results for all noise densities and complex image structures.

When an image is corrupted with AWGN, the EPAT scheme based image denoising has provided better experimental results. As the fine details of an image especially edges may be over-smoothen during the traditional image denoising in wavelet domain. Morphological operations are used for recovering the over-smoothing of edges or extraction of other features of images. The concatenating morphological opening with closing can improve the experimental results more efficiently.

The proposed efficient EPAT algorithm provides higher PSNR and better edge preserving than traditional wavelet based IDAs as seen from denoised images and PSNR comparison using Daubechies ($Db3$ and $Db8$) wavelets as shown in performance graphs. It produces the better PSNR values and image sharpness for higher noise standard deviations compared to multiresolution bilateral filtering and edge preserving IDA proposed in Chapter 3. The output denoised images from proposed algorithm are much closer to the real images and there is no blurring in the them.

EPAT based IDA is performed better than that of bilateral filtering in wavelet domain for medium level of noise standard deviations. The proposed adaptive thresholding scheme performs much better than the bilateral filtering in wavelet domain for higher noise standard deviations. All denoised images and PSNR results of the proposed denoising algorithm show that edges of the test images are more preserved with enhanced sharpness than the traditional adaptive thresholding based algorithms.

The standard DWT is widely used in image denoising because it provides localization in both time and frequency domain but it suffers some deficiency in handling the fine details and color components of images very well. When a color image is corrupted with AWGN, the traditional wavelet coefficients

thresholding based image denoising has been proved an optimal technique for graycale images, but they have some drawbacks when used for color image denoising

UDWT is widely used in many applications because it provides the solution of each drawbacks of traditional DWT. Specially, UDWT based spatially correlated coefficients thresholding provides better results for a color image corrupted with AWGN. The basic features of UDWT like shift-invariance and directional selectivity perform better in preserving the color components and other fine details of color images.

All considered algorithms for comparison are spatially adaptive in denoising the color images. Each of these algorithms are analyzed and compared in terms of the PSNR values and visual perception. The proposed spatial correlation of UDWT coefficients thresholding algorithm which provides higher PSNR and better edge and color components. It produces the better PSNR values and color image sharpness compared to bilateral filtering in wavelet domain and spatial correlation of DWT coefficients thresholding. The output parameters from proposed spatially adaptive thresholding algorithm are much closer to the parameters of original image. Subjective and objective results of the proposed denoising algorithm show that edges of the test images are more preserved with enhanced sharpness than the traditional EPAT scheme both in terms of PSNR values and visual perception.

This work proposed a comparative analysis between newly designed complex wavelet transform IDA with the existing IDAs. Traditional DWT does not provide satisfactory results due to the lack of shift-invariance and poor directional selectivity. The Wiener filter in the wavelet domain reduces the noise pretty well in the smooth regions but performs poorly along the edges and other fine details of the images as reported in literature.

The major factor is the application of pre-processing in DDT-CWT based IDA is to reduce the heavy additive noises. In this proposal, edge preserving and other fine details in denoised images are achieved more in all subbands as compared to traditional DWT domain and DT-CWT domain image denoising. The Wiener filter in wavelet domain performs better in flatten image in snaps like *Barbara*, but not in more complex structural images like *Mandrill* as shown from the graphs. The proposed DDT-CWT based IDA minimizes pitfalls of wavelet based IDAs and Wiener filtering in wavelet domain.

7.2 Future Scope

In the experimental analysis, the best adaptive thresholding scheme which preserve the image edges and other fine details more is finalized. The drawbacks of bilateral filtering, BM3D filtering can be eliminated by using edge preserving adaptive wavelet coefficients thresholding scheme. Spatially correlation of wavelet coefficients using UDWT can improve the performance and efficiency because it considers additional local information of the color images (identification of color components or edge regions) to be included into the algorithm. DDT-CWT based IDA has been proposed which minimizes limitations of standard DWT based IDAs and Wiener filtering in wavelet domain.

In the experimental result analysis for color image denoising, it is tried to determine the best adaptive algorithm which preserve the image edges and color components more. The drawbacks of bilateral filtering and spatially correlation thresholding using DWT can be recovered by using spatially correlated wavelet coefficients thresholding using UDWT. Spatially correlation of wavelet coefficients using UDWT can improve the performance and efficiency because it considers additional local information of the color images (identification of color components or edge regions) to be included into the algorithm. The spatial correlated thresholding may be extended to various other wavelet families depending upon the number of vanishing points. This thresholding scheme may also be extended to various complex wavelets like DT-CWT and DDT-CWT domain, which yield better results while preserving the color image fine details. Similar bodies of research work may be conducted for other kinds of grayscale and medical images.

In this work, DDT-CWT based IDA has been proposed which minimizes drawbacks of wavelet based IDAs and Wiener filtering in wavelet domain. The adaptive wavelet coefficients thresholding scheme in DDT-CWT domain allows additional local information like smoothen or edge regions identification of the image very well. It will enhance the visual quality of the denoised images and they will look like original image with their fine details preserving. This algorithm can be extended to wavelet packet domain and for color images. In briefing, further enhancement of thesis work will be completed by considering these points:

- Advance transform like Counterlet and Curvelet Transforms can make IDA more efficient by

preserving the curved edges.

- Spatially adaptive threshold selection can preserve all the fine details and color components well.
- Hybrid thresholding application can enhance the performance.
- The work can be extended to denoisie non-square images directly.
- Joint use of traditional and DWT based IDA can improve the results.
- The efficiency of an IDA may be enhanced by using EPAT in multiwavelets and wavelet packets.
- The same work can be extended to other type of images like Medical, SAR, Multispectral etc.

Bibliography

Abramov, S., Krivenko, S., Roenko, A., Lukin, V., Djurović, I. and Chobanu, M.: 2013, Prediction of filtering efficiency for dct-based image denoising, *2013 2nd Mediterranean Conference on Embedded Computing*, IEEE, pp. 97–100.

Abramovich, F. and Benjamini, Y.: 1996, Adaptive thresholding of wavelet coefficients, *Computational Statistics & Data Analysis* **22**(4), 351–361.

Athira, T. and George, G. C.: 2014, Complex wavelet transform based image denoising and zooming under the lmmse framework, *International Journal of Computer, Electrical, Automation, Control and Information Engineering* **8**(6), 1034–1037.

Azzalini, A., Farge, M. and Schneider, K.: 2005, Nonlinear wavelet thresholding: A recursive method to determine the optimal denoising threshold, *Applied and Computational Harmonic Analysis* **18**(2), 177–185.

Bacchelli, S. and Papi, S.: 2004, Filtered wavelet thresholding methods, *Journal of Computational and Applied Mathematics* **164**, 39–52.

Bala, E. and Ertüzün, A.: 2005, A multivariate thresholding technique for image denoising using multiwavelets, *EURASIP Journal on Applied Signal Processing,* pp. 1205–1211.

Balster, E. J., Zheng, Y. F. and Ewing, R. L.: 2005, Feature-based wavelet shrinkage algorithm for image denoising, *IEEE Transactions on Image Processing* **14**(12), 2024–2039.

Banham, M. R. and Katsaggelos, A. K.: 1996, Spatially adaptive wavelet-based multiscale image restoration, *IEEE Transactions on Image Processing* **5**(4), 619–634.

Basu, M.: 2002, Gaussian-based edge-detection methods-a survey, *IEEE Transactions on Systems, Man, and Cybernetics, Part C (Applications and Reviews)* **32**(3), 252–260.

Beghdadi, A. and Khellaf, A.: 1997, A noise-filtering method using a local information measure, *IEEE Transactions on Image Processing* **6**(6), 879–882.

Bhonsle, D. and Dewangan, S.: 2012, Comparative study of dual-tree complex wavelet transform and double density complex wavelet transform for image denoising using wavelet-domain, *International Journal of Scientific and Research Publications* **2**(7), 1–5.

Bhujle, H. and Chaudhuri, S.: 2014, Novel speed-up strategies for non-local means denoising with patch and edge patch based dictionaries, *IEEE Transactions on Image Processing* **23**(1), 356–365.

Blu, T. and Luisier, F.: 2007, The sure-let approach to image denoising, *IEEE Transactions on Image Processing* **16**(11), 2778–2786.

Bo, C., Zexun, G., Yang, Y. and Tianshuang, S.: 2007, Dual-tree complex wavelets transforms for image denoising, *in Proceeding of IEEE International Conference on Software Engineering, Artificial Intelligence, Networking, and Parallel/Distributed Computing*, Vol. 1, pp. 70–74.

Bolster, E., Zheng, Y. F. and Ewing, R. L.: 2003, Fast, feature-based wavelet shrinkage algorithm for image denoising, *in Proceeding of IEEE International Conference onIntegration of Knowledge Intensive Multi-Agent Systems*, pp. 722–728.

Brox, T., Kleinschmidt, O. and Cremers, D.: 2008, Efficient nonlocal means for denoising of textural patterns, *IEEE Transactions on Image Processing* **17**(7), 1083–1092.

Buades, A., Coll, B. and Morel, J.-M.: 2005a, Image denoising by non-local averaging, *in Proceeding of IEEE International Conference on Acoustics, Speech, and Signal Processing*, Vol. 2, pp. 11–25.

Buades, A., Coll, B. and Morel, J.-M.: 2005b, A review of image denoising algorithms, with a new one, *Multiscale Modeling & Simulation* **4**(2), 490–530.

Bui, T. D. and Chen, G.: 1998, Translation-invariant denoising using multiwavelets, *IEEE Transactions on Signal Processing* **46**(12), 3414–3420.

Chan, T. F. and Chen, K.: 2006, An optimization-based multilevel algorithm for total variation image denoising, *Multiscale Modeling & Simulation* **5**(2), 615–645.

Chang, S. G., Yu, B. and Vetterli, M.: 2000, Adaptive wavelet thresholding for image denoising and compression, *IEEE Transactions on Image Processing* **9**(9), 1532–1546.

Chappelier, V. and Guillemot, C.: 2006, Oriented wavelet transform for image compression and denoising, *IEEE Transactions on Image Processing* **15**(10), 2892–2903.

Chatterjee, P. and Milanfar, P.: 2012, Patch-based near-optimal image denoising, *IEEE Transactions on Image Processing* **21**(4), 1635–1649.

Chaux, C., Pesquet, J.-C. and Duval, L.: 2007, Noise covariance properties in dual-tree wavelet decompositions, *IEEE Transactions on Information Theory* **53**(12), 4680–4700.

Chen, G., Bui, T. D. and Krzyżak, A.: 2005, Image denoising with neighbour dependency and customized wavelet and threshold, *Pattern recognition* **38**(1), 115–124.

Chen, G. and Kégl, B.: 2007, Image denoising with complex ridgelets, *Pattern Recognition* **40**(2), 578–585.

Chen, P.-Y. and Lien, C.-Y.: 2008, An efficient edge-preserving algorithm for removal of salt-and-pepper noise, *IEEE Signal Processing Letters* **15**, 833–836.

Cho, D., Bui, T. D. and Chen, G.: 2009, Image denoising based on wavelet shrinkage using neighbor and level dependency, *International Journal of Wavelets, Multiresolution and Information Processing* **7**(03), 299–311.

Coifman, R. R. and Donoho, D. L.: 1995, Translation-invariant de-noising, *Wavelets and Statistics*, Springer, pp. 125–150.

Coupier, D., Desolneux, A. and Ycart, B.: 2005, Image denoising by statistical area thresholding, *Journal of Mathematical Imaging and Vision* **22**(2-3), 183–197.

Dabov, K., Foi, A., Katkovnik, V. and Egiazarian, K.: 2006, Image denoising with block-matching and 3d filtering, *Image Processing: Algorithms and Systems, Neural Networks, and Machine Learning*, Vol. 6064, pp. 1–12.

Dabov, K., Foi, A., Katkovnik, V. and Egiazarian, K.: 2009, Bm3d image denoising with shape-adaptive principal component analysis, *Signal Processing with Adaptive Sparse Structured Representations*, pp. 1–20.

Dai, S.-w., Sun, Y.-k., Tian, X.-l. and Tang, Z.-s.: 2007, Image denoising based on complex contourlet transform, *in Proceeding of IEEE International Conference on Wavelet Analysis and Pattern Recognition*, Vol. 4, pp. 1742–1747.

Danielyan, A. and Foi, A.: 2009, Noise variance estimation in nonlocal transform domain, *in Proceeding of International Workshop on Local and Non-Local Approximation in Image Processing*, pp. 41–45.

Dengwen, Z. and Wengang, C.: 2008, Image denoising with an optimal threshold and neighbouring window, *Pattern Recognition Letters* **29**(11), 1694–1697.

Donoho, D. L.: 1995, De-noising by soft-thresholding, *IEEE Transactions on Information Theory* **41**(3), 613–627.

Donoho, D. L. and Johnstone, I. M.: 1995, Adapting to unknown smoothness via wavelet shrinkage, *Journal of the American Statistical Association* **90**(432), 1200–1224.

Donoho, D. L., Johnstone, I. M., Kerkyacharian, G. and Picard, D.: 1996, Density estimation by wavelet thresholding, *The Annals of Statistics* **24**(2), 508–539.

Donoho, D. L. and Johnstone, J. M.: 1994, Ideal spatial adaptation by wavelet shrinkage, *Biometrika* **81**(3), 425–455.

Easley, G. R., Labate, D. and Colonna, F.: 2009, Shearlet-based total variation diffusion for denoising, *IEEE Transactions on Image processing* **18**(2), 260–268.

Edoh, K. and Roop, J. P.: 2009, A fast wavelet multilevel approach to total variation image denoising, *International Journal of Signal Processing, Image Processing and Pattern Recognition* **2**(3), 57–74.

Elad, M. and Aharon, M.: 2006, Image denoising via sparse and redundant representations over learned dictionaries, *IEEE Transactions on Image processing* **15**(12), 3736–3745.

Eng, H.-L. and Ma, K.-K.: 2001, Noise adaptive soft-switching median filter, *IEEE Transactions on Image Processing* **10**(2), 242–251.

Ertuzun, A. B. and Bala, E.: 2002, Applications of multiwavelet techniques to image denoising, *in proceeding of International Conference on Image Processing*, Vol. 2, pp. 581–584.

Faghih, F. and Smith, M.: 2002, Combining spatial and scale-space techniques for edge detection to provide a spatially adaptive wavelet-based noise filtering algorithm, *IEEE Transactions on Image Processing* **11**(9), 1062–1071.

Feng, J., Ding, M. and Zhang, X.: 2014, Decision-based adaptive morphological filter for fixed-value impulse noise removal, *Optik-International Journal for Light and Electron Optics* **125**(16), 4288–4294.

Fodor, I. and Kamath, C.: 2001, On denoising images using wavelet-based statistical techniques, *Lawrence Livermore National Laboratory Technical Report* .

Foi, A., Katkovnik, V. and Egiazarian, K.: 2007, Pointwise shape-adaptive dct for high-quality denoising and deblocking of grayscale and color images, *IEEE Transactions on Image Processing* **16**(5), 1395–1411.

Ge, J. and Mirchandani, G.: 2003, A simple and efficient wavelet-based denoising algorithm using joint interand intrascale statistics adaptively, *in Proceeding of International Symposium on Signal Processing and Its Applications*, Vol. 1, pp. 429–432.

Ghouti, L. and Bouridane, A.: 2005, Two-step variance-adaptive image denoising, *in Proceeding of International Conference on Image Processing*, Vol. 3, pp. 344–348.

Gnanadurai, D. and Sadasivam, V.: 2006, An efficient adaptive thresholding technique for wavelet based image denoising, *International Journal of Signal Processing* **2**(2), 114–119.

Grossmann, A., Kronland-Martinet, R. and Morlet, J.: 1989, Reading and understanding continuous wavelet transforms, *In Wavelets: Time-Frequency Methods and Phase Space* **1**, 2–20.

Hammond, D. K. and Simoncelli, E. P.: 2006, Image denoising with an orientation-adaptive gaussian scale mixture model, *in Proceeding of International Conference on Image Processing*, pp. 1433–1436.

Hamza, A. B. and Krim, H.: 2001, Image denoising: A nonlinear robust statistical approach, *IEEE Transactions on Signal Processing* **49**(12), 3045–3054.

Hassan, H. and Saparon, A.: 2011, Still image denoising based on discrete wavelet transform, *in Proceeding of International Conference on System Engineering and Technology*, pp. 188–191.

Hawwar, Y. and Reza, A.: 2002, Spatially adaptive multiplicative noise image denoising technique, *IEEE Transactions on Image Processing* **11**(12), 1397–1404.

Hedaoo, P. and Godbole, S. S.: 2011, Wavelet thresholding approach for image denoising, *International Journal of Network Security & Its Applications* **3**(4), 16–21.

Hel-Or, Y. and Shaked, D.: 2008, A discriminative approach for wavelet denoising, *IEEE Transactions on Image Processing* **17**(4), 443–457.

Hirakawa, K. and Parks, T. W.: 2006, Image denoising using total least squares, *IEEE Transactions on Image Processing* **15**(9), 2730–2742.

Ho, J. and Hwang, W.-L.: 2013, Wavelet bayesian network image denoising, *IEEE Transactions on Image Processing* **22**(4), 1277–1290.

Hongqiao, L. and Shengqian, W.: 2009, A new image denoising method using wavelet transform, *International Forum on Information Technology and Applications*, Vol. 1, pp. 111–114.

Hosseini, H., Anpalagan, A., Raahemifar, K. and Erkucuk, S.: 2016, Wavelet-based cognitive scma system for mmwave 5g communication networks, *IET Communications* **11**(6), 831–836.

Hu, J., Pu, Y., Wu, X., Zhang, Y. and Zhou, J.: 2012, Improved dct-based nonlocal means filter for mr images denoising, *Computational and mathematical methods in medicine* **2012**.

Huang, D.-A., Kang, L.-W., Wang, Y.-C. F. and Lin, C.-W.: 2014, Self-learning based image decomposition with applications to single image denoising, *IEEE Transactions on multimedia* **16**(1), 83–93.

Hui, T., Zengli, L., Lin, C. and Zaiyu, C.: 2013, Wavelet image denoising based on the new threshold function, *in Proceedings of International Conference on Computer Science and Electronics Engineering* pp. 2749–2752.

Hussain, A. J., Al-Jumeily, D., Radi, N. and Lisboa, P.: 2015, Hybrid neural network predictive-wavelet image compression system, *Neurocomputing* **151**, 975–984.

Islam, S., Balasubramaniam, S., Goyal, P., Sati, M. and Goyal, N.: 2017, A domain specific language for clustering, *in Proceeding of International Conference on Distributed Computing and Internet Technology*, Springer, pp. 231–234.

Jain, P. and Tyagi, V.: 2015, Adaptive edge-preserving image denoising using arbitrarily shaped local windows in wavelet domain, *International Journal of Computer Applications* **114**(16).

Jansen, M. and Bultheel, A.: 2001, Empirical bayes approach to improve wavelet thresholding for image noise reduction, *Journal of the American Statistical Association* **96**(454), 629–639.

Jin, F., Fieguth, P., Winger, L. and Jernigan, E.: 2003, Adaptive wiener filtering of noisy images and image sequences, *in Proceedings of International Conference on Image Processing*, Vol. 3, pp. 343–349.

Joshi, J., Nabar, N. and Batra, P.: 2006, Reconfigurable implementation of wavelet based image denoising, *International Midwest Symposium on Circuits and Systems*, Vol. 1, pp. 475–478.

Jung, C. R. and Schacanski, J.: 2001, Adaptive image denoising in scale-space using the wavelet transform, *Brazilian Symposium onomputer Graphics and Image Processing*, pp. 172–178.

Kalavathy, S. and Suresh, R.: 2011, Analysis of image denoising using wavelet coefficient and adaptive subband thresholding technique, *International Journal of Computer Science Issues* **8**(6), 166–172.

Kaur, R. and Kaur, R.: 2013, Survey of de-noising methods using filters and fast wavelet transform, *International Journal of Advanced Research in Computer Science and Software Engineering* **3**(2), 133–136.

Kervrann, C. and Boulanger, J.: 2006, Optimal spatial adaptation for patch-based image denoising, *IEEE Transactions on Image Processing* **15**(10), 2866–2878.

Khmag, A., Ramli, A. R., Al-haddad, S., Kamarudin, N. and Aqel, M. O.: 2015, Robust natural image denoising in wavelet domain using hidden markov models, *Indian Journal of Science and Technology* **8**(32), 1–9.

Krishnamoorthi, R.: 2007, Transform coding of monochrome images with a statistical design of experiments approach to separate noise, *Pattern Recognition Letters* **28**(7), 771–777.

Kumar, R. and Saini, B.: 2012, Improved image denoising technique using neighboring wavelet coefficients of optimal wavelet with adaptive thresholding, *International Journal of Computer Theory and Engineering* **4**(3), 395–400.

Kumar, S., Kumar, S., Sukavanam, N. and Raman, B.: 2014, Dual tree fractional quaternion wavelet transform for disparity estimation, *ISA Transactions* **53**(2), 547–559.

Lal, S. and Chandra, M.: 2012, Image denoising of wavelet based compressed images corrupted by additive white gaussian noise, *Research Journal of Applied Sciences, Engineering and Technology* **4**(17), 3108–3118.

Lang, M., Guo, H., Odegard, J. E., Burrus, C. S. and Wells, R. O.: 1996, Noise reduction using an undecimated discrete wavelet transform, *IEEE Signal Processing Letters* **3**(1), 10–12.

Lazzaro, D. and Montefusco, L.: 2007, Edge-preserving wavelet thresholding for image denoising, *Journal of Computational and Applied Mathematics* **210**(1-2), 222–231.

Lee, Y.-H. and Rhee, S.-B.: 2005, Wavelet-based image denoising with optimal filter, *Journal of Information Processing Systems* **1**(1), 32–35.

Li, J., Mohamed, S., Salama, M. M. and Freeman, G. H.: 2007, Subband-adaptive and spatially-adaptive wavelet thresholding for denoising and feature preservation of texture images, *International Conference Image Analysis and Recognition*, Springer, pp. 24–37.

Lian, N.-X., Zagorodnov, V. and Tan, Y.-P.: 2006, Edge-preserving image denoising via optimal color space projection, *IEEE Transactions on Image Processing* **15**(9), 2575–2587.

Liao, Z., Hu, S. and Chen, W.: 2010, Determining neighborhoods of image pixels automatically for adaptive image denoising using nonlinear time series analysis, *Mathematical Problems in Engineering* **2010**, 1–14.

Lin, L. and Lingfu, K.: 2009, Image denoising based on non-local means with wiener filtering in wavelet domain, *International Conference on Intelligent Information Hiding and Multimedia Signal Processing*, pp. 471–474.

Liu, W. and Ma, Z.: 2006, Wavelet image threshold denoising based on edge detection, *Multiconference on Computational Engineering in Systems Applications*, Vol. 1, pp. 72–78.

Liu, Z., Mi, Y. and Mao, Y.: 2014, Improved real-time denoising method based on lifting wavelet transform, *Measurement Science Review* **14**(3), 152–159.

Luisier, F. and Blu, T.: 2007, Image denoising by pointwise thresholding of the undecimated wavelet coefficients: A global sure optimum, *IEEE International Conference on Acoustics, Speech and Signal Processing*, Vol. 1, pp. 593–596.

Luisier, F., Blu, T. and Unser, M.: 2007, A new sure approach to image denoising: Interscale orthonormal wavelet thresholding, *IEEE Transactions on Image Processing* **16**(3), 593–606.

Luo, G.: 2006, Fast wavelet image denoising based on local variance and edge analysis, *International Journal of Intelligent Technology* **1**(2), 165–175.

Mahalakshmi, B. and Anand, M.: 2014, Adaptive wavelet packet decomposition for efficient image denoising by using neighsure shrink method, *International Journal of Comput.er Science Information Technolog* **5**(4), 5003–5009.

Malfait, M. and Roose, D.: 1997, Wavelet-based image denoising using a markov random field a priori model, *IEEE Transactions on Image Processing* **6**(4), 549–565.

Meher, S. K. and Singhawat, B.: 2014, An improved recursive and adaptive median filter for high density impulse noise, *AEU-International Journal of Electronics and Communications* **68**(12), 1173–1179.

Mihcak, M. K., Kozintsev, I., Ramchandran, K. and Moulin, P.: 1999, Low-complexity image denoising based on statistical modeling of wavelet coefficients, *IEEE Signal Processing Letters* **6**(12), 300–303.

Miller, M. and Kingsbury, N.: 2008, Image denoising using derotated complex wavelet coefficients, *IEEE Transactions on Image Processing* **17**(9), 1500–1511.

Mittal, R. and Kumar, S.: 2006, Numerical study of fisher's equation by wavelet galerkin method, *International Journal of Computer Mathematics* **83**(3), 287–298.

Mohideen, S. K.: 2012, Denosing of images using complex wavelet transform, *International Journal Advanced Scientific and Technical Research* **1**(2), 176–184.

Mohideen, S. K., Perumal, S. A., Krishnan, N., Sathik, M. M. and Kumar, T. R.: 2008, Image denoising multi-wavelet and threshold, *in Proceeding of International Conference on Computing, Communication and Networking*, pp. 1–5.

Montefusco, L. B., Lazzaro, D. and Papi, S.: 2011, Fast sparse image reconstruction using adaptive nonlinear filtering, *IEEE Transactions on Image Processing* **20**(2), 534–544.

Moulin, P. and Liu, J.: 1999, Analysis of multiresolution image denoising schemes using generalized gaussian and complexity priors, *IEEE Transactions on Information Theory* **45**(3), 909–919.

Naimi, H., Adamou-Mitiche, A. B. H. and Mitiche, L.: 2015, Medical image denoising using dual tree complex thresholding wavelet transform and wiener filter, *Journal of King Saud University-Computer and Information Sciences* **27**(1), 40–45.

Nandal, S. and Kumar, S.: 2018, Image denoising using fractional quaternion wavelet transform, *Proceedings of International Conference on Computer Vision & Image Processing*, Springer, pp. 301–313.

Nason, G. P.: 1996, Wavelet shrinkage using cross-validation, *Journal of the Royal Statistical Society. Series B (Methodological),* pp. 463–479.

Nikpour, M. and Hassanpour, H.: 2010, Using diffusion equations for improving performance of wavelet-based image denoising techniques, *IET Image Processing* **4**(6), 452–462.

Oktem, R. and Ponomarenko, N.: 2007, Image filtering based on discrete cosine transform, *Telecommunications and Radio Engineering* **66**(18).

Oten, R. and de Figueiredo, R. J.: 2004, Adaptive alpha-trimmed mean filters under deviations from assumed noise model, *IEEE Transactions on Image Processing* **13**(5), 627–639.

Ouarti, N. and Peyré, G.: 2009, Best basis denoising with non-stationary wavelet packets, *in Proceeding of International Conference on Image Processing*, pp. 3825–3828.

Ozkan, M. K., Erdem, A. T., Sezan, M. I. and Tekalp, A. M.: 1992, Efficient multiframe wiener restoration of blurred and noisy image sequences, *IEEE Transactions on Image Processing* **1**(4), 453–476.

Pan, Q., Zhang, L., Dai, G. and Zhang, H.: 1999, Two denoising methods by wavelet transform, *IEEE Transactions on Signal Processing* **47**(12), 3401–3406.

Pizurica, A.: 2002, *Image denoising using wavelets and spatial context modeling*, PhD thesis, Ghent University.

Pizurica, A., Vanhamel, I., Sahli, H., Philips, W. and Katartzis, A.: 2006, A bayesian formulation of edge-stopping functions in nonlinear diffusion, *IEEE Signal Processing Letters* **13**(8), 501–504.

Portilla, J., Strela, V., Wainwright, M. J. and Simoncelli, E. P.: 2001, Adaptive wiener denoising using a gaussian scale mixture model in the wavelet domain, *in Proceeding of International Conference on Image Processing*, Vol. 2, pp. 37–40.

Pragada, S. and Sivaswamy, J.: 2008, Image denoising using matched biorthogonal wavelets, *Indian Conference on Computer Vision, Graphics and Image Processing*, pp. 25–32.

Prudyus, I., Voloshynovskiy, S. and Synyavskyy, A.: 2001, Wavelet-based map image denoising using provably better class of stochastic iid image models, *in Proceeding of International Conference on Telecommunications in Modern Satellite, Cable and Broadcasting Service*, Vol. 2, pp. 583–586.

Rabbani, H. and Vafadoost, M.: 2006, Wavelet based image denoising based on a mixture of laplace distributions, *Iranian Journal of Science and Technology* **30**(B6), 711–733.

Radi, N., Hussain, A. and Al-Jumeily, D.: 2011, Hybrid predictive, wavelet and arithmetic (hpwa) image coding system, *in Proceeding of Developments in E-systems Engineering*, pp. 558–563.

Rafsanjani, H. K., Sedaaghi, M. H. and Saryazdi, S.: 2017, An adaptive diffusion coefficient selection for image denoising, *Digital Signal Processing* **64**, 71–82.

Raghuvanshi, D., Jain, D. and Jain, P.: 2013, Performance analysis of non local means algorithm for denoising of digital images, *International Journal Adv Res Computer Science Software Engineering* **3**(1), 94–100.

Rajpoot, K., Rajpoot, N. and Noble, J. A.: 2008, Discrete wavelet diffusion for image denoising, *International Conference on Image and Signal Processing*, Springer, pp. 20–28.

Ranganathan, A. and Von Borries, R.: 2006, Sliced ridgelet transform for image denoising, *Digital Signal Processing Workshop*, pp. 209–213.

Rank, K. and Unbehauen, R.: 1992, An adaptive recursive 2-d filter for removal of gaussian noise in images, *IEEE Transactions on Image Processing* **1**(3), 431–436.

Ranta, R., Heinrich, C., Louis-Dorr, V. and Wolf, D.: 2003, Interpretation and improvement of an iterative wavelet-based denoising method, *IEEE Signal Processing Letters* **10**(8), 239–241.

Raokhande, N. M. A. and Marathe, N.: 2012, Image denoising using trivariate shrinkage filter in wavelet domain, *International Journal of Emerging Technology and Advanced Engineering* **2**(3), 323–326.

Raphan, M. and Simoncelli, E. P.: 2008, Optimal denoising in redundant representations, *IEEE Transactions on Image Processing* **17**(8), 1342–1352.

Ray, S. and Mallick, B. K.: 2003, A bayesian transformation model for wavelet shrinkage, *IEEE Transactions on Image Processing* **12**(12), 1512–1521.

Rehman, A. and Wang, Z.: 2011, Ssim-based non-local means image denoising, *in Proc. of 18th IEEE International Conference on Image Processing*, pp. 217–220.

Routray, S., Ray, A. K., Mishra, C. and Palai, G.: 2018, Efficient hybrid image denoising scheme based on svm classification, *Optik-International Journal for Light and Electron Optics* **157**, 503–511.

Sadeghipour, Z., Babaie-Zadeh, M. and Jutten, C.: 2009, An adaptive thresholding approach for image denoising using redundant representations, *IEEE International Workshop on Machine Learning for Signal Processing*, pp. 1–6.

Sahu, D. and Dewangan, R. K.: 2014, Analysis of image denoising technique based on wavelet thresholding along with preserving edge information, *International Journal of Research in Advent Tech nology* **2**(1), 441–446.

Scharcanski, J., Jung, C. R. and Clarke, R. T.: 2002, Adaptive image denoising using scale and space consistency, *IEEE Transactions on Image Processing* **11**(9), 1092–1101.

Scheunders, P.: 2004, Wavelet thresholding of multivalued images, *IEEE Transactions on Image Processing* **13**(4), 475–483.

Selesnick, I. W.: 2008, The estimation of laplace random vectors in additive white gaussian noise, *IEEE Transactions on Signal Processing* **56**(8), 3482–3496.

Sethunadh, R. and Thomas, T.: 2014, Spatially adaptive image denoising using inter-scale dependence in directionlet domain, *IET Image Processing* **9**(2), 142–152.

Shao, L., Yan, R., Li, X. and Liu, Y.: 2014, From heuristic optimization to dictionary learning: A review and comprehensive comparison of image denoising algorithms, *IEEE Transactions on Cybernetics* **44**(7), 1001–1013.

Shensa, M. J.: 1992, The discrete wavelet transform: wedding the a-trous and mallat algorithms, *IEEE Transactions on Signal Processing* **40**(10), 2464–2482.

Shi, Y., Yang, X. and Guo, Y.: 2014, Translation invariant directional framelet transform combined with gabor filters for image denoising, *IEEE Transactions on Image Processing* **23**(1), 44–55.

Shiguo, C., Ruanyu, Z., Peng, W. and Taihua, L.: 2004, Enhance accuracy in pole identification of system by wavelet transform de-noising, *IEEE Transactions on Nuclear Science* **51**(1), 250–255.

Shikkenawis, G., Mitra, S. K. and Rajwade, A.: 2015, Image denoising using orthogonal locality preserving projections, *Journal of Electronic Imaging* **24**(4), 43–48.

Shu, Y., Chen, Y. and Su, Y.: 2013, Fast adaptive bilateral filtering with fixed parameters for sharpness enhancement and noise reduction, *in Proceeding of IEEE International Conference on Information Science and Cloud Computing Companion*, pp. 640–645.

Shui, P.-L.: 2005, Image denoising algorithm via doubly local wiener filtering with directional windows in wavelet domain, *IEEE Signal Processing Letters* **12**(10), 681–684.

Shui, P.-L.: 2009, Image denoising using 2-d separable oversampled dft modulated filter banks, *IET Image processing* **3**(3), 163–173.

Starck, J.-L., Candès, E. J. and Donoho, D. L.: 2002, The curvelet transform for image denoising, *IEEE Transactions on image processing* **11**(6), 670–684.

Suresh, S. and Lal, S.: 2017, Two-dimensional cs adaptive fir wiener filtering algorithm for the denoising of satellite images, *IEEE Journal of Selected Topics in Applied Earth Observations and Remote Sensing* **10**(12), 5245–5257.

Tasdizen, T.: 2009, Principal neighborhood dictionaries for nonlocal means image denoising, *IEEE Transactions on Image Processing* **18**(12), 2649–2660.

Tessens, L., Pižurica, A., Alecu, A., Munteanu, A. and Philips, W.: 2006, Spatially adaptive image denoising based on joint image statistics in the curvelet domain, *in Proceeding of Wavelet Applications in Industrial Processing*, Vol. 6383, pp. 1–12.

Thaipanich, T., Oh, B. T., Wu, P.-H., Xu, D. and Kuo, C.-C. J.: 2010, Improved image denoising with adaptive nonlocal means algorithm, *IEEE Transactions on Consumer Electronics* **56**(4), 2623 – 2630.

Thakur, R.: 2013, Analysis of orthogonal and biorthogonal mother wavelet using gaussian noise for image denoising, *International Journal of Application or Innovation in Engineering and Management* **12**, 2623 – 2630.

Verd-Monedero, R., Angulo, J. and Serra, J.: 2011, Anisotropic morphological filters with spatially-variant structuring elements based on image-dependent gradient fields, *IEEE Transactions on Image Processing* **20**(1), 200–212.

Verma, D. and Mathur, S.: 2012, Image denoising based on averaging of two wavelet transformed images, *International Journal of Engineering Research and Applications* **2**(5), 2112–2119.

Verma, R. and Pandey, R.: 2017, Adaptive selection of search region for nlm based image denoising, *Optik-International Journal for Light and Electron Optics* **147**, 151–162.

Vidakovic, B.: 1998, Nonlinear wavelet shrinkage with bayes rules and bayes factors, *Journal of the American Statistical Association* **93**(441), 173–179.

Voloshynovskiy, S., Koval, O. and Pun, T.: 2005, Image denoising based on the edge-process model, *Signal Processing* **85**(10), 1950–1969.

Wang, X.-Y., Yang, H.-Y. and Fu, Z.-K.: 2010, A new wavelet-based image denoising using undecimated discrete wavelet transform and least squares support vector machine, *Expert Systems with Applications* **37**(10), 7040–7049.

Wang, Y. and Zhou, H.: 2006, Total variation wavelet-based medical image denoising, *International Journal of Biomedical Imaging* **2006**, 1–12.

Weyrich, N. and Warhola, G. T.: 1998, Wavelet shrinkage and generalized cross validation for image denoising, *IEEE Transactions on Image Processing* **7**(1), 82–90.

Wu, X., Guo, B., Qu, S. and Wang, Z.: 2009, A new adaptive image denoising method combining the nonsubsampled contourlet transform and total variation, *in Proc. of Fifth International Conference on Information Assurance and Security*, pp. 581–584.

Xie, J., Zhang, D. and Xu, W.: 2004, Spatially adaptive wavelet denoising using the minimum description length principle, *IEEE Transactions on Image Processing* **13**(2), 179–187.

Yang, L., Parton, R., Ball, G., Qiu, Z., Greenaway, A. H., Davis, I. and Lu, W.: 2010, An adaptive non-local means filter for denoising live-cell images and improving particle detection, *Journal of Structural Biology* **172**(3), 233–243.

Yoo, J.-C. and Ahn, C. W.: 2014, Image restoration by blind-wiener filter, *IET Image Processing* **8**(12), 815–823.

You, X. and Crebbin, G.: 1995, Robust adaptive estimator for filtering noise in images, *IEEE Transactions on Image Processing* **4**(5), 693–699.

Yu, H., Zhao, L. and Wang, H.: 2009, Image denoising using trivariate shrinkage filter in the wavelet domain and joint bilateral filter in the spatial domain, *IEEE Transactions on Image Processing* **18**(10), 2364–2369.

Yüksel, M. E.: 2006, A median/anfis filter for efficient restoration of digital images corrupted by impulse noise, *AEU-International Journal of Electronics and Communications* **60**(9), 628–637.

Zervakis, M. E., Sundararajan, V. and Parhi, K. K.: 2001, Vector processing of wavelet coefficients for robust image denoising, *Image and Vision Computing* **19**(7), 435–450.

Zhang, B. and Allebach, J. P.: 2008, Adaptive bilateral filter for sharpness enhancement and noise removal, *IEEE Transactions on Image Processing* **17**(5), 664–678.

Zhang, L. and Bao, P.: 2003, Denoising by spatial correlation thresholding, *IEEE Transactions on Circuits and Systems for Video Technology* **13**(6), 535–538.

Zhang, X. and Feng, X.: 2014, Hybrid gradient-domain image denoising, *AEU-International Journal of Electronics and Communications* **68**(3), 179–185.

Zhang, X.-P. and Desai, M. D.: 1998, Adaptive denoising based on sure risk, *IEEE Signal Processing Letters* **5**(10), 265–267.

Zhu, S., Li, Y. and Li, Y.: 2014, Two-stage non-local means filtering with adaptive smoothing parameter, *Optik-International Journal for Light and Electron Optics* **125**(23), 7040–7044.